# Product Design Optimization Under Epistemic Uncertainty

by

Xiaotian Zhuang

A Dissertation Presented in Partial Fulfillment
of the Requirements for the Degree
Doctor of Philosophy

Approved April 2012 by the
Graduate Supervisory Committee:

Rong Pan, Chair
Muhong Zhang
Xiaoping Du
Douglas C. Montgomery

ARIZONA STATE UNIVERSITY

May 2012

ABSTRACT

This dissertation is to address product design optimization including reliability-based design optimization (RBDO) and robust design with epistemic uncertainty. It is divided into four major components as outlined below.

Firstly, a comprehensive study of uncertainties is performed, in which sources of uncertainty are listed, categorized and the impacts are discussed. Epistemic uncertainty is of interest, which is due to lack of knowledge and can be reduced by taking more observations. In particular, the strategies to address epistemic uncertainties due to implicit constraint function are discussed.

Secondly, a sequential sampling strategy to improve RBDO under implicit constraint function is developed. In modern engineering design, an RBDO task is often performed by a computer simulation program, which can be treated as a black box, as its analytical function is implicit. An efficient sampling strategy on learning the probabilistic constraint function under the design optimization framework is presented. The method is a sequential experimentation around the approximate most probable point (MPP) at each step of optimization process. It is compared with the methods of MPP-based sampling, lifted surrogate function, and non-sequential random sampling.

Thirdly, a particle splitting-based reliability analysis approach is developed in design optimization. In reliability analysis, traditional simulation methods such as Monte Carlo simulation may provide accurate results, but are often accompanied with high computational cost. To increase the efficiency, particle splitting is integrated into RBDO. It is an improvement of subset simulation with multiple particles to enhance the diversity and stability of simulation samples. This method is further extended to address problems with multiple probabilistic constraints and compared

with the MPP-based methods.

Finally, a reliability-based robust design optimization (RBRDO) framework is provided to integrate the consideration of design reliability and design robustness simultaneously. The quality loss objective in robust design, considered together with the production cost in RBDO, are used formulate a multi-objective optimization problem. With the epistemic uncertainty from implicit performance function, the sequential sampling strategy is extended to RBRDO, and a combined metamodel is proposed to tackle both controllable variables and uncontrollable variables. The solution is a Pareto frontier, compared with a single optimal solution in RBDO.

ACKNOWLEDGEMENTS

As I come to the accomplishment of my four-year doctoral study in Arizona State University, I would like to give my sincere gratitude to faculties, friends and my family members. Without their support and help, my doctoral study and dissertation would not have been possible.

I especially would like to thank my advisor Dr. Rong Pan for his patient guidance and assistance throughout my four-year doctoral study. Dr. Pan not only gave me mentoring and coaching during the research and dissertation writing process, but also encouraged me to keep a good attitude to face difficulties and challenges in future.

I would like to thank other committee members Drs. Muhong Zhang, Xiaoping Du and Douglas C. Montgomery. To Dr. Zhang, I appreciate her help in my optimization algorithm improvement. To Dr. Du, thanks for his guidance in my research direction especially in my third journal paper. To Dr. Montgomery, thanks for his suggestions in the experiment selection and model construction in my dissertation.

My doctoral study would not have been the same without my friends' support. I appreciate the help of my lab-mates Jinsuk Lee, Eric Monroe, Luis Mejia Sanchez in my research and job hunting guidance. I would like to thank my friend Zhun Han and Liangjie Xue in learning the Latex syntax used to format my dissertation. I also would like to thank my friends Mengqi Hu, Junzilan Cheng, Mingjun Xia, Tao Yang, Houtao Deng, Ning Wang, Hairong Xie, Min Zhang, Cheng Xu, Huying Liu and Lizhi Wang. Thanks for their time, support and patience over the years. I would like to express my gratitude to the faculty and staff of the Industrial Engineering department for their assistance during my course of study.

Finally, I wish to acknowledge all of my friends and family members. Thanks for their encouragement and support through my four-year overseas doctoral study. I wish to especially thank my parents, who provided me never-ending love and always stood behind me no matter what happened.

TABLE OF CONTENTS

Page

LIST OF TABLES . . . . . ix

LIST OF FIGURES . . . . . x

CHAPTER

1 INTRODUCTION . . . . . 1

1.1 Background . . . . . 1

1.2 Motivation . . . . . 5

Deterministic Design Optimization vs. Reliability-Based Design Optimization . . . . . 5

Aleatory Uncertainty vs. Epistemic Uncertainty . . . . . 5

Metamodel-Based Approach & Simulation-Based Approach . . . . 6

Reliability & Robustness . . . . . 7

1.3 Dissertation Organization . . . . . 7

1.4 Literature Review . . . . . 9

RBDO Approaches . . . . . 9

Reliability Analysis Approaches . . . . . 10

Reliability and Robustness Integration . . . . . 11

2 EPISTEMIC UNCERTAINTY IN PRODUCT DESIGN OPTIMIZATION 12

2.1 Introduction . . . . . 12

2.2 Reliability-Based Design Optimization . . . . . 12

2.3 Epistemic Uncertainty in RBDO . . . . . 14

Sources of Uncertainties . . . . . 14

Categorizing Epistemic Uncertainty . . . . . 16

Impacts of Epistemic Uncertainty on RBDO . . . . . 16

2.4 Epistemic Uncertainty Strategy in RBDO . . . . . 19

CHAPTER Page

Implicit Constraint Function . . . . . 19
Unknown Random Variable Distribution . . . . . 21
2.5 I-Beam Example . . . . . 22
Effects of Implicit Constraint Functions . . . . . 24
Effects of Unknown Random Variable Distributions . . . . . 25
2.6 Conclusion . . . . . 25
3 A SEQUENTIAL SAMPLING STRATEGY TO IMPROVE RELIABILITY-BASED DESIGN OPTIMIZATION WITH IMPLICIT CONSTRAINT FUNCTIONS . . . . . 27
3.1 Introduction . . . . . 27
3.2 Reliability Analysis in RBDO . . . . . 29
First-Order Reliability Analysis in RIA and PMA . . . . . 29
Sequential Optimization and Reliability Analysis (SORA) . . . . . 31
Metamodeling Techniques and Comparisons . . . . . 32
3.3 Sequential Expected Improvement Sampling . . . . . 34
Initial Latin Hypercube Sampling . . . . . 34
Expected Improvement Criterion . . . . . 34
RBDO Solution Using Sequential ERI-Based Sampling Strategy . . 36
Other Methods . . . . . 42
3.4 I-Beam Performance Comparison . . . . . 43
Solution with the True Constraint Function . . . . . 43
Solution with the Sequential ERI-Based Sampling Strategy . . . . . 44
Solutions by Other Methods . . . . . 47
Efficiency and Accuracy Comparison Between Different Methods . 51

CHAPTER Page

3.5 Application to A Thin Walled Box Beam . . . . . 53
3.6 Conclusion and Future Work . . . . . 56
4 DESIGN OPTIMIZATION WITH PARTICLE SPLITTING-BASED RELIABILITY ANALYSIS . . . . . 60
4.1 Introduction . . . . . 60
4.2 Simulation-Based Reliability Analysis . . . . . 61
4.3 SORA with Particle Splitting-Based Reliability Analysis . . . . . 64
Particle Splitting . . . . . 65
SORA with Particle Splitting-Based Reliability Assessment . . . . . 69
Extension to RBDO with Multiple Probabilistic Constraints . . . . . 73
4.4 Examples . . . . . 76
I-Beam Example . . . . . 76
An Example with Multiple Constraints . . . . . 78
4.5 Conclusion and Future Work . . . . . 82
5 RELIABILITY-BASED ROBUST DESIGN OPTIMIZATION UNDER IMPLICIT PERFORMANCE FUNCTIONS . . . . . 84
5.1 Introduction . . . . . 84
5.2 Reliability-Based Robust Design Optimization . . . . . 88
RBRDO Formulation . . . . . 89
Sequential Optimization and Reliability Analysis (SORA) in RBRDO 90
5.3 Sequential Sampling Strategy in RBRDO Under Implicit Performance Function . . . . . 90
Hybrid Design and Combined Metamodel in RBRDO . . . . . 91
Expected Improvement Criterion . . . . . 91

CHAPTER Page

RBRDO Solution by Sequential EI-Based Sampling Strategy . . . . 92

5.4 I-Beam Example . . . . . 96

5.5 Conclusion and Future Work . . . . . 99

6 CONCLUSION AND FUTURE RESEARCH . . . . . 101

6.1 Conclusions . . . . . 101

6.2 Future Work . . . . . 102

REFERENCES . . . . . 104

LIST OF TABLES


| Table | | Page |
|---|---|---|
| 1 | Approaches for Unknown Distribution | 21 |
| 2 | Epistemic Uncertainty Impact on I-Beam Case | 24 |
| 3 | Results of SORA for I-Beam with True Constraint | 43 |
| 4 | Initial Samples by Latin Hypercube | 46 |
| 5 | Results of SORA for I-Beam with Sequential ERI Sampling Strategy | 46 |
| 6 | Additional Samples by Sequential ERI Sampling Strategy | 48 |
| 7 | Additional Samples by Uniform Sampling | 51 |
| 8 | Results Comparison Between Methods in I-Beam Case | 52 |
| 9 | Efficiency in Thin Walled Box Beam Demo | 56 |
| 10 | Initial Samples by Latin Hypercube | 57 |
| 11 | Results of Sequential ERI Sampling of the Thin Walled Box Beam | 59 |
| 12 | Sample Size Requirement for Different Number of Subsets When $\delta = 0.1$ | 68 |
| 13 | Solution Steps by the Particle Splitting-Based Approach | 77 |
| 14 | I-Beam Accuracy Comparison | 78 |
| 15 | Results by the Particle Splitting-Based Approach | 80 |
| 16 | Comparing Accuracy of the Solutions by Different Methods | 82 |
| 17 | Initial Samples by Cross Array Design | 98 |
| 18 | Pareto Solutions for I-Beam Design | 99 |

LIST OF FIGURES


| Figure | | Page |
|---|---|---|
| 1 | Research overall vision | 8 |
| 2 | Implicit constraint function infeasible impact | 17 |
| 3 | Implicit constraint function conservative impact | 18 |
| 4 | Unknown random variable distribution impact | 19 |
| 5 | I-beam case study | 23 |
| 6 | Implicit constraint function impact on I-beam | 24 |
| 7 | Unknown distribution impact on I-beam | 25 |
| 8 | Max ERI sample point in design space. The initial samples are marked by "+", additional samples are marked by "o", and $G'_{min}$ is the latest additional sample selected by the ERI criterion. | 37 |
| 9 | Algorithmic flowchart | 38 |
| 10 | Max ERI sample point in response space | 41 |
| 11 | 3D shape of G function | 44 |
| 12 | Feasible region with true G function | 45 |
| 13 | RBDO feasible region of $\hat{G}$ by sequential ERI sampling | 47 |
| 14 | RBDO feasible region $\hat{G}$ function by MPP-based sampling | 49 |
| 15 | RBDO feasible region by lifting response function | 50 |
| 16 | RBDO feasible region of $\hat{G}$ by non-sequential random sampling | 51 |
| 17 | A thin walled box beam demo | 53 |
| 18 | Preprocess model in ANSYS | 54 |
| 19 | Deformed shape | 55 |
| 20 | Contour plots of Von-Mises | 55 |
| 21 | Sample size requirement for different coefficient of variation and number of subsets. | 67 |

22 Particle splitting-based reliability assessment . . . . . 70
23 Particle splitting samples . . . . . 72
24 TPP location by particle splitting . . . . . 73
25 Particle splitting samples in multiple constraints . . . . . 76
26 Particle splitting optimal solution . . . . . 81
27 Noise variable impacts on performance function . . . . . 88
28 RBRDO algorithm . . . . . 93
29 RBRDO Pareto frontier . . . . . 100

# CHAPTER 1

# INTRODUCTION

## 1.1 Background

Product design optimization is concerned with efficient and effective methods leading to new products. Uncertainty always exists during the process of design and production and may come from various sources, such as modeling approximation, imperfect manufacturing, etc. Taking from an epistemological perspective, uncertainties to be considered at the product design stage can be categorized into objective and subjective ones ([9, 74, 41]).

Objective uncertainties are also called aleatory uncertainties (AU). The word aleatory derives from the Latin *alea*, which means the rolling of dice. Aleatory uncertainty exists because of natural variation in the system performance. Aleatory uncertainties can be quantified but cannot be reduced, because they are the intrinsic randomness of a phenomenon. Examples are environmental parameter such as humidity, temperature and wind load, or material property parameters such as stiffness, yielding strength and conductivity.

Subjective uncertainties are also called epistemic uncertainties (EU). The word epistemic derives from the Greek $\varepsilon\pi\iota\sigma\tau\eta\mu\eta$, which means knowledge. Epistemic uncertainties exist because of lack of knowledge, and they are reducible to aleatory uncertainty by understanding the design or by obtaining more data. For example, the random variable's distribution is unknown or the systems' performance function is unknown or implicit due to lack of knowledge.

For the epistemic uncertainty with unknown random variable's distribution, two typical methods are employed. One method is possibility and evidence theory. A comparison of probability and possibility of design under uncertainty was

proposed in [63]; Reliability estimation based on possibility theory was presented in [61]; Du proposed a possibility-based design optimization (PBDO) instead of RBDO due to epistemic uncertainty in [20]. Zhang presented a mixed variable (random and fuzzy variables) multidisciplinary design optimization with the framework of SORA in [98]. The other method is statistical inference approach, in which finite samples obtained from experiments are used to estimate unknown random variables's or performance function's distribution by statistical inference (e.g. Bayesian inference). Strategies are developed to take more efficient and effective samples to update the distribution estimate based on Bayesian inference. A beta conjugate Bayesian inference was employed in [30, 92] to deal with RBDO with incomplete information of design variables; A Bayesian RBDO method combined with eigenvector dimension reduction (EDR) was proposed in [93]; A Kriging dimension reduction method was employed to promote efficient implementation of the reliability analysis in [16].

For the epistemic uncertainty with implicit system's performance function, systems' performance function is evaluated by computer models such as Finite Element Model (FEM) ([72, 67]); therefore, the true analytical performance functions are implicit. Metamodels, which are constructed by computer experiments, are used to approximate this function. The two most common types of metamodels are response surface model (RSM) and Kriging model. A sequential sampling RSM was proposed by [99, 89]. An RSM with prediction interval estimation was proposed by [40]. An RBDO using moment method and a Kriging metamodel was provided by [39], in which a Kriging metamodel that can carry out reliability analysis based on the moment method was presented. Also a comparative study of polynomial model, Kriging model and radial basis function can be found in [37], in which the accuracy of Kriging model was compared with polynomial model.

In order to design and manufacture high quality products, product design optimization under uncertainty has been widely discussed in recent years, techniques are employed to control and minimize impact of uncertainty. Robustness and reliability are two important aspects of design optimization based on different design scenarios ([44]).

Robust design, firstly proposed by Taguchi, is a method which focuses on minimizing performance variation without eliminating the sources of variation. Robust design is actually from the point of view of quality engineers, who concern with the product performance variation for a given performance target. Taguchi provides a three-stage robust design methodology: systems design, parameter design and tolerance design. The difference between robust design optimization and ordinary optimization lies in the consideration for performance variations due to uncontrolled noise factors. In actual product design, two kinds of variables or parameters exist: control factors $\mathbf{x}$, which are controllable and can be tuned for optimal system performance; noise factors $\xi$, which are uncontrollable, such as production tolerances (e.g., length variation) and environmental conditions (e.g. humidity and temperature). Signal-to-noise ratio (SNR), one important measure of quality loss, is proposed by Taguchi as design objective in robust design:

$$SNR := -10log_{10}(MSD) \tag{1.1}$$

where maximum $SNR$ is desired, and $MSD = \frac{1}{k}\sum_{i=1}^{k}(y_i(\mathbf{x},\xi_\mathbf{i}) - y_t)^2$, which means the mean square deviation. $y_i(\mathbf{x},\xi_\mathbf{i})$ is the quality value of a single sample and $y_t$ is the desired target value. MSD can have other definitions according to different objectives (e.g. close to zero or as large as possible). $SNR$ is optimized by design of experiments (DOE) in Taguchi method. Controllable parameters $\mathbf{x}$ are systematically changed based on a predefined lattice (inner array). At each design

point $\mathbf{x}$, noise factors $\xi$ are also changed according to an outer array. Thus a set of $(y_i, \ldots, y_k)$ w.r.t $\mathbf{x}$ is derived and $SNR(\mathbf{x})$ can be calculated. Finally we can find the $\mathbf{x}$ which produces the maximum $SNR$ based on statistical data analysis.

Reliability-based design is another aspect of design optimization from the viewpoint of mechanical engineers. In structure design, it is critical to maintain the design feasibility (or reliability). Then the paradigm of RBDO is proposed for design under uncertainty. RBDO typically considers the uncertainties in some design variables and uses a probabilistic constraint function to guarantee a system's reliability (i.e., performance or safety requirement). A generic formulation is given below.

$$\text{Minimize: } f(\mathbf{d}, \mu_{\mathbf{X}}, \mu_{\mathbf{P}}) \tag{1.2}$$

$$\text{Subject to: } Prob[G_i(\mathbf{d}, \mathbf{x}, \mathbf{p}) \geq 0] \geq R_i, \quad i = 1, 2, \ldots, m \tag{1.3}$$

$$\mathbf{d^L} \leq \mathbf{d} \leq \mathbf{d^U}, \mu_{\mathbf{X}}^{\mathbf{L}} \leq \mu_{\mathbf{X}} \leq \mu_{\mathbf{X}}^{\mathbf{U}}, \mu_{\mathbf{P}}^{\mathbf{L}} \leq \mu_{\mathbf{P}} \leq \mu_{\mathbf{P}}^{\mathbf{U}} \tag{1.4}$$

The objective function can be viewed as a production cost function of the system. Note that the objective function above is the first-order Taylor expansion approximation of the mean cost function $E[f(\mathbf{d}, \mathbf{x}, \mathbf{p})]$ due to the randomness of $\mathbf{X}$ and $\mathbf{P}$. This approximation is generally acceptable for linear and close-to-linear cost function. However, we are more interested in the probabilistic constraint function, which is the key difference of RBDO from other engineering optimizations. The function $G_i(\mathbf{d}, \mathbf{x}, \mathbf{p}) > 0$ is the system's performance or safety requirement, where $G_i > 0$ denotes safe or successful region, $G_i < 0$ denotes failure region, and $G_i = 0$ is defined as limit state surface which is the boundary between success and failure. The value $R_i$ is the target probability of the constraint function. Thus, this probabilistic constraint guarantees the system's reliability.

## 1.2 Motivation

*Deterministic Design Optimization vs. Reliability-Based Design Optimization*

Optimization techniques have been extensively employed in product design and manufacturing in order to decrease cost and augment quality. Traditionally, product design is formulated as a deterministic design optimization, which assumes that there is no model or input variable uncertainty. In product design, however, there exist uncertainties that can affect system performance and result in output variation. The optimal designs obtained from deterministic optimization often reach the limit state surface of design constraints, without tolerance region for uncertainties. Hence the deterministic optimal designs cannot satisfy constraints with small deviations. In other words, the optimal solutions are unreliable or too sensitive to variation in reality. To achieve reliable designs, RBDO is employed in the presence of uncertainties. Probabilistic constraints are used to consider stochastic nature of variables and parameters, and a mean performance measure is optimized subject to probabilistic constraints. However, efficient and effective probabilistic constraints evaluation is the major challenge in RBDO. It is necessary and valuable, therefore, to develop strategies to handle the problem.

*Aleatory Uncertainty vs. Epistemic Uncertainty*

Traditional probabilistic analysis approaches are very effective to handle product and system's inherent randomness, or we call aleatory uncertainties when sufficient data is available. In other words, enough data about the product or system is known to construct exact performance functions or constraint functions, and quantify uncertainties with probability distributions.

However, in many cases sufficient information assumption is not realistic; insufficient data prevents correct probability distribution inference and causes errors in performance function construction. For many engineering tasks, system's performance or safety criterion is evaluated by computer models (e.g., finite element model). Metamodels are constructed based on the computer experiment sample points. Ideally, the metamodel is perfectly the same as the true model if we do experiments to exhaust the sample space. However, in reality computer experiments could be very expensive and time consuming, so taking a lot of sample points is unaffordable. Therefore, the true probability distribution or analytical constraint function is unknown or implicit due to lack of knowledge or epistemic uncertainty, and the solutions derived without considering epistemic uncertainty are unreliable. Our research focuses on the RBDO with epistemic uncertainty.

*Metamodel-Based Approach* & *Simulation-Based Approach*

Under epistemic uncertainty with implicit constraint or performance functions, two types of approach can be used. The first one is the metamodel-based approach. In this approach, a design of experiment is implemented to generate a few initial samples so that the metamodel is constructed to replace the implicit constraint function. In order to reduce the metamodel prediction error between metamodel and true model, sequential sampling strategies are required to select additional samples to update the metamodel and improve the RBDO solution. This approach takes very few samples and is efficient for the problem in which the implicit function evaluation is very expensive.

The second one is the simulation-based approach. In this approach the implicit function is simulated as a black-box. The probabilistic constraints evaluation is conducted by simulation directly. Traditional Monte Carlo simulation can reach

high accurate results, but are often accompanied with high computational cost. Instead, the importance simulation such as particle splitting is integrated in the probabilistic constraints evaluation process. Thus the efficiency dramatically increases without losing accuracy. This approach provides accurate solutions and is useful when the implicit function evaluation is affordable.

*Reliability & Robustness*

Although reliability and robustness are different aspects of design optimization from mechanical engineering and quality engineering, respectively, they are both important attributes in design optimization. RBDO provides the optimum designs in the presence of uncertainty, in which probabilistic distributions are employed to describe the stochastic nature of design variables and parameters, and standard deviations are typically assumed to be constant. Robust design is widely used to improve product quality. It minimizes performance variation without eliminating the sources of variation. Many methods using mean and standard deviation of performance have been proposed in [22] to estimate product quality loss. It is necessary, therefore, to improve robustness and reliability simultaneously. A multi-objective optimization problem is established to integrate robustness and reliability, where the quality loss due to performance variation and production cost are simultaneously minimized, subject to probabilistic constraints.

## 1.3 Dissertation Organization

In this research, we develop a general framework to evaluate the impact of epistemic uncertainty to design optimization including RBDO and robust design. The overall vision of research is described in Figure 1. The work of three phases are shown as follows:

**Phase I**: A metamodel-based approach with sequential sampling strategy

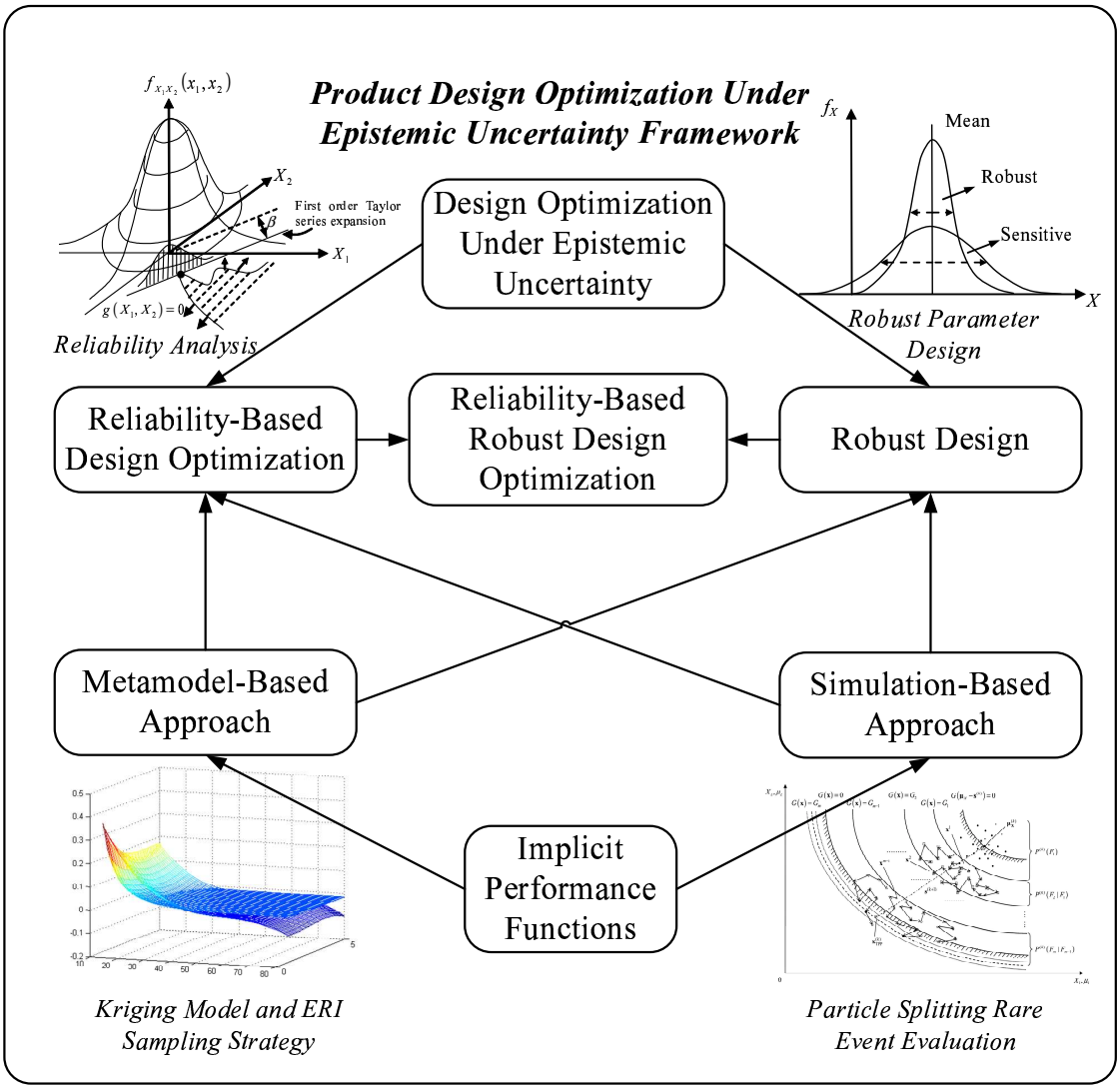


Figure 1.Research overall vision

is developed to improve RBDO under epistemic uncertainty of implicit constraint functions. An initial Kriging metamodel is constructed to replace the true model in RBDO, then a sequential sampling strategy is developed to add samples around the approximate MPP and update metamodel. Thus the RBDO solution is improved.

**Phase II**: A simulation-based approach is developed in reliability analysis in RBDO. Traditional simulation methods such as Monte Carlo simulation may provide accurate results in reliability analysis in RBDO, but they often lead to high computational cost. In order to tackle the efficiency problem, a particle splitting approach is introduced and integrated into reliability analysis.

**Phase III**: A framework integrating RBDO and robust design under epistemic uncertainty of implicit performance functions is proposed. The sequential sampling strategy in Phase I is extended to a multi-objective optimization problem. In order to address impacts of noise variables, a hybrid design is implemented and a combined Kriging metamodel is constructed.

## 1.4 Literature Review

### *RBDO Approaches*

Solving an RBDO problem demands two steps – the design optimization loop and the reliability assessment loop, and two loops are nested. Many techniques have been developed and can be broadly classified into nested double-loop methods, decoupled-loop methods, and single-loop methods. The nested double-loop methods are the traditional approaches which require large computational work. The decoupled-loop methods are based on the elements of the sequential optimization. A sequential optimization and reliability assessment (SORA) method was presented in [23], which was also employed to improve the efficiency of probabilistic structural optimization by [52]. A single-loop approach for RBDO was presented in

[78, 48, 76].

*Reliability Analysis Approaches*

SORA is employed in this research because of its high accuracy and efficiency. We focus on the evaluation of probabilistic constraints. According to [44], the methods of evaluating probabilistic constraints can be classified into five categories as follows:

1. *Simulation-based method* – Monte Carlo simulation (MSC) ([22]) is a basic method to evaluate probabilistic feasibility. However, the computation cost is high especially for high target reliability (approaching 1.0). Then importance sampling is employed to improve the sampling efficiency. A sampling method around the MPP was provided in [22]; The importance sampling in reduced region was developed in [33, 46]; Importance sampling was also employed to improve sampling efficiency and estimation accuracy in [58, 42].

2. *Local expansion-based method* – Taylor series method ([55, 31]) belongs to this category, which could not be efficient dealing with high dimension input and nonlinear performance functions. Functional expansion based method such as the polynomial chaos expansion ([18]) is in this category as well.

3. *MPP-based method* – This method is typically based on first-order reliability method (FORM) ([15, 57]). Two alternative ways can be used to evaluate probabilistic constraints: The direct reliability analysis method is reliability index approach (RIA) ([90, 88, 91]) in which the first-order safety reliability index ([28, 97]) and MPP are obtained using FORM by formulating an optimization problem. Since the convergence efficiency is low in traditional RIA, a modified RIA ([50]) revises the reliability index definition and im-

proves the efficiency. Also, a new approach for RIA based on minimum error point (MEP) ([51]) was presented to minimize the error produced by approximating performance functions. Another indirect reliability analysis method is performance measure approach (PMA) ([90, 21]), which is more robust and effective than RIA. An integrated framework using PMA was provided by [25] to assess probabilistic constraints.

4. *Response surface approximate method* – RSM builds metamodels based on the limited number of samples to replace the true system response [62]. The accuracy of this method depends on the accuracy of RSM model. An efficient global reliability analysis (EGRA) was proposed in [10], [11], [12] to effectively add samples to update metamodels. A sequential sampling strategy to improve reliability-based optimization under implicit constraints was proposed in [100].

5. *Numerical integration based method* – Dimension reduction (DR) ([96, 71, 95, 94, 43]) is one common method of this category, which deals with high dimension numerical integration.

*Reliability and Robustness Integration*

Multi-objective optimization is one approach to integrate reliability and robustness. Li presented a robust multi-objective genetic algorithm (RMOGA) in [47], in which a robustness index was proposed to measure robustness; Mourelatos provided a probabilistic multi-objective optimization problem in [60], where variation was expressed in terms of a percentile difference. Another approach in [2] is to use a weighted sum single objective optimization to improve reliability and robustness.

# CHAPTER 2

# EPISTEMIC UNCERTAINTY IN PRODUCT DESIGN OPTIMIZATION

## 2.1 Introduction

RBDO considers various types of uncertainties during the process of product design and production. As mentioned in Chapter 1, uncertainties to be considered at a product's design stage can be categorized into aleatory uncertainties (AU) and epistemic uncertainties (EU) [41]. This chapter focuses on the impact of EU on RBDO. Also uncertainty sources of EU are categorized and methods are summarized to address two important types of EU in RBDO.

To deal with the epistemic uncertainty of unknown distributions of design variables, two methods are typically employed as mentioned in Section 1.1. One method is the possibility and evidence theory. The other method is statistical inference approach. For the epistemic uncertainty of unknown or implicit product's performance function. RSM and Kriging model are two commonly used Metamodels to approximate true functions.

The remaining chapter is organized as follows: Section 2.2 reviews basic concept and formulation of RBDO. Section 2.3 proposes the uncertainty sources of EU and assesses their impacts on RBDO. Section 2.4 presents several effective strategies for tackling the RBDO problem with EU. Section 2.5 provides an I-beam case study to illustrate the effect of EU on RBDO.

## 2.2 Reliability-Based Design Optimization

In product design under uncertainty, RBDO is employed to maintain design feasibility, which is shown in Formulation 1.2 to 1.4. The uncertainties as represented by random variables and probabilistic constraints are aleatory uncertainties. In reality, however, epistemic uncertainties always exist due to lack of knowledge of the

variables and processes of the system. They could be reduced by understanding the design or by obtaining more relevant data. The RBDO formulation can be rewritten in different form according to the type of epistemic uncertainty.

For the epistemic uncertainty of unknown random variable's distribution, the RBDO formulation becomes:

$$\text{Minimize: } f(\mathbf{d}, \mu_{\mathbf{X}}, \mu_{\mathbf{Y}}, \mu_{\mathbf{P}}) \tag{2.1}$$

$$\text{Subject to: } P_{\hat{\mathbf{Y}}}\{P_{\mathbf{X}}[G_i(\mathbf{d}, \mathbf{x}, \mathbf{p}) \geq 0] \geq R_i\} \geq 1 - \alpha_i, \quad i = 1, 2, \ldots, m \tag{2.2}$$

$$\mathbf{d}^{\mathbf{L}} \leq \mathbf{d} \leq \mathbf{d}^{\mathbf{U}}, \mu_{\mathbf{X}}^{\mathbf{L}} \leq \mu_{\mathbf{X}} \leq \mu_{\mathbf{X}}^{\mathbf{U}}, \mu_{\mathbf{Y}}^{\mathbf{L}} \leq \mu_{\mathbf{Y}} \leq \mu_{\mathbf{Y}}^{\mathbf{U}}, \mu_{\mathbf{P}}^{\mathbf{L}} \leq \mu_{\mathbf{P}} \leq \mu_{\mathbf{P}}^{\mathbf{U}} \tag{2.3}$$

where $\mathbf{x}$ denotes the vector of aleatory random variables with complete information and their distribution are known; the vector $\hat{\mathbf{y}}$ denotes the vector of epistemic random variables with incomplete information and their distribution or parameters are estimate based on limited samples. Thus a double-loop probabilistic constraint is derived, in which the inner loop is due to aleatory variable $\mathbf{x}$ and the outer loop is due to epistemic variable $\hat{\mathbf{y}}$. The outer loop demands that the confidence level of the design satisfying the reliability constraint for the given information of the epistemic variable is at least $(1 - \alpha_i)\%$.

For the epistemic uncertainty of implicit constraint function, the RBDO formulation becomes:

$$\text{Minimize: } f(\mathbf{d}, \mu_{\mathbf{X}}, \mu_{\mathbf{P}}) \tag{2.4}$$

$$\text{Subject to: } P_{\hat{G}}\{P_{\mathbf{X}}[\hat{G}_i(\mathbf{d}, \mathbf{x}, \mathbf{p}) \geq 0] \geq R_i\} \geq 1 - \alpha_i, \quad i = 1, 2, \ldots, m \tag{2.5}$$

$$\mathbf{d}^{\mathbf{L}} \leq \mathbf{d} \leq \mathbf{d}^{\mathbf{U}}, \mu_{\mathbf{X}}^{\mathbf{L}} \leq \mu_{\mathbf{X}} \leq \mu_{\mathbf{X}}^{\mathbf{U}}, \mu_{\mathbf{P}}^{\mathbf{L}} \leq \mu_{\mathbf{P}} \leq \mu_{\mathbf{P}}^{\mathbf{U}} \tag{2.6}$$

where $\hat{G}_i$ is a metamodel of system performance function, which is constructed based on the results of computer experiments, and it is used to approximate the

constraint function. Therefore a double-loop probabilistic constraint is obtained, in which the inner loop is due to aleatory uncertainty and outer loop is due to epistemic uncertainty of modeling error.

Solving an RBDO problem requires two loops - the optimization loop and the reliability assessment loop. The nested loops problem could be computationally intensive. In particular, the latter loop involves rare event probability evaluation. To have a balanced trade-off between efficiency and accuracy, many approaches such as the double-loop methods, decoupled-loop methods and single-loop methods are developed and applied. In this chapter we choose the SORA method which is a decoupled-loop method. Our focus is to evaluate the impact of EU on RBDO using the SORA method.

## 2.3 Epistemic Uncertainty in RBDO

### *Sources of Uncertainties*

Engineers have to face uncertainties from different sources during the product design and manufacturing process. A natural distinction between these AU and EU does not always exist. Perhaps it is just a matter of time to obtain enough information about missing variables and learn model formulation. In such a world, if uncertainty exists, it will only be aleatory.

In the context of the problem mentioned above, uncertainty sources can be identified as follows [41, 9]:

1. *Uncertainty from material property and operating conditions change* – This is the uncertainty inherent in material property, operation environment, and it can be categorized to aleatory uncertainty. Examples are material properties drift, operating temperature, pressure, humidity, etc. They can be expressed

by random parameter $\mathbf{p}$ in objective or constraint function. However, when these uncertainties cannot be fully characterized due to lack of data, they become epistemic.

2. *Imprecise production* – The design parameter in production and manufacturing can only be achieved to a certain degree of accuracy, as high precision machinery naturally leads to high manufacturing expense. To a design engineer, these manufacturing errors are often unknown; thus this kind of uncertainty belongs to epistemic uncertainty. It is typically represented by the perturbations of the design variable $\mathbf{x}$, i.e. $f = f(\mathbf{x}+\delta,\mathbf{p})$ and $G = G(\mathbf{x}+\delta,\mathbf{p})$. Note that if the manufacturing errors are adequately studied and modeled in the design process, they will become aleatory uncertainties as some random parameters.

3. *Uncertainties in modeling and measurement* – This type of uncertainty includes modeling errors and measurement errors, which belongs to epistemic uncertainty. Modeling errors result from employing empirical model instead of the true model. Measurement errors may include the errors involved in indirect measurement. This type of uncertainty is expressed by the approximated function $\hat{f}(\mathbf{x},\mathbf{p})$ and $\hat{G}(\mathbf{x},\mathbf{p})$.

4. *Uncertainty from computational errors, numerical approximations or truncations* – One example is the computational error in a finite element analysis of load effects in a high nonlinear structure [41]. Another example is the mesh size and convergence stopping criterion settings. They are aleatory in nature.

5. *Uncertainty from human activities and decisions* – Human errors, such as unintentional errors in design, modeling and operations, are inherent in nature and can be categorized as aleatory uncertainty.

*Categorizing Epistemic Uncertainty*

Epistemic uncertainty typically arises from an absence of information or data, which causes vagueness in parameter definition, simplification and idealization in system modeling, as well as subjection in numerical implementation. Three categories of epistemic are included in [32] as follows:

1. *Lack of knowledge or vagueness,* e.g. unknown random variable's distribution type and distribution parameters due to sparse or imprecise information (i.e. sparse point data or interval data) regarding to stochastic quantity.

2. *Errors or defects in modeling*, e.g. systems' performance function is implicit or can only capture part of the real system. It includes the idealization or simplification due to a linearization of the model equations or the assumption of linear model behavior, etc.

3. *Subjectivity in implementation*, e.g. the selection of different methods of numerical evaluation by using different finite element solvers and mesh refinement, expert judgment about an uncertain parameter, etc.

*Impacts of Epistemic Uncertainty on RBDO*

In this section, we mainly discuss the first two types of epistemic uncertainty and their impacts on RBDO.

Probabilistic constraint evaluation is the critical piece in RBDO. By the SORA decoupled-loop method, once an optimal solution $\mu$ is derived from the optimization loop, the corresponding MPP [33] is calculated and evaluated in the reliability assessment loop. If MPP is feasible, $\mu$ is the optimal solution; if MPP is infeasible, it enters the next iteration in SORA. However, the derived MPP could

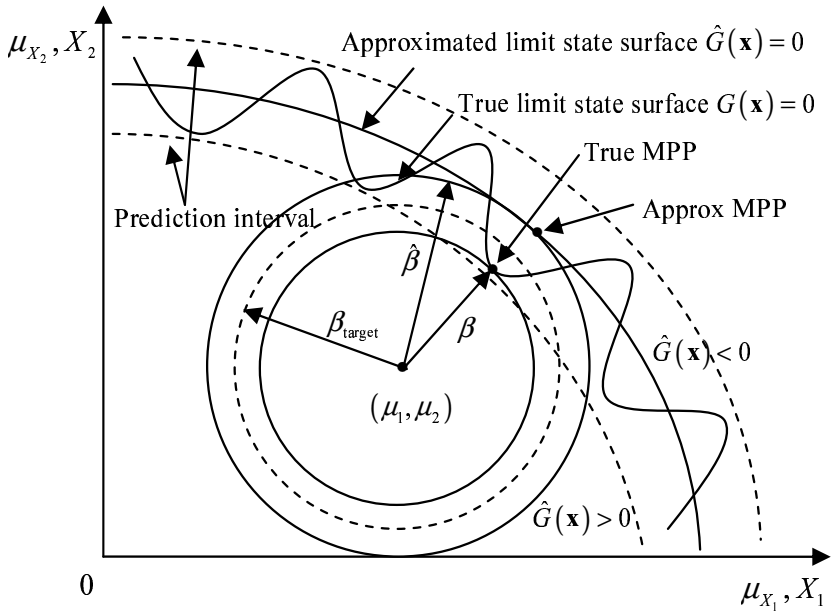


Figure 2.Implicit constraint function infeasible impact

not be accurate enough under epistemic uncertainty. The approximated MPP could be either infeasible or too conservative.

(1) Implicit constraint function

Suppose the analytical performance function G unavailable, but it can be evaluated by a computer model. Then samples are taken from computer experiments and G is replaced by a metamodel $\hat{G}$. According to RIA in reliability analysis, MPP is the point which locates on the limit state surface G with the smallest distance to $\mu$. Since G is replaced by metamodel $\hat{G}$, true MPP is replaced by approximated MPP. Therefore epistemic uncertainty of implicit constraint function will lead to either infeasible or conservative optimal solution.

In Fig. 2, the approximated MPP leads to a reliability index $\hat{\beta}$ which is evaluated to be greater than $\beta_{\text{target}}$. Thus the SORA algorithm stops and current $\mu$ is selected as the optimal solution. However, the true reliability index is proved to

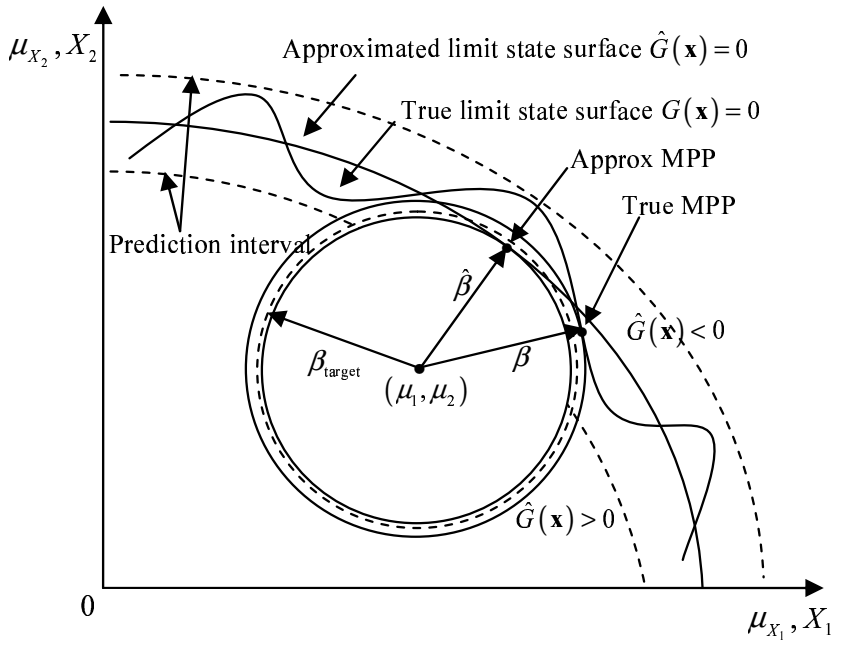


Figure 3.Implicit constraint function conservative impact

less than $\beta_{\text{target}}$, which means the current $\mu$ is actually an infeasible solution.

In Fig. 3, current approximated MPP leads to a reliability index $\hat{\beta}$ which is evaluated to be less than $\beta_{\text{target}}$. Thus SORA enters next iteration to resolve the optimization loop and obtain a more conservative solution. Actually the true reliability $\hat{\beta}$ is proved to be greater than $\beta_{\text{target}}$, and current optimal solution $\mu$ is a feasible optimal solution. In this case, epistemic uncertainty leads to a conservative solution.

(2) Unknown random variable distribution

Suppose we can assume the design variable **x** follows normal distribution with unknown parameter $\sigma$. Then a set of samples are taken to derive a parameter estimate $\hat{\sigma}$. Based on the first-order Taylor expansion, $\hat{\sigma}$ can be derived.

According to the definition of reliability index $\beta = \frac{\mu_G}{\sigma_G}$. In reliability index

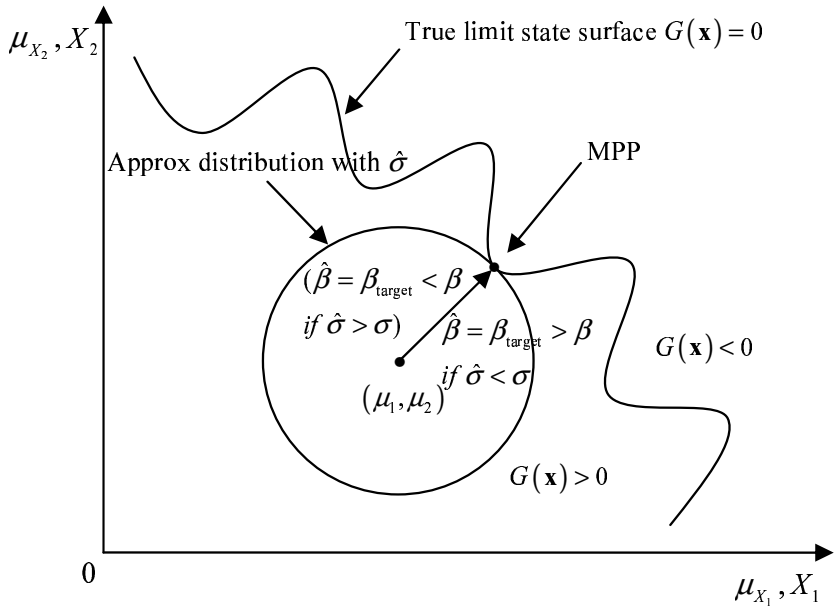


Figure 4.Unknown random variable distribution impact

analysis method, the safety constraint is satisfied if $\beta \geq \beta_{\text{target}}$. However, under unknown variable distribution, $\hat{\beta} = \frac{\mu_G}{\sigma_G}$ may not be accurate enough. It could be either infeasible or conservative.

As shown in Fig. 4, an optimal solution $\mu$ is derived with the reliability index $\beta = \beta_{\text{target}}$. Thus it is a feasible RBDO optimal solution. However, since the estimate $\hat{\sigma}$ is less than true parameter $\sigma$, the true $\beta$ is smaller than $\hat{\beta}$. Thus the optimal solution derived here is actually infeasible. On the other hand, if the estimate $\hat{\sigma}$ is greater than true parameter $\sigma$, true $\beta$ is greater than $\hat{\beta}$. Thus the optimal solution derived is too conservative comparing with the true optimal solution.

## 2.4 Epistemic Uncertainty Strategy in RBDO

### *Implicit Constraint Function*

To address epistemic uncertainty of implicit constraint function, a typical two-step strategy is developed: First, metamodels are constructed based on the initial sam-

ples given by computer experiments. Then additional samples are selected and added to update the metamodel step by step until the accuracy stopping criterion is satisfied.

In metamodel selection, three typical metamodels are employed: polynomial model, radial basis function model and Kriging model. Polynomial model is a widely employed parametric model since it is easy to implement. Better performance is expected for low order response functions. However, less efficiency and large computation work are expected when it is applied to problems with highly non-linear and irregular performance functions. Radial basis function (RBF) is a commonly used nonparametric model. It is a real-valued function whose value depends only on the distance from some other point c, called a center, so that $\phi(\mathbf{x},\mathbf{c}) = \phi(\|\mathbf{x}-\mathbf{c}\|)$. Kriging model is a semi-parametric model which allows much more flexibility than parametric models since no specific model structure is used. It contains a linear regression part (parametric) and a non-parametric part considered as the realization of a random process. Thus Kriging model can capture the nonlinear and irregular function shape well and requires fewer sample points.

Typically RBDO accuracy largely depends on whether the Kriging model can capture the general tendencies of the design behavior. In order to enhance the metamodel accuracy, additional samples are selected step by step to update the metamodel. The procedure ends until a stopping criterion is satisfied. Many accuracy metrics and algorithm criteria are proposed, for examples, R square metric, rooted mean square error (RMSE), relative absolute max error (RAME), maximum absolute error (MAXERR), etc.

Table 1.Approaches for Unknown Distribution

| Epistemic uncertainty with unknown distribution | | | |
|---|---|---|---|
| Fit distribution | | Do not fit distribution | |
| Bayesian approach Youn (2008) | Assume $N(\mu, \sigma^2)$ with unknown $\sigma$ Picheny (2007) | Interval variables Du (2005) | Decision framework Samson (2009) |

*Unknown Random Variable Distribution*

Some distribution fitting is typically used to characterize the unknown random variable distribution. The goodness of fit largely depends on the quality of the available data of the variable.

To address RBDO with unknown variable distribution, the approaches appeared in literature are summarized in Table 1:

The first category of approach is to fit a distribution of epistemic variable:

(1) A Bayesian inference approach is employed in [93]. Since distribution parameters $\theta$ are unknown under epistemic uncertainty, Bayes' theorem is used to estimate parameters as:

$$f(\theta|\mathbf{x}) = f(\mathbf{x}|\theta)f(\theta)/c \tag{2.7}$$

where $f(\theta|\mathbf{x})$ is the posterior PDF of $\theta$ conditional on the observed data $\mathbf{x}$, $f(\mathbf{x}|\theta)$ is the likelihood of observed data $\mathbf{x}$ conditional on $\theta$, and $f(\theta)$ is the prior PDF of $\theta$. Under unknown parameters, the failure probability P or reliability R becomes a random variable which is bounded between 0 and 1. Thus uniform distribution is selected as the prior distribution of P, and the posterior distribution is a Beta distribution.

(2) Another approach is to assume normal distribution, and estimate parameter based on the provided data. In [70], an empirical CDF is first built as:

$$F_X(x) = \begin{cases} 0, & \text{for } x \geq x_1; \\ (k-0.5)/n, & \text{for } x_k \leq x \leq x_{k+1}; \\ 1, & \text{for } x_n \leq x. \end{cases} \tag{2.8}$$

An RMSE criterion is employed to calculate the unknown parameter $\sigma$ by solving the following optimization problem:

$$\text{Minimize: } \sqrt{\frac{1}{n}\sum_{k=1}^{n}\left[F(x_k) - \frac{k-0.5}{n}\right]^2} \tag{2.9}$$

The second category is to treat epistemic variable as interval variables or constants instead of fitting distributions, which is used in the case of very few data. In [26] epistemic variables are treated as interval variables without assuming any probability distribution. Under the worst case combination of interval variables, RBDO is solved with only aleatory variables. In [74] continuous epistemic uncertainty intervals are first discretized into $n$ scenarios, then a decision framework is proposed to the best scenario with only aleatory uncertainty.

## 2.5 I-Beam Example

To design an I-beam [75], two design variables $X_1$ and $X_2$ are geometric parameters of the cross-section as shown in Fig. 5. Due to manufacturing variability, we treat these two variables as random variables and assume they are normally distributed with $\sigma_1 = 2.025$ and $\sigma_2 = 0.225$. The beam is loaded by the mutually independent vertical and lateral loads parameters $P \sim N(600, 10)KN$ and $Q \sim N(50, 1)KN$. The maximum bending stress of the beam is $\sigma = 16kn/cm^2$, the target reliability index $\beta = 3(R = 99.87\%)$.

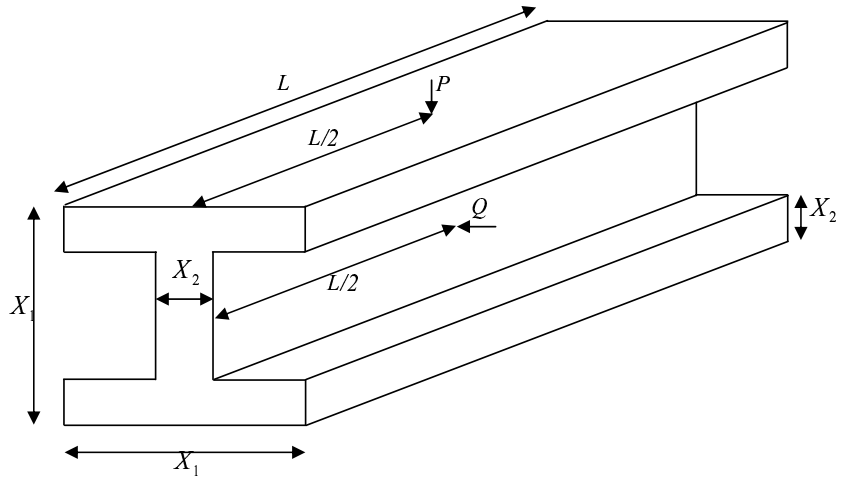


Figure 5.I-beam case study

The objective is the production cost which is the weight of the beam. Assuming the beam length and the material density are constants, minimizing this function is equivalent to minimizing the cross-section area, $f(\mathbf{x}) = 2x_1x_2 + x_2(x_1 - 2x_2)$. Since $x_1$ and $x_2$ are random variables, the cost function $f(\mu) = 2\mu_1\mu_2 + \mu_2(\mu_1 - 2\mu_2) = 3\mu_1\mu_2 - 2\mu_2^2$ is derived. The single probabilistic constraint is given as $P(G(x_1,x_2) \geq 0) \geq R$, where $G(x_1,x_2)$ is the bending threshold subtracted by actual bending stress, so $G(x_1,x_2) \geq 0$ denotes the feasible region. The analytical $G$ function is available as

$$G(x_1,x_2) = \sigma - (\frac{M_Y}{Z_Y} + \frac{M_Z}{Z_Z}) \tag{2.10}$$

$$\frac{M_Y}{Z_Y} + \frac{M_Z}{Z_Z} = \frac{0.3px_1}{x_2(x_1-2x_2)^3 + 2x_1x_2(4x_2^2 + 3x_1^2 - 6x_1x_2)} + \frac{0.3qx_1}{(x_1-2x_2)x_2^3 + 2x_2x_1^3} \tag{2.11}$$

For the purpose of simplicity, the random parameters $P$ and $Q$ and equal to their mean values, respectively. The effects of the two types of epistemic uncertainty on the RBDO solution in this example are discussed in the following.

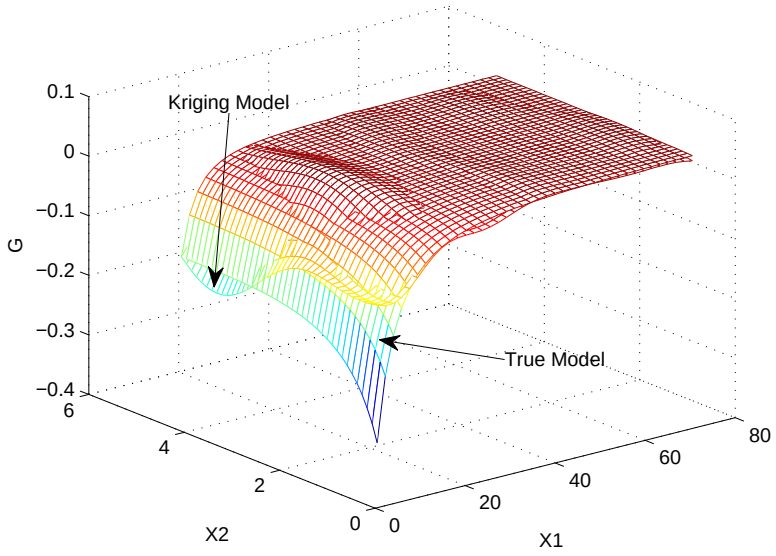


Figure 6.Implicit constraint function impact on I-beam

Table 2.Epistemic Uncertainty Impact on I-Beam Case

| | $(\mu_1, \mu_2)$ | Objective |
|---|---|---|
| True G and $\sigma$ | (49.7275, 0.9173) | 135.1594 |
| Kriging model | (52.8422, 1.0603) | 168.8332 |
| Estimate $\hat{\sigma}$ | (53.8285, 0.9599) | 153.1716 |

*Effects of Implicit Constraint Functions*

For the purpose of comparison, true G function is assumed to be implicit. A Latin hypercube design is employed to select 29 sample points to construct the Kriging model, which is used to approximate the true model. The comparison between true model and Kriging model is shown in Fig. 6. Then RBDO is solved with both true constraint function and Kriging model, and results comparison is in Table 2. From Table 2 we conclude that the optimal solution under Kriging model is too conservative comparing with true optimal solution.

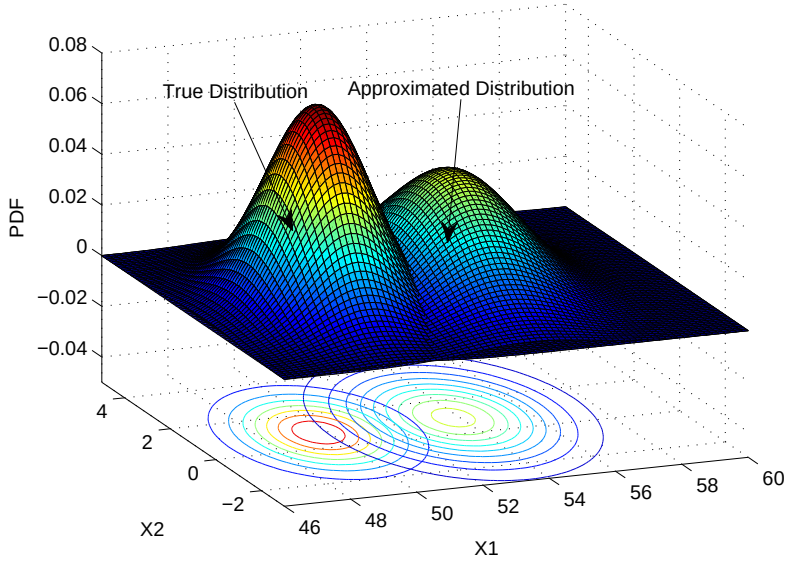


Figure 7.Unknown distribution impact on I-beam

*Effects of Unknown Random Variable Distributions*

For the purpose of comparison, design variable's distribution is assumed to be unknown. Taken from the existing I-beam designs, 29 samples are selected above to estimate $\sigma_1$ and $\sigma_2$ based on the RMSE criterion.

The results are $\hat{\sigma}_1 = 3.380$ and $\hat{\sigma}_2 = 0.312$, respectively. Then RBDO is solved with both the true $\sigma$ and the estimate $\hat{\sigma}$, and their optimal solutions are compared in Table 2. The comparison between true distribution and estimate distribution at optimal solution is shown in Fig. 7. Thus we can see that the optimal solution under estimate $\hat{\sigma}$ is more conservative than true optimal solution.

## 2.6 Conclusion

In this chapter, epistemic uncertainties and their impacts on RBDO are discussed. We first review the generic formulation of RBDO, then extend it to take into account of epistemic uncertainties due to unknown random variable distributions and

implicit constraint functions.

Secondly, the sources of epistemic uncertainties are explained, and their impacts on the RBDO solution are discussed. Comparing with the true RBDO optimal solution, the solution for the problem where epistemic uncertainty exists can be either infeasible or too conservative. To address the issues with epistemic uncertainties, we summarize several approaches in literature.

Finally, an I-beam example is used to illustrate the effects of the two types of epistemic uncertainty on RBDO solution.

# CHAPTER 3

# A SEQUENTIAL SAMPLING STRATEGY TO IMPROVE RELIABILITY-BASED DESIGN OPTIMIZATION WITH IMPLICIT CONSTRAINT FUNCTIONS

## 3.1 Introduction

As mentioned in Section 1.4, to trade off between the efficiency and accuracy of the solution to an RBDO problem, many approaches such as the double-loop method [13], decoupled-loop method [23] and single-loop method are developed [78, 48, 76]. However, all these approaches are based on the assumption that the constraint functions, $G_i$'s, are given analytically. Our focus in this chapter is to develop a decoupled-loop RBDO approach with implicit constraint functions, i.e., black-box constraints.

In this chapter we employ the Kriging method as the metamodeling method for the implicit constraint function. Consequentially, we need to consider how to take efficient samples to fit and update the metamodel, as the accuracy of metamodel largely depends on the choice of sample points. The more samples we have, in general, the more accurate model can be derived. However, in reality computer experiments could be very expensive and time-consuming, so taking a lot of sample points is unaffordable. Some common sampling methods such as Latin Hypercube experimental design, uniform experimental design has been employed in RBDO for implicit constraints. For examples, in [39] a maximum mean square sampling technique was employed; [45] provided a constraint boundary sampling strategy to enhance accuracy and efficiency of metamodel based on the RIA in RBDO; [10, 11, 12] proposed the efficient global reliability analysis (EGRA), in which an expected feasibility function criterion was used to add samples to obtain an accurate limit state function, then the reliability analysis was implemented by im-

portance simulation; in [8, 5, 6, 7] DOE was performed to generate initial samples and support vector machine (SVM) algorithm was employed to derive the failure domain boundary; and in [3] SVM was also used to calculate failure probabilities in RBDO. In addition, to better approximate the limit state function, methods such as polynomial chaos expansion (PCE, [85]), adaptive-sparse PCE ([34]), asymmetric dimension-adaptive tensor-product (ADATP, [35]) and sparse grid interpolation (SGI, [86]) have been developed for stochastic response surface.

In this chapter, we propose a sequential maximum expected improvement sampling strategy based on the PMA. In the PMA, the reliability assessment step is replaced by a process of minimizing the R-percentile derived from the constraint function. Since the true constraint function is implicit and a metamodel is used, we employ an expected improvement criterion to propose additional sampling points so as to update the metamodel and to locate the global minimum R-percentile.

Our research contributions include: First, an integrated scheme of the decoupled loop approach and the sequential sampling of implicit constraints is proposed. Our method is different from other existing methods in that we use the PMA for reliability assessment and our sequential sampling strategy focuses on the MPP approximation instead of the entire limit state function or the whole response surface of the constraint function. Secondly, we extend our method to handle multiple implicit constraints, and compare the efficiency and accuracy of several competitive methods.

The rest of the chapter is organized as follows: Section 3.2 introduces SORA method and the metamodeling technique employed in the chapter. Section 3.3 proposes a sequential maximum expected improvement sampling strategy and compare with other strategies to update Kriging model. Section 3.4 presents

an I-beam case study to illustrate the efficiency and accuracy of proposed methods. Section 3.5 provides another engineering demo to show the extension of our method to the RBDO problem with multiple probabilistic constraints. Finally, Section 3.6 gives the discussion and conclusion.

## 3.2 Reliability Analysis in RBDO

It is well known that uncertainty is inevitable in engineering design. Traditional RBDO deals with this type of uncertainty. That is, it tries to optimize designs when some design variables are random with assumed distributions. Epistemic uncertainty deals with lack of knowledge. For example, the random variable's distribution is unknown [64] or the system's performance function is implicit due to lack of knowledge. In this chapter, we study the latter case, where there is not an analytical function to explicitly describe system's performance, i.e., the $G$ function in Formulation 1.3 is unknown, so we construct a metamodel, $\hat{G}$, based on computer experiments.

In this section we briefly review the approaches to solving RBDO problems with known constraint functions. Due to the existence of uncertainty, a design solution based on the deterministic approach could be too conservative. Ref. [22] summarized some reliability analysis approaches.

### *First-Order Reliability Analysis in RIA and PMA*

RIA and PMA are two common reliability assessment approaches. These approaches employ the concepts of the reliability index ([28, 97]) and the MPP ([33]). Assuming the output of performance function $G_i$ follows normal distribution, the probabilistic constraint function can be characterized by the cumulative distribution func-

tion $F_{G_i}(0)$ and the target reliability index $\beta_i$ as follows:

$$\begin{aligned} Prob[G_i(\mathbf{d},\mathbf{x},\mathbf{p}) \geq 0] &= \int_0^\infty \frac{1}{\sqrt{2\pi}} exp[-\frac{1}{2}(\frac{g_i-\mu_{G_i}}{\sigma_{G_i}})^2] d(\frac{g_i-\mu_{G_i}}{\sigma_{G_i}}) \\ &= \int_{-\beta_i}^\infty \frac{1}{\sqrt{2\pi}} exp(-\frac{1}{2}t^2) dt \\ &= 1-\Phi(-\beta_i) = \Phi(\beta_i) \end{aligned} \tag{3.1}$$

where $t = \frac{g_i-\mu_{G_i}}{\sigma_{G_i}}$ and $\beta_i = \frac{\mu_{G_i}}{\sigma_{G_i}}$. Here, $\beta_i$ is defined as the safety index or reliability index of the $i^{\text{th}}$ constraint, and $\mu_{G_i} = \beta_i \sigma_{G_i}$ indicates that a reliability index measures the distance between the mean margin and the limit state surface, as we may consider $\sigma_{G_i}$ as a constant scale parameter. For simplicity, we will remove the index $i$ and consider only the deterministic vector $\mathbf{d}$ and random design vector $\mathbf{x}$ in our later discussion.

In the Hasofer and Lind approach [33], the original random vector $\mathbf{x}$ is transformed into an independent and standardized normal random vector $\mathbf{u}$. MPP becomes a point on the limit state surface in the U-space that has the minimum distance to the origin, and $\beta$ is this minimum distance. MPP represents the worst case on the limit state surface; i.e., if MPP can satisfy the required reliability level, so does any other point on the limit state surface. Therefore, the probabilistic constraint evaluation can be converted to an optimization problem to find the MPP and the reliability index. The probabilistic constraint can be expressed through inverse transformation in two alternative ways, leading to two different optimization problems.

In the RIA([53, 29, 84]), the reliability assessment becomes the reliability index assessment such as

$$\beta = -\Phi^{-1}(F_G(0)) \geq \beta_{\text{target}} \tag{3.2}$$

In the U-space, the following optimization problem is solved to find the MPP and $\beta$:

$$\begin{aligned} &\text{Minimize } \| \mathbf{u} \| \\ &\text{Subject to } G(\mathbf{u}) = 0 \end{aligned} \tag{3.3}$$

where the optimal solution on the limit state surface ($G(\mathbf{u}) = 0$) is the MPP in the U-space and $\beta = \| \mathbf{u} \|_{\text{MPP}}$.

In the PMA([84, 17, 24]), the reliability assessment is converted to the R-percentile assessment such as

$$G^R = F_G^{-1}(\Phi(-\beta_{\text{target}})) \geq 0 \tag{3.4}$$

where $G^R$ is the R-percentile of $G(\mathbf{d}, \mathbf{x})$ and $P(G(\mathbf{d}, \mathbf{x}) \geq G^R) = R$. In the U-space, an optimization problem is employed to find the most probable point of inverse reliability (MPPIR) [25] and the minimum R-percentile, i.e.,

$$\begin{aligned} &\text{Minimize } G(\mathbf{u}) \\ &\text{Subject to } \| \mathbf{u} \| = \beta_{\text{target}} \end{aligned} \tag{3.5}$$

where the optimal solution on the targeted reliability surface is the MPPIR. MPPIR is the point on the target reliability level which has the smallest performance function value in the U-space, and $G^R = G(\mathbf{u}_{\text{MPPIR}})$.

*Sequential Optimization and Reliability Analysis (SORA)*

Du [24] developed the SORA method for efficiently solving RBDO problems, in which the nested-loop of optimization and reliability assessment steps are replaced by two decoupled-loop steps. SORA employs a series of cycles of optimization and reliability assessment. In each cycle an equivalent deterministic optimization problem is solved first, and a design variable $\mu_X$ is proposed. Then the X-space is

transformed to the U-space based on $\mu_X$ and $\sigma_X$, and the MPP(or MPPIR) is found by the PMA optimization method. Next, the current MPP is checked against the R-percentile constraints of each performance function $G_i$. If $G_i^R = G_i(\mathbf{d}, \mathbf{x}_{\text{MPP}}) \geq 0$, design variable $\mu_X$ is feasible and it is the final solution; otherwise, a shifting vector is derived to modify the current decision variable.

For the deterministic optimization in the first cycle, there is no information about the MPP, so the values of $\mathbf{x}_{\text{MPP}}$ are conveniently set as the means of the random variable. The deterministic optimization model in the first cycle becomes

$$\begin{aligned} &\text{Minimize } f(\mathbf{d}, \mu_{\mathbf{X}}) \\ &\text{Subject to } G_i(\mathbf{d}, \mu_{\mathbf{X}}) \geq 0 \quad i = 1, 2, \ldots, m \end{aligned} \tag{3.6}$$

The solution of 3.6 is fed into 3.5 to find the MPP. Let $\mathbf{s}$ denote the shifting vector, the new constraint in the deterministic optimization in next cycle is reformulated as

$$G_i(\mathbf{d}, \mu_{\mathbf{X}} - \mathbf{s}^{(2)}) \geq 0 \quad i = 1, 2, \ldots, m \tag{3.7}$$

where $\mathbf{s}^{(2)} = \mu_{\mathbf{X}}{}^{(1)} - \mathbf{x}_{\text{MPP}}^{(1)}$. The process will continue until the R-percentile $G^R(\mathbf{d}, \mathbf{x}_{\text{MPP}}) \geq 0$.

*Metamodeling Techniques and Comparisons*

When the performance function $G$ is a computer model, we sample it by conducting computer experiments and replace $G$ by a metamodel $\hat{G}$. Due to limited sampling points, it is critical to select a good surrogate function to fit computer outputs. Polynomial model and Kriging model are presented and compared in this section.

As mentioned in [37], polynomial functions are widely employed as metamodels. The sample size is suggested to be two or three times the number of model

parameters. However, the number of parameters of the polynomial model will increase dramatically as the order of the model increases. Due to the cost and computation limitation, quadratic and cubic polynomial models are typically suggested. In many engineering design problems, however, high nonlinearity and twisting may happen such that even the cubic polynomial model cannot capture the performance variation well. In addition, polynomial models are not robust to outliers.

Kriging model (also called Gaussian process, or GP, model), firstly proposed by a South African geo-statistician Krige [73], is a suitable model for modeling computer experiments. In a Kriging model, the response at a certain sample point not only depends on the settings of the design parameters, but is also affected by the points in its neighborhood. The spatial correlation between design points is considered. A Kriging model combines a polynomial function for the output means and a random process for the output variance, and it is given as follows ([54]):

$$\hat{y} = \beta_0 + \sum_{j=1}^{k} \beta_j f_j(x_j) + Z(x) \tag{3.8}$$

where $\beta_0 + \sum_{j=1}^{k} \beta_j f_j(x_j)$ is the polynomial component and $Z(x)$ is the random process. Typically, the polynomial component is reduced to $\beta_0$, and the random process $Z(x)$ is assumed to have a zero mean and a spatial covariance function between $Z(x_i)$ and $Z(x_j)$ is

$$\begin{aligned} Cov[Z(x_i), Z(x_j)] &= E[Z(x_i)Z(x_j)] - E[Z(x_i)]E[Z(x_j)] \\ &= \sigma^2 R(\theta, x_i, x_j) \end{aligned} \tag{3.9}$$

where $\sigma^2$ is the process variance and $R(\theta, x_i, x_j)$ is the correlation model with parameters $\theta$. The correlation model may have one of several different kernel func-

tions. For details, refer to, e.g., [73, 54].

In a Kriging model, the number of parameter can be reduced to the dimension of input vector, which is much fewer than the cubic polynomial model, so fewer samples are needed for building a robust Kriging model. In addition, Kriging model is suitable for modeling high nonlinearity and twisty because of the flexibility of the correlation function. Hence, Kriging model $\hat{y} = \beta_0 + Z(x)$ is selected in this chapter.

## 3.3 Sequential Expected Improvement Sampling

The sampling strategy for deriving the metamodel $\hat{G}$ needs to be carefully constructed, as in RBDO we must consider the additional epistemic uncertainty brought by the constraint function estimation; otherwise, the optimal solution obtained may be actually infeasible because $\hat{G}$ is not the true function. As we know, reliability assessment in the RBDO solution is equivalent to the MPP optimization, thus our strategy is to deploy more samples subject to the MPP constraint so that the metamodel becomes more accurate in the area of the most importance to RBDO. In this section, we present a sequential sampling strategy based on a criterion called expected improvement (EI).

### *Initial Latin Hypercube Sampling*

The statistical method of Latin hypercube sampling (LHS) is employed in this chapter for initial sampling to build a Kriging model. LHS was first described in [56], and was further elaborated in [36]. LHS is particularly good for sampling a complex computer model that is computationally demanding and expensive.

### *Expected Improvement Criterion*

A metamodel $\hat{G}$ is constructed based on initial samples. If the input space was entirely sampled, then $\hat{G}$ surface would get close enough to the true surface; however,

as only a few samples are obtained in reality, $\hat{G}$ surface is different from the true surface. In addition, the prediction error by $\hat{G}$ is different from area to area on the metamodel surface. Some areas have larger prediction errors than others because they have fewer sample points in the neighborhood. Therefore, the area with large prediction error has the potential of containing the true MPP, instead of the current minimum point. In other words, the area with large prediction error is less explored and may bring bigger improvement to the metamodel if additional samples are taken in this area. Thus, we use the EI as the criterion for adding the next sampling point.

The EI criterion proposed by [38] is computed as follows. Suppose there are $n$ initial samples, and $G^{(1)},\ldots,G^{(n)}$ are the outputs by the computer model. Let $G_{\min}=\min(G^{(1)},\ldots,G^{(n)})$ be the current minimum. The improvement at a point $\mathbf{x}$ towards the global minimum is $I(\mathbf{x})=\max(G_{\min}-G(\mathbf{x}),0)$, where $G(\mathbf{x})$ follows a normal distribution, $N(\hat{G}(\mathbf{x}),s^2(\mathbf{x}))$, and $\hat{G}$ and $s$ denote the Kriging predictor and its standard error. The expected improvement is

$$E[I(\mathbf{x})]=E[\max(G_{\min}-G,0)] \tag{3.10}$$

In RBDO, we often need to consider more than one constraints. In order to compare EIs from different constraints and to select the additional sample point with the maximum EI, we propose an expected relative improvement criterion as follows:

Let $RI=max(\frac{G_{\min}-G}{G_a},0)$, where $G_a=\frac{|G^{(1)}|+\cdots+|G^{(n)}|}{n}$. The expected relative improvement (ERI) is

$$E[RI(\mathbf{x})]=E[\max\Big(\frac{G_{\min}-G}{G_a},0\Big)] \tag{3.11}$$

After applying integrations, we have

$$E[RI(\mathbf{x})] = \frac{1}{G_a}[(G_{\min} - \hat{G})\Phi\Big(\frac{G_{\min} - \hat{G}}{s}\Big) + s\phi\Big(\frac{G_{\min} - \hat{G}}{s}\Big)] \tag{3.12}$$

where $\Phi(\cdot)$ and $\phi(\cdot)$ denote the cumulative distribution function and the probability density function of standard normal distribution, respectively.

The definition of ERI indicates that both the Kriging predictor $\hat{G}$ and its standard error $s$ can affect the ERI value. Taking the derivative of ERI with respect to $\hat{G}$ and $s$, we can derive the following properties:

$$\frac{\partial E[RI]}{\partial \hat{G}} = -\frac{1}{G_a}\Phi\Big(\frac{G_{\min} - \hat{G}}{s}\Big) < 0 \tag{3.13}$$

$$\frac{\partial E[RI]}{\partial s} = \frac{1}{G_a}\phi\Big(\frac{G_{\min} - \hat{G}}{s}\Big) > 0 \tag{3.14}$$

Due to the monotonicity, we conclude that a larger standard error ($s$) or a larger difference between the current minimum and the prediction $(G_{\min} - \hat{G})$ will lead to a larger expected relative improvement value.

*RBDO Solution Using Sequential ERI-Based Sampling Strategy*

Based on the PMA mentioned above, Formula 3.5 is used to find the MPP and check the R-percentile, which is equivalent to reliability assessment. In this chapter, we maximize the ERI to find new sample points because they are the best for searching for $G$'s minimum value when the true function of $G$ is unknown or implicit. Note that the optimization Formula 3.5 is a constrained optimization, where the feasible $\mathbf{u}$ points are located on a circle with its center at the origin of the U-space and its radius as $\beta_{\text{target}}$. (For visualization, we assume a two-dimensional case here.) This corresponds to an ellipsis on the X-space as shown in Fig. 8. In essence, the additional samples are taken from this ellipsis, so only a local area of the $G$ surface around the current RBDO solution will be mostly improved. This is in contrast with

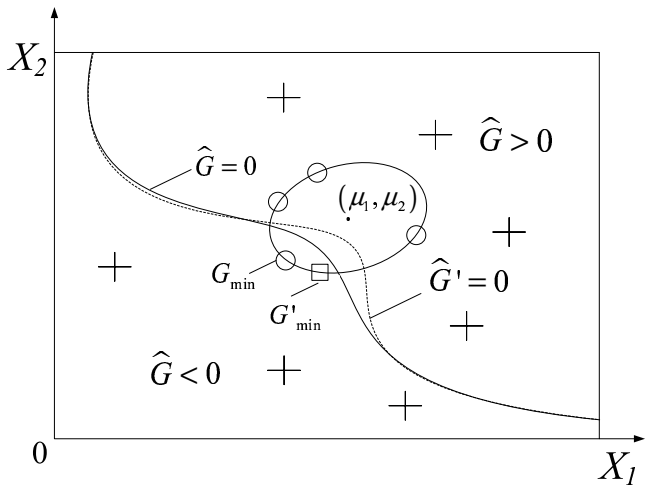


Figure 8.Max ERI sample point in design space. The initial samples are marked by "+", additional samples are marked by "o", and $G'_{min}$ is the latest additional sample selected by the ERI criterion.

random sampling on the whole X-space or on the limit state function. Our purpose is not to obtain a better overall estimation of the constraint function or the limit state function, but rather to find an accurate MPP; therefore, it is reasonable to sample an area that is close to the region of limit state function that contains the true MPP. The SORA procedure of RBDO with implicit constraint functions is outlined in Fig. 9.

We detail our sequential sampling strategy in the following steps:

1). After the initial sampling, a Kriging metamodel $\hat{G}$ is built. A deterministic optimization is then solved for decision vectors, $\mathbf{d}$ and $\mu_{\mathbf{X}}$. Note that in the first cycle, the shifting vector, $\mathbf{s}$, equals $\mathbf{0}$.

$$\begin{aligned} &\text{Minimize } f(\mathbf{d}, \mu_{\mathbf{X}}) \\ &\text{Subject to } \hat{G}_i(\mathbf{d}, \mu_{\mathbf{X}} - \mathbf{s}) \geq 0 \quad i = 1, 2, \ldots, m \end{aligned} \tag{3.15}$$

2). Given $\mu_{\mathbf{X}}$ and $\sigma_{\mathbf{X}}$, the X-space can be transformed to the standardized

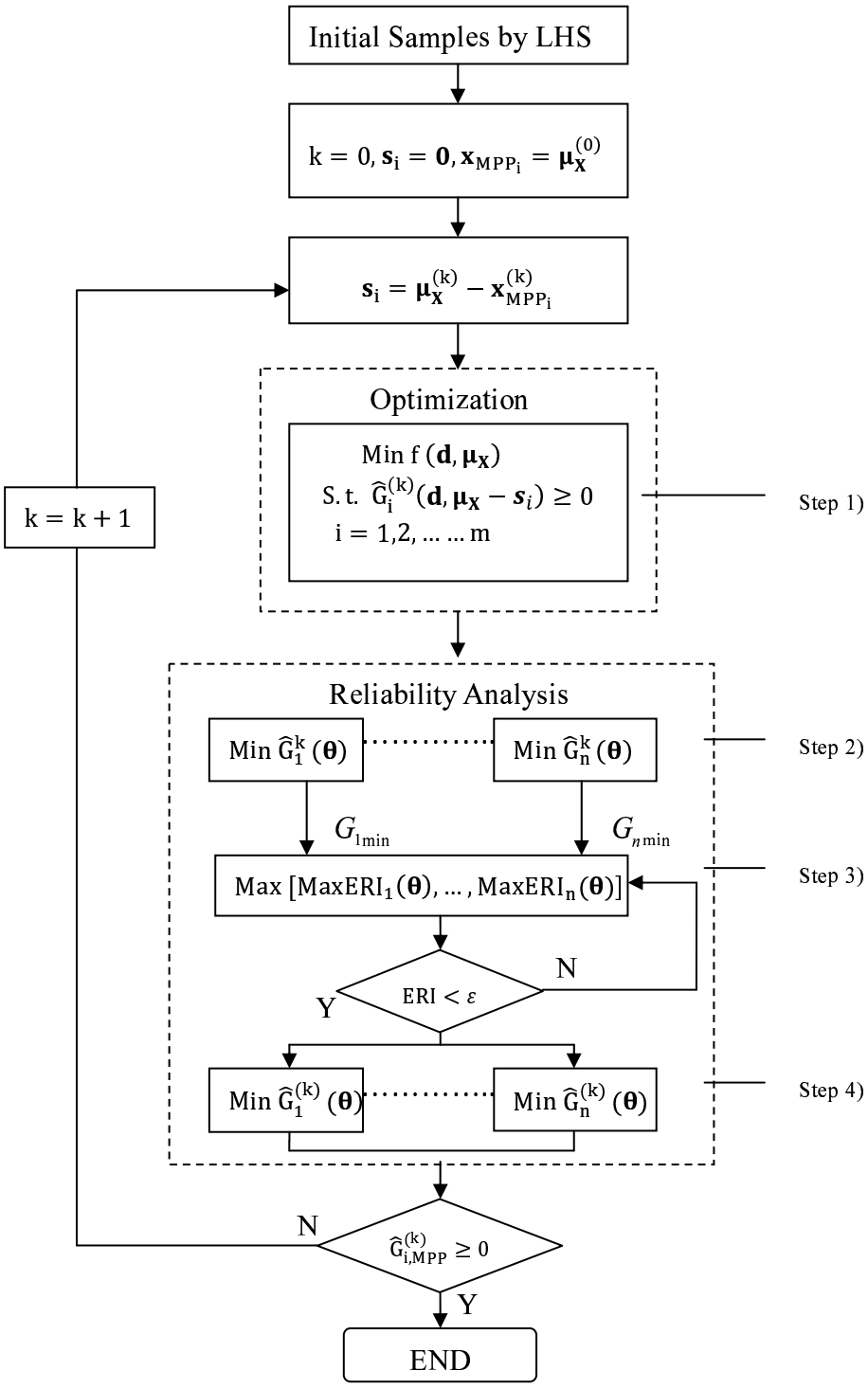


Figure 9.Algorithmic flowchart

U-space. Following PMA, the reliability analysis optimization is as follows:

$$\begin{aligned} &\text{Minimize } \hat{G}(\mathbf{u}) \\ &\text{Subject to } \parallel \mathbf{u} \parallel = \beta_{\text{target}} \end{aligned} \tag{3.16}$$

However, $\hat{G}$ is only a metamodel based on initial samples and the MPP derived by Formula 3.16 may not be accurate enough. Therefore, the ERI criterion is employed to find additional sample points that can make large expected improvement on the objective function. In order to find global minimum in the design space, the above optimization problem is first transformed to an unconstrained optimization problem by using a polar coordinate system. For example, when there are three variables, set $u_1 = \beta_{\text{target}} cos(\theta), u_2 = \beta_{\text{target}} sin(\theta) cos(\alpha), u_3 = \beta_{\text{target}} sin(\theta) sin(\alpha)$, then the optimization becomes:

$$\text{Minimize } \hat{G}(\theta, \alpha) \tag{3.17}$$

After solving this unconstrained optimization, the optimal solution $(\theta, \alpha)$ will be transformed back to the X-space and evaluated by the computer experiment, and it becomes the current minimum, $G_{\text{min}}$. If there are multiple constraints, each constraint will produce a $G_{\text{i, min}}$.

3). To find an additional sampling point, which has the potential to maximize the relative improvement on the $G$ function estimation, we solve the following maximization problem to locate the next sampling point.

$$\text{Maximize } \frac{1}{G_a}[(G_{\text{min}} - \hat{G})\Phi(\frac{G_{\text{min}} - \hat{G}}{s}) + s\phi(\frac{G_{\text{min}} - \hat{G}}{s})] \tag{3.18}$$

If there is only one constraint, the point with the maximum ERI should be evaluated by experiment and then added into the sample pool; while if there are

multiple constraints, the point associated with the largest maximum ERI is added into the sample pool.

The optimal solution of Equation 3.18 is a point located on the circle centered at the origin and with radius as $\beta_{\text{target}}$ in the U-space. This point is supposed to bring the maximum improvement to the $G$ function estimation subject to the MPP constraint. The corresponding point in the X-space is depicted in Fig. 8. The curve in Fig. 8 represents the current limit state surface $\hat{G} = 0$, and the areas of $\hat{G} > 0$ and $\hat{G} < 0$ denote the successful region and the failure region, respectively. The plus marks represent the initial sample points, and the point $(\mu_1, \mu_2)$ is the optimal solution obtained from deterministic optimization in Step (1). As the current MPP may not be accurate enough due to the prediction error of metamodel $\hat{G}$, the ERI criterion is employed to find a new sampling point (denoted by the square mark) on the ellipsis. Then the Kriging metamodel is reconstructed and the prediction error in the neighborhood of MPP will decrease.

Plotting along the angle coordinate, the solid curve on the upper panel of Fig. 10 is the metamodel predictor for the $\hat{G}$ function; while the dotted curve is the updated response curve after a new sample point is added. From the lower panel of Fig. 10 we can see that the response prediction error decreases dramatically around the new sample area after the new sample point is added. If the new sample point is evaluated to be smaller than the current minimum, it will be closer to global minimum and it is a more accurate candidate for MPP.

Repeat Step (3) to select the maximum ERI among constraint(s), until the maximum ERI is less than a small number (stopping rule), which means the prediction error of $\hat{G}$ around its global minimum is very small, so the current minimum of $\hat{G}$ shall be closer to the true global minimum.

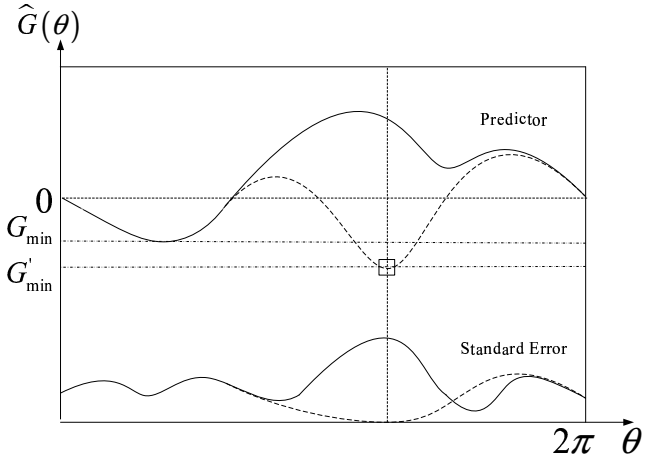


Figure 10.Max ERI sample point in response space

4). The metamodel $\hat{G}$ is updated with all samples and the MPPs for all constraints are derived. If all $\hat{G}_{\text{i,MPP}} \geq 0, i = 1, \ldots, m$, then $\mathbf{d}$ and $\mu_{\mathbf{X}}$ are the desired solution of RBDO and the algorithm stops. If any constraint $\hat{G}_{\text{i,MPP}} < 0$, a shift vector is computed based on current $\mu_{\mathbf{X}}$ and $\mathbf{x}_{\text{MPP}}$. Then return to Step (1) with the modified shift vector $\mathbf{s}$.

In the first cycle of sequential ERI, since there is no information about the MPPs, $\mathbf{x}_{\text{MPP}}$ is set as $\mu_{\mathbf{X}}$ and the shifting vector $\mathbf{s}$ is $\mathbf{0}$. Step (1) to Step (4) are repeated in each cycle to solve decision vectors, update Kriging metamodel and locate accurate MPPs until all $\hat{G}_{\text{i,MPP}} \geq 0$, which means all probabilistic constraints are feasible.

Comparing with the traditional SORA algorithm with explicit constraint functions, sequential ERI has one more loop in Step (3) because of the epistemic uncertainty associated with implicit constraint functions. That is, in each cycle, due to the prediction error of the estimated constraint function we cannot decide whether or not the constraint is feasible simply by the MPP calculated in Step (2). Instead, Step (3) is employed to add new sample points until there are no more allowable po-

tential improvement on the estimation of constraint function, so the updated Kriging metamodel is closer to the true model in the area of interests. Finally, the new MPP calculated in Step (4) is used to assess the feasibility of probabilistic constraint.

*Other Methods*

For the purpose of comparison, three other methods dealing with RBDO under implicit constraints are listed below.

*RBDO Solution Using Sequential MPP-Based Sampling Strategy* – This method is to add each MPP point to the sample pool without considering additional sampling points based on ERI. As at Step (2) MPPs are evaluated by computer experiments at each iteration, it is natural to add them to update the estimation of function $G$. This method is similar to the sequential ERI-based sampling strategy, but remove Step (3).

*RBDO Solution Using Lifted Metamodel Function* – In order to guarantee the optimal solution given by $\hat{G}$ function is feasible, a conservative approach is to replace $\hat{G}$ function by a predicted lower bound function. Since $\hat{G}$ function approximately follows a normal distribution, the lifted response function is $\hat{G} - t_{\alpha/2,n-p}\sqrt{Var(\hat{G})}$. Then the RBDO formulation becomes:

$$\text{Minimize } f(\mathbf{d}, \mu_{\mathbf{X}}) \tag{3.19}$$

$$\text{Subject to } Prob[\hat{G}(\mathbf{d},\mathbf{x}) - t_{\alpha/2,n-p}\sqrt{Var(\hat{G}(\mathbf{d},\mathbf{x}))} \geq 0] \geq R \tag{3.20}$$

$$\mathbf{d}^{\mathbf{L}} \leq \mathbf{d} \leq \mathbf{d}^{\mathbf{U}}, \mu_{\mathbf{X}}^{\mathbf{L}} \leq \mu_{\mathbf{X}} \leq \mu_{\mathbf{X}}^{\mathbf{U}} \tag{3.21}$$

where $\sqrt{Var(\hat{G}(\mathbf{d},\mathbf{x}))}$ is the standard error of prediction. It is expected that the true function value will fall in the prediction interval $[\hat{G}(\mathbf{d},\mathbf{x}) - t_{\alpha/2,n-p}\sqrt{Var(\hat{G}(\mathbf{d},\mathbf{x}))}, \hat{G}(\mathbf{d},\mathbf{x}) + t_{\alpha/2,n-p}\sqrt{Var(\hat{G}(\mathbf{d},\mathbf{x}))}]$ at the $(1-\alpha)$% confidence level. This method

is very conservative. It requires large initial sample size for reducing the prediction error. Typically $t_{\alpha/2,n-p}\sqrt{Var(\hat{G})} \propto \frac{c}{\sqrt{n}}$ , where c is a constant.

*RBDO Solution Based on Non-sequential Random Sampling Strategy* – As mentioned in Section 3.3, LHS is used to construct initial sample pool. Latin hypercube sampling or any other random sampling method can also be used subsequently to add more samples to update $\hat{G}$ function. The result will be compared with the sequential ERI-based sampling and the MPP-based sampling strategies in the following example.

## 3.4 I-Beam Performance Comparison

In the I-beam example mentioned in Section 2.5, as the true G function is known, we can use it to evaluate the fitness of metamodel $\hat{G}$ and to compare different sampling strategies for improving the MPP estimation. The RBDO problem is formulated as:

$$\text{Minimize: } 3\mu_1\mu_2 - 2\mu_2^2 \tag{3.22}$$

$$\text{Subject to: } Prob[\hat{G}(x_1,x_2) \geq 0] \geq 99.87\% \tag{3.23}$$

$$10 \leq \mu_1 \leq 80, 0.9 \leq \mu_2 \leq 5 \tag{3.24}$$

*Solution with the True Constraint Function*

Following the SORA procedure, we obtain the following solution using genetic algorithm (GA) with 100 initial population and 5 iterations.

Table 3.Results of SORA for I-Beam with True Constraint

| | Optimization | | | Constraint | | |
|---|---|---|---|---|---|---|
| Cycle | $\mu_1$ | $\mu_2$ | Obj | $MPP_1$ | $MPP_2$ | $G^R$ |
| 1 | 49.94 | 0.91 | 120.44 | 38.85 | 0.91 | -0.004 |
| 2 | 49.73 | 0.92 | 135.16 | 43.63 | 0.92 | 0.0003 |

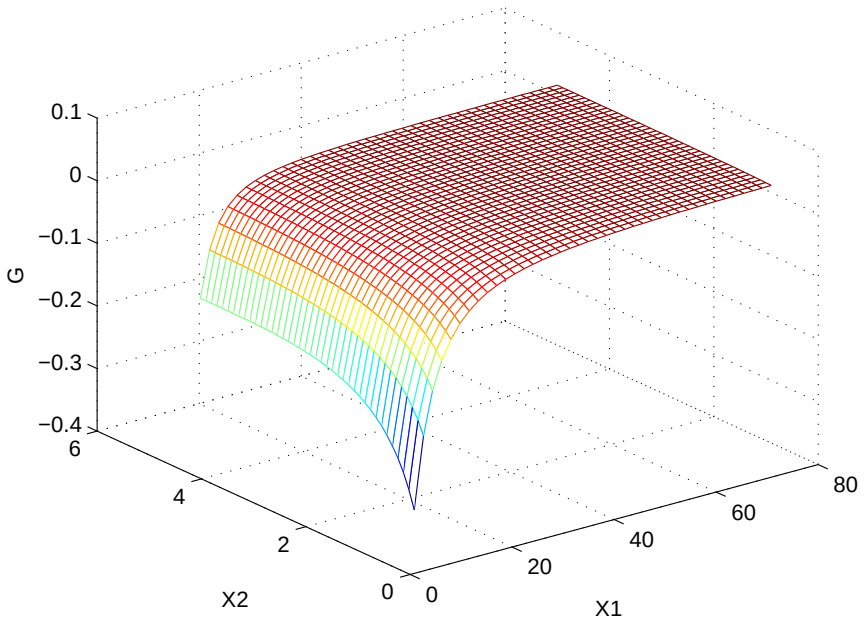


Figure 11.3D shape of G function

From Table 3 we can see that after two cycles the decision variable $(49.73,$ $0.92)$ can satisfy the probabilistic constraint with the R-percentile $G^R = 0.0003 > 0$. The objective value of RBDO is 135.16 based on the true constraint function. The 3-D graph of $G$ function is shown in Fig. 11. If we cut 3-D G function with plane $G = 0$, the feasible region of the deterministic constraint by SORA (the dark blue dot) and the shifted constraint region by SORA (the light blue star) in the X-space are shown in Fig. 12.

*Solution with the Sequential ERI-Based Sampling Strategy*

In this section, the sequential ERI-based sampling strategy is employed as we treat the constraint function as implicit. First, 20 initial sample points are generated by LHS as shown in Table 4. These sample points are evaluated by the G function, which we assume to be a black box. A Kriging model $\hat{G}$ is built with these initial

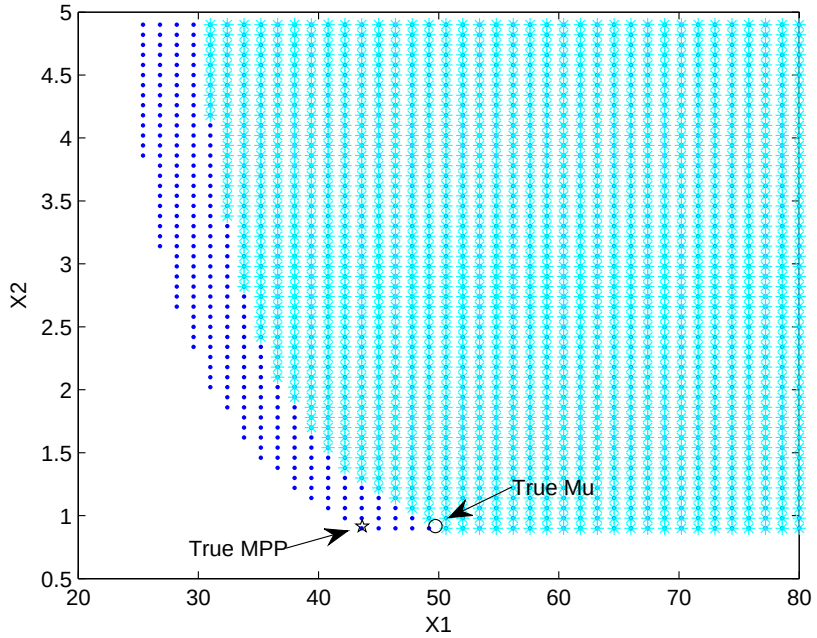


Figure 12.Feasible region with true G function

20 samples. We set the stopping criterion of the sequential ERI-sampling strategy to be $\max ERI < 0.005$ and obtain the results as in Table 5.

Similar to the results in Table 3, after two cycles our method obtains a feasible solution $(51.31, 0.91)$ with the value of the cost function to be 138.32. The additional sample points needed in each cycle are provided in Table 6. The feasible region in the X-space is shown in Fig. 13. The black dotted area is the true feasible region of deterministic constraint $G(\mu) \geq 0$ by SORA, and it is partially overlapped by the star area. The light blue star area is the shifted feasible region of $\hat{G}(\mu - \mathbf{s}) \geq 0$ when the sequential ERI sampling is applied; while the dark blue x-mark area is the shifted feasible region of $G(\mu - \mathbf{s}) \geq 0$ by SORA when the true constraint function is known. The red circle denotes the approximated optimal solution $(\mu_1, \mu_2) = (51.31, 0.91)$, and the red pentagram represents the approximated

Table 4.Initial Samples by Latin Hypercube

| Obs | $X_1$ | $X_2$ | $G$ |
|---|---|---|---|
| 1 | 32.11 | 2.63 | 0.004 |
| 2 | 24.74 | 0.90 | -0.036 |
| 3 | 65.26 | 2.19 | 0.013 |
| 4 | 10.00 | 3.71 | -0.173 |
| 5 | 61.58 | 3.27 | 0.014 |
| 6 | 50.53 | 5.00 | 0.013 |
| 7 | 54.21 | 4.14 | 0.013 |
| 8 | 72.63 | 3.92 | 0.015 |
| 9 | 35.79 | 3.49 | 0.008 |
| 10 | 57.89 | 1.12 | 0.009 |
| 11 | 80.00 | 3.06 | 0.015 |
| 12 | 28.42 | 1.76 | -0.006 |
| 13 | 39.47 | 4.35 | 0.011 |
| 14 | 21.05 | 4.57 | -0.007 |
| 15 | 76.32 | 1.33 | 0.013 |
| 16 | 68.95 | 4.78 | -0.015 |
| 17 | 13.68 | 1.55 | -0.106 |
| 18 | 43.16 | 1.98 | 0.008 |
| 19 | 46.84 | 2.84 | 0.011 |
| 20 | 17.37 | 2.41 | -0.036 |

Table 5.Results of SORA for I-Beam with Sequential ERI Sampling Strategy

| | Optimization | | | Constraint | | |
|---|---|---|---|---|---|---|
| Cycle | $\mu_1$ | $\mu_2$ | Obj | $MPP_1$ | $MPP_2$ | $G^R$ |
| 1 | 40.92 | 0.95 | 115.35 | 34.83 | 0.92 | -0.009 |
| 2 | 51.31 | 0.91 | 138.32 | 45.21 | 0.91 | 0.001 |

MPP $(45.21, 0.91)$. One can see that the approximated MPP is in the true feasible region. For the purpose of comparison, $\mu$ and MPP given by the true G function are also shown in Fig. 13. The additional sample points selected by the sequential ERI sampling strategy are represented by diamonds. We notice that these additional samples appear in both feasible and infeasible regions, and they cluster around the

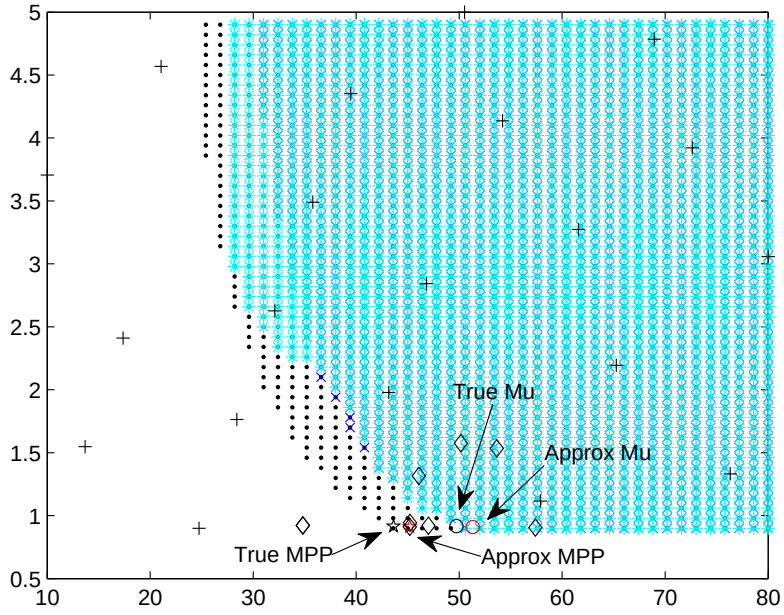


Figure 13.RBDO feasible region of $\hat{G}$ by sequential ERI sampling

optimal solution of ($\mu_1$, $\mu_2$). In consequence, the estimated shifted limit state function, $\hat{G}(\mu - \mathbf{s}) = 0$, is more accurate in the area around the true optimal solution. In fact, the dark blue (the true shifted feasible region by SORA) and light blue (the estimated shifted feasible region) regions are quite different in the upper part of the graph, but almost identical in the lower part of the graph, which is the area of the most importance to RBDO.

*Solutions by Other Methods*

*RBDO Solution using Sequential MPP-Based Sampling Strategy* – The MPP-based sampling strategy is employed to deal with the I-beam example with implicit constraint function. The initial sample points are the same as in Table 4. After two cycles an approximated optimal solution $(49.21, 0.90)$ is obtained with the objective value of 131.66. Note that the objective value is smaller than the value given by

Table 6.Additional Samples by Sequential ERI Sampling Strategy

| Obs | $X_1$ | $X_2$ | $G$ |
|---|---|---|---|
| 21 | 34.8290 | 0.9226 | -0.0088 |
| 22 | 47.0108 | 0.9198 | 0.0026 |
| 23 | 46.0796 | 1.3158 | 0.0060 |
| 24 | 34.8294 | 0.9216 | -0.0088 |
| 25 | 45.2150 | 0.9427 | 0.0018 |
| 26 | 53.6512 | 1.5349 | 0.0097 |
| 27 | 57.4040 | 0.9050 | 0.0070 |
| 28 | 50.1729 | 1.5752 | 0.0089 |
| 29 | 45.2076 | 0.9108 | 0.0014 |

the true function, but an evaluation of the obtained solution $(49.21, 0.90)$ shows that it is indeed an infeasible solution to the probabilistic constraint 3.23. The reason is that the current MPP $(55.31, 0.92)$ is obtained by the $\hat{G}$ function instead of the true G function and the $\hat{G}$ function is not accurate enough to locate the true MPP. We see that the prediction errors are high at the area around the current MPP. The feasible region is shown in Fig. 14.

In Fig. 14, the star area is the feasible region of $\hat{G}(\mu - \mathbf{s}) \geq 0$ given by the MPP-based sampling strategy. Same as before, the dotted area is the true feasible region of $G(\mu) \geq 0$ and the x-mark area is the feasible region of $G(\mu - \mathbf{s}) \geq 0$. The red circle denotes optimal solution given by the sequential MPP-based sampling strategy, and the red pentagram represents the approximated MPP. One can see that the approximated MPP falls out of deterministic feasible region.

*RBDO Solution using the Lifted Response Function* – Using the method provided in Section 3.3, a lifted response function is employed to replace $\hat{G}$. Hence

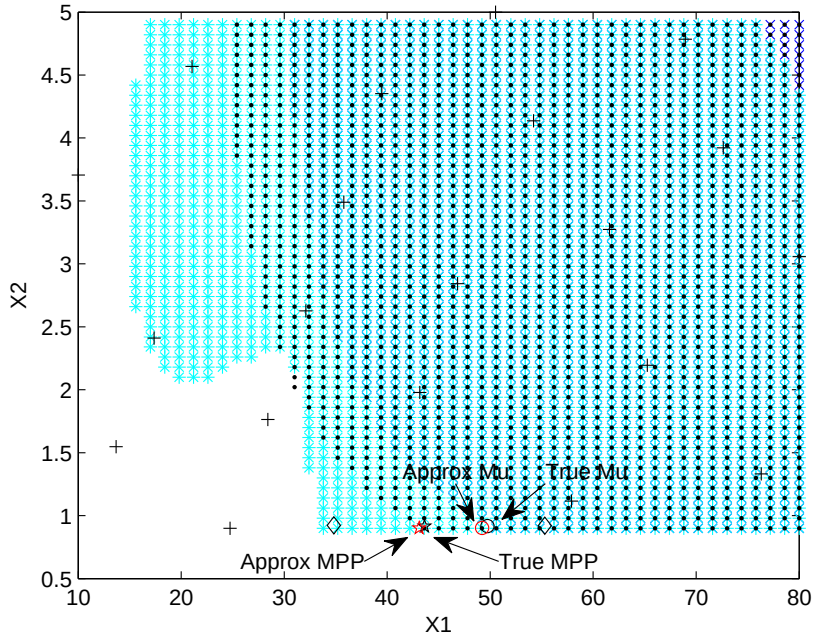


Figure 14.RBDO feasible region $\hat{G}$ function by MPP-based sampling

the RBDO formulation becomes

$$\text{Minimize: } 3\mu_1\mu_2 - 2\mu_2^2 \tag{3.25}$$

$$\text{Subject to: } P[\hat{G}(x_1,x_2) - t_{\alpha/2,n-p}\sqrt{Var(\hat{G}(x_1,x_2))} \geq 0] \geq 99.87\% \tag{3.26}$$

$$10 \leq \mu_1 \leq 80, 0.9 \leq \mu_2 \leq 5 \tag{3.27}$$

where $n$ is equal to 20, which is the initial sample size; $p$ is equal to 3 since there are one parameter for the linear term and two parameters for the correlation term in the Kriging model. In this case no additional samples are added and the SORA converges after 12 cycles. The feasible region is shown in Fig. 15.

In Fig. 15, the dotted area is the true feasible region of $G(\mu) \geq 0$, the x-mark area is the feasible region of $G(\mu - \mathbf{s}) \geq 0$, and star area is the feasible region by prediction lower bound function $\hat{G}(\mathbf{x}) - t_{\alpha/2,n-p}\sqrt{Var(\hat{G}(\mathbf{x}))} \geq 0$. The red circle denotes the approximated optimal solution $(\mu_1,\mu_2) = (52.74, 1.04)$ given by the

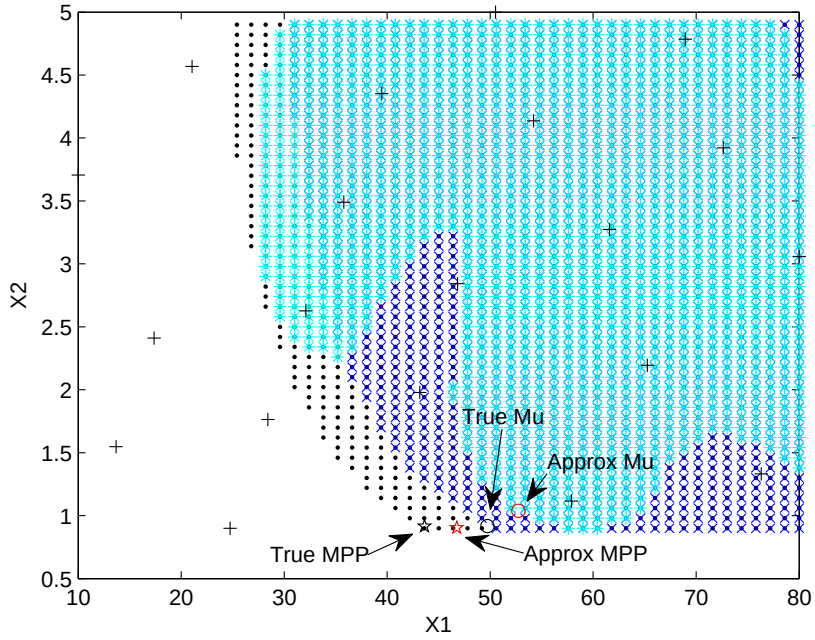


Figure 15.RBDO feasible region by lifting response function

lifting response function, and the red pentagram represents the approximated MPP $(46.76, 0.90)$. One can see that although the approximated MPP falls in the feasible region, its corresponding solution $\mu$ is too conservative and far from the true optimum.

*RBDO Solution using Random Additional Samples* – To compare with the sequential ERI-sampling strategy, we uniformly take 9 additional sample points. These additional sample points are shown in Table 7. A Kriging model is constructed based on the total 29 samples, and the RBDO result is given by SORA. In the X-space, the feasible region is shown in Fig. 16. One can see that the approximated feasible region and the true feasible region are quite different in the lower part of the graph. This causes that the approximated optimal solution $(\mu_1, \mu_2) = (52.84, 1.06)$, denoted by the red circle, and the approximated MPP

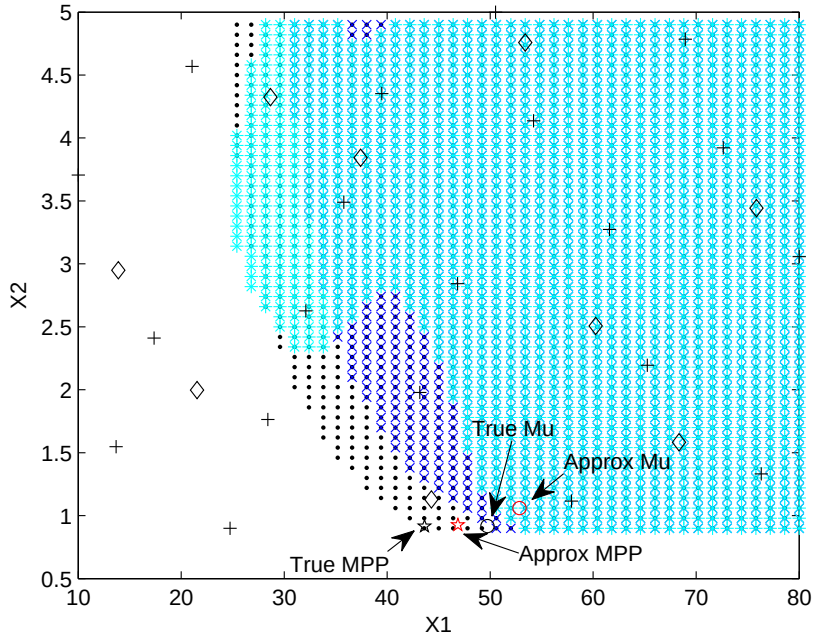


Figure 16.RBDO feasible region of $\hat{G}$ by non-sequential random sampling

Table 7.Additional Samples by Uniform Sampling

| Obs | $X_1$ | $X_2$ | $G$ |
|---|---|---|---|
| 21 | 13.8889 | 2.9500 | -0.0658 |
| 22 | 28.6680 | 4.3240 | 0.0049 |
| 23 | 68.3334 | 1.5833 | 0.0123 |
| 24 | 44.3002 | 1.1289 | 0.0035 |
| 25 | 21.5410 | 1.9975 | -0.0201 |
| 26 | 37.4270 | 3.8430 | 0.0096 |
| 27 | 75.8626 | 3.4424 | 0.0145 |
| 28 | 53.4068 | 4.7577 | 0.0136 |
| 29 | 60.2463 | 2.5064 | 0.0128 |

$(46.86, 0.93)$, denoted by the red pentagram, are far from their true optimums.

*Efficiency and Accuracy Comparison Between Different Methods*

We summarize the results of the I-beam example solved by different methods in Table 8 and compare their merits. The column of function calls is defined as the

number of optimization function calls including the deterministic optimization, the ERI optimization and MPP optimization. It takes 2 cycles to solve RBDO with true model in SORA, thus there are 2 deterministic optimization calls and 2 MPP optimization calls. Similarly, the MPP-based sampling strategy and the non-sequential random sampling strategy take 2 cycles to achieve their optimal solutions, so 4 function calls are needed. It takes 2 cycles in the sequential ERI-based sampling strategy, and there are 2 function calls in Step (1), 2 in Step (2), 5 in Step (3) and 2 Step (4); hence, the ERI-based strategy takes 11 function calls in total. In the lifted metamodel function approach, 24 optimization calls are executed since it takes 12 cycles to achieve the optimal solution. The columns of $(\mu_1, \mu_2)$ is the approximated optimal solution and the last column is the obtained minimum objective value.

Table 8.Results Comparison Between Methods in I-Beam Case

| Method | Cycles | Function calls | New pts | $(\mu_1, \mu_2)$ | Obj |
|---|---|---|---|---|---|
| True | 2 | 4 | NA | (49.7, 0.92) | 135.16 |
| ERI | 2 | 11 | Yes | (51.3, 0.91) | 138.32 |
| MPP | 2 | 4 | Yes | (49.2, 0.90) | 131.66 infeasible |
| Lifted | 12 | 24 | No | (52.7, 1.04) | 162.08 |
| Random | 2 | 4 | Yes | (52.8, 1.06) | 165.83 |

First, we can see that the sequential ERI-sampling strategy provides a good approximated optimal solution that is close to the true optimal solution, but it needs to take additional samples. Second, the MPP-based sampling may also provide a near optimal solution with even fewer function calls; however, as mentioned above, the feasible region derived from the MPP-based sampling is proved to be infeasible in this example, because the metamodel $\hat{G}$ around the MPP area is not accurate enough. Third, although the RBDO solution using the lifted response function

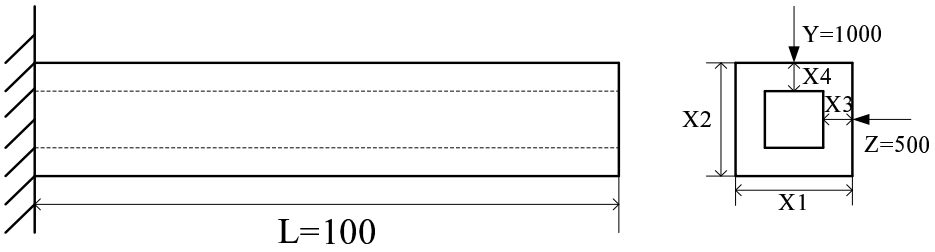


Figure 17.A thin walled box beam demo

needs no additional samples, thus it has lower sampling cost, it requires a larger number of function calls to converge to an optimal solution than any other methods. Furthermore, the solution it provided is far from the true optimum. Finally, the non-sequential random sampling method cannot give an accurate optimal solution because the additional samples are not taken from the MPP area. In summary, the sequential ERI-based sampling strategy provides the most accurate optimal solution when the constraint function of RBDO is a black box.

### 3.5 Application to A Thin Walled Box Beam

In this section we demonstrate the applicability of the sequential ERI-based sampling strategy for multiple constraints using a thin walled box beam example. As shown in Fig. 17, the beam is clamped at one end and loaded at the tip of the other end. The objective is to minimize the weight of the thin-walled box beam under both the vertical and lateral loads. Since the beam length $L = 100cm$ is kept as a constant and the material is assumed to be isotropic, minimizing the beam weight is equivalent to minimizing the cross-section area. Four random variables $X_1, X_2, X_3, X_4$ describe the cross-section area, and they follow normal distributions as $X_1 \sim N(\mu_1, 0.225^2), X_2 \sim N(\mu_2, 0.225^2), X_3 \sim N(\mu_3, 0.03^2), X_4 \sim N(\mu_4, 0.03^2)$. The vertical load Y is equal to $1000kN$ and the horizontal load Z is equal to $500kN$.

There are two implicit black box constraints – the bending moment con-

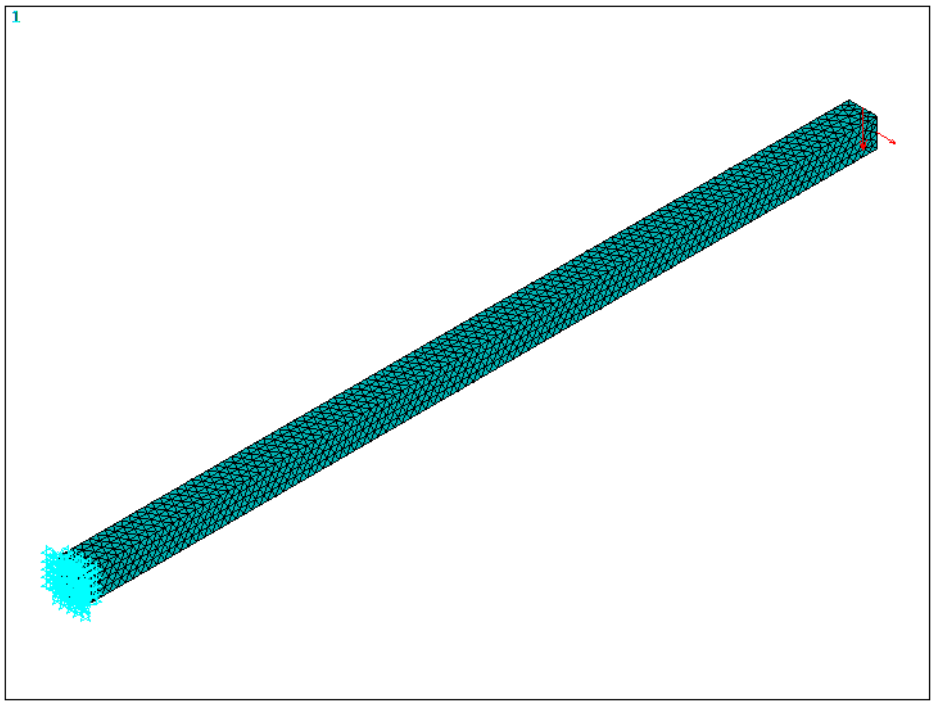


Figure 18.Preprocess model in ANSYS

straint and the displacement constraint. As shown in Fig. 17, the vertical and horizontal loads are applied on the free end of the beam, thus the bending moment stress is not uniform on the beam and the maximum value takes place on the clamped left end. To satisfy the yield bending moment threshold $\sigma_t^1 = 24000kN/cm^2$, the maximum $\sigma^1$ should be less or equal to $\sigma_t^1$. The displacement constraint requires the maximum displacement of the beam, which happens at the free end, to be less or equal to $\sigma_t^2$, where $\sigma_t^2 = 1.6cm$ is the displacement threshold.

The demo is ran in ANSYS 10.0, in which the material's elastic modulus is set as $E = 2.9 \times 10^7 psi$, and Poisson's ratio is 0.3. The size element edge length is set to be $1cm$ in finite element analysis. The finite element model in ANSYS is shown in Fig. 18. After finite element analysis (FEA), the deformed shape and the contour plots of Von-Mises are shown in Fig. 19 and Fig. 20, respectively.

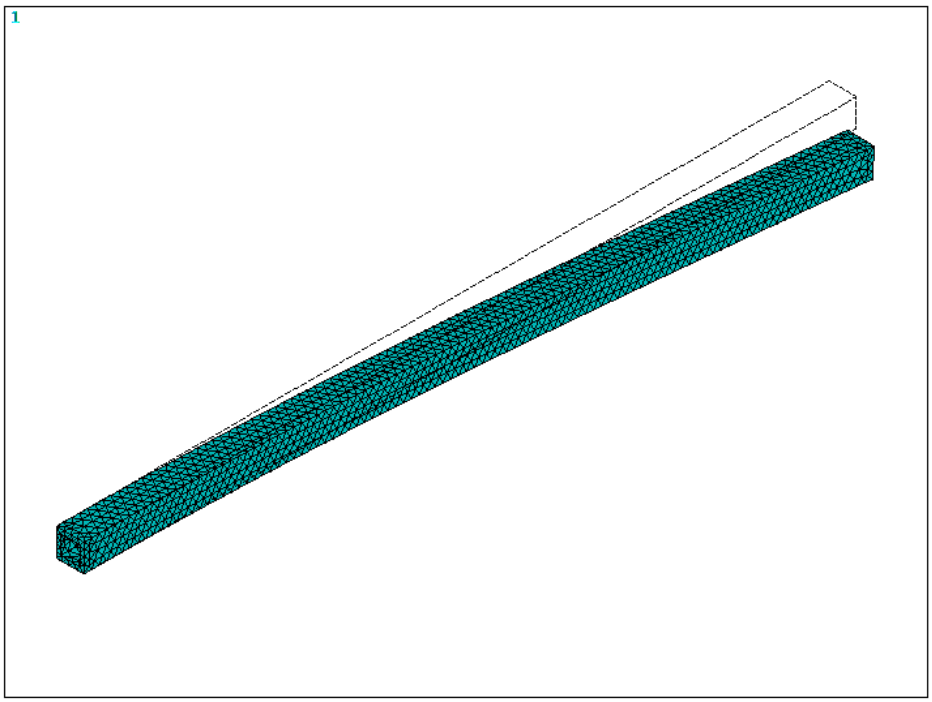


Figure 19.Deformed shape

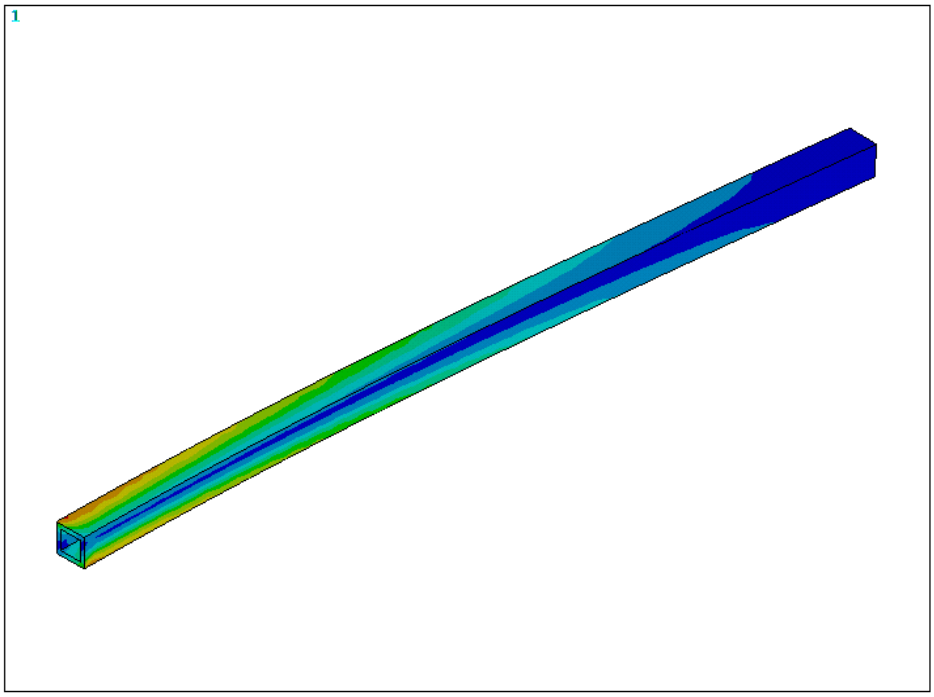


Figure 20.Contour plots of Von-Mises

The 20 initial Latin Hypercube samples are evaluated by the FEM computer experiment, which are listed in Table 10. Following the sequential ERI-sampling strategy with multiple constraints as described in Section 3.3, we set the stopping criterion as 0.1, then 23 additional samples are taken. Table 9 provides the number of function calls, FEM evaluation and additional samples required for solving this box beam RBDO problem. The details of each iteration are given in Table 11. In summary, there are 3 deterministic optimization calls, 28 ERI optimization calls and 6 MPP optimization calls in the three cycles. The column "FEM No." denotes the number of finite element analysis. There are 43 FEM models, for the 20 original samples and 23 additional samples, evaluated in this case. After three SORA cycles the MPPs of the two constraints become feasible.

Table 9.Efficiency in Thin Walled Box Beam Demo

| Method | Function calls | FEM No. | New samples | $(\mu_1, \mu_2, \mu_3, \mu_4)$ | Obj. |
|---|---|---|---|---|---|
| ERI | 37 | 43 | 23 | (4.02, 4.00, 0.53, 0.59) | 7.75 |

## 3.6 Conclusion and Future Work

In this chapter, an RBDO problem under implicit constraint function is discussed. Metamodels are used to approximate the true constraint functions in RBDO. We discuss and compare two different metamodels – polynomial model and Kriging model, and Kriging model is selected as our empirical metamodels in RBDO because it not only requires fewer parameter estimations but also fits well for high nonlinear functions. Based on Kriging model, we propose a sequential ERI-based sampling strategy to improve the solution of RBDO, and compare it with the methods of the MPP-based sampling, lifted response function and non-sequential random sampling. Among all of them, the sequential ERI-based sampling provides

Table 10.Initial Samples by Latin Hypercube

| Obs | $X_1$ | $X_2$ | $X_3$ | $X_4$ | $G_1$ | $G_2$ |
|---|---|---|---|---|---|---|
| 1 | 3.58 | 3.74 | 0.73 | 0.71 | 5704 | 0.68 |
| 2 | 4.21 | 5.00 | 0.58 | 0.73 | 12948 | 1.19 |
| 3 | 4.37 | 3.11 | 0.9 | 0.77 | 5998 | 0.53 |
| 4 | 2.32 | 3.26 | 0.82 | 0.79 | -9070 | -0.57 |
| 5 | 2.95 | 2.16 | 0.54 | 0.63 | -25286 | -2.23 |
| 6 | 3.42 | 2.32 | 0.67 | 0.84 | -12013 | -1.03 |
| 7 | 2.16 | 3.42 | 0.71 | 0.58 | -11569 | -0.66 |
| 8 | 3.89 | 2.95 | 0.69 | 0.52 | -2067 | 0.04 |
| 9 | 4.84 | 3.89 | 0.86 | 0.56 | 10860 | 0.98 |
| 10 | 4.53 | 2.00 | 0.75 | 0.67 | -9770 | -1.58 |
| 11 | 2.63 | 4.21 | 0.5 | 0.65 | -544 | 0.35 |
| 12 | 3.74 | 4.37 | 0.84 | 0.88 | 10920 | 1.02 |
| 13 | 4.05 | 4.53 | 0.61 | 0.5 | 9040 | 1.00 |
| 14 | 5.00 | 3.58 | 0.63 | 0.86 | 10853 | 0.94 |
| 15 | 2.47 | 4.84 | 0.77 | 0.75 | 5444 | 0.70 |
| 16 | 2.00 | 2.79 | 0.56 | 0.82 | -26039 | -1.88 |
| 17 | 3.11 | 4.68 | 0.79 | 0.54 | 8005 | 0.90 |
| 18 | 3.26 | 2.63 | 0.88 | 0.61 | -7846 | -0.58 |
| 19 | 2.79 | 4.05 | 0.65 | 0.9 | 3666 | 0.52 |
| 20 | 4.68 | 2.47 | 0.52 | 0.69 | -127 | -0.07 |

more reliable optimal solution than the MPP-based sampling method, and more accurate solution than the lifting response function and the random sampling methods. The strength of our proposed method lies on that it will add samples around the current RBDO solution to maximally improve the MPP estimation, while ignore other areas of the constraint function that are not important to the RBDO solution.

As mentioned in Section 3.2, implicit constraint function is just one type of epistemic uncertainty due to lack of knowledge. Unknown distributions of random variables, for example, is another type of epistemic uncertainty and it is not discussed in this chapter. In future the sampling strategy could be developed to make an accurate inference of random variable distributions. Our method can also be ex-

tended and applied on more complex problems, such as the RBDO problem with multiple objectives. In addition, since reliability and robustness are two important attributes of product design optimization, robust design method, which focuses on minimizing performance variation without eliminating the sources of variation, can be combined with RBDO.

Table 11.Results of Sequential ERI Sampling of the Thin Walled Box Beam

| Cycle 1 | | | | |
|---|---|---|---|---|
| $\mu_1, \mu_2, \mu_3, \mu_4$ | | | Objective Value | |
| 3.21, 3.77, 0.52, 0.50 | | | 6.09 | |
| $X_1, X_2, X_3, X_4$ | $ERI_{\hat{G}_1}$ | $ERI_{\hat{G}_2}$ | $\hat{G}_1$ | $\hat{G}_2$ |
| 3.06, 3.11, 0.52, 0.51 | | | -7631 | |
| 2.83, 3.22, 0.52, 0.52 | | | | -0.337 |
| 2.61, 3.47, 0.51, 0.50 | | $0.083 < \varepsilon$ | -8101 | -0.289 |
| $MPP_1, MPP_2, MPP_3, MPP_4$ | | | $\hat{G}_1$ | $\hat{G}_2$ |
| 2.75, 3.28, 0.51, 0.51 | | | -9256($<0$) | |
| 2.77, 3.26, 0.52, 0.51 | | | (infeasible) | -0.346($<0$) |
| Cycle 2 | | | | |
| $\mu_1, \mu_2, \mu_3, \mu_4$ | | | Objective Value | |
| 2.76, 4.82, 0.57, 0.50 | | | 7.14 | |
| $X_1, X_2, X_3, X_4$ | $ERI_{\hat{G}_1}$ | $ERI_{\hat{G}_2}$ | $\hat{G}_1$ | $\hat{G}_2$ |
| 2.15, 4.67, 0.55, 0.53 | | | -2158 | |
| 2.21, 4.45, 0.55, 0.50 | | | | 0.081 |
| 3.17, 4.91, 0.50, 0.52 | | 0.590 | 6672 | 0.844 |
| 2.46, 4.98, 0.51, 0.56 | | 0.112 | 2542 | 0.517 |
| 2.17, 4.50, 0.58, 0.50 | $0.094 < \varepsilon$ | | -3135 | 0.075 |
| $MPP_1, MPP_2, MPP_3, MPP_4$ | | | $\hat{G}_1$ | $\hat{G}_2$ |
| 2.21, 4.43, 0.56, 0.51 | | | -2789($<0$) | |
| 2.11, 4.65, 0.56, 0.50 | | | (infeasible) | 0.051($<0$) |
| Cycle 3 | | | | |
| $\mu_1, \mu_2, \mu_3, \mu_4$ | | | Objective Value | |
| 4.02, 4.00, 0.53, 0.59 | | | 7.75 | |
| $X_1, X_2, X_3, X_4$ | $ERI_{\hat{G}_1}$ | $ERI_{\hat{G}_2}$ | $\hat{G}_1$ | $\hat{G}_2$ |
| 3.85, 3.35, 0.53, 0.58 | | | 2164 | |
| 3.71, 3.40, 0.53, 0.59 | | | | 0.415 |
| 3.41, 4.06, 0.51, 0.55 | 1.689 | | 3431 | 0.666 |
| 4.64, 4.27, 0.52, 0.59 | 1.068 | | 10481 | 1.037 |
| 3.61, 3.66, 0.51, 0.54 | 0.407 | | 1636 | 0.516 |
| 3.44, 4.33, 0.52, 0.59 | 0.327 | | 5780 | 0.795 |
| 4.04, 3.95, 0.52, 0.50 | 0.289 | | 5654 | 0.774 |
| 3.46, 3.74, 0.50, 0.61 | 0.200 | | 2261 | 0.540 |
| 3.53, 3.63, 0.56, 0.56 | $0.096 < \varepsilon$ | | 1748 | 0.493 |
| $MPP_1, MPP_2, MPP_3, MPP_4$ | | | $\hat{G}_1$ | $\hat{G}_2$ |
| 3.55, 3.55, 0.52, 0.56 | | | 911($>0$) | |
| 3.60, 3.49, 0.52, 0.58 | | | (feasible) | 0.423($>0$) |

# CHAPTER 4

# DESIGN OPTIMIZATION WITH PARTICLE SPLITTING-BASED RELIABILITY ANALYSIS

## 4.1 Introduction

The simulation-based method is the rudimentary method of assessing a probability function in RBDO. However, it is also the most accurate method if the sample size is large enough. The computation burden is typically large, but it can be greatly reduced by some advanced sampling methods as discussed in the later sections of this chapter. In this chapter, our approach replaces the MPP-based reliability assessment step by a new simulation-based reliability assessment method – particle splitting. Therefore, the probabilistic constraint is not longer evaluated by the worst case scenario, but by the whole feasible design space. We introduce the concept of target probable point (TPP), which is derived from the desirable sampling points from simulation directly. The mean performance measure is feasible if TPP can satisfy the constraint. Our approach takes the advantages of both the merit of efficiency from the sequential loop method and the merit of accuracy from the simulation-based reliability assessment method.

Our research contributions are: First, the rare-event simulation technique (i.e., subset simulation and particle splitting) is integrated into RBDO. However, different from the typical rare-event simulation application that aims to evaluate probabilistic constraints, we employ the rare-event simulation in an optimization aiming to find optimal random properties under a target probability. Secondly, particle splitting is proposed as an improvement of subset simulation in rare-event simulation, and the trade-off balance among number of subsets, simulation sample size and coefficient of variation is investigated, which provides a guidance for determining the simulation process. Finally, we extend our particle splitting-based

reliability analysis approach to address multiple constraints without significantly increasing simulation efforts.

The remaining part of the chapter is organized as follows: In Section 4.2 we specify the simulation-based sequential optimization reliability assessment approach employed in the chapter. A particle splitting-based reliability analysis approach is proposed in Section 4.3. In Section 4.4 we provide an I-beam case to illustrate the proposed method and a mathematical example to demonstrate the extension of our algorithm on handling the problem with multiple probabilistic constraints. Finally, we draw the conclusion and propose our future work in Section 4.5.

## 4.2 Simulation-Based Reliability Analysis

Monte Carlo simulation (MCS) with large sample size generally provides high accuracy in estimating the probability of an event; however, it requires tremendous amount of event evaluation, when the event probability is very small (a rare event), in order to get lower estimation error. This computational issue has been addressed recently by applying other simulation methods, such as importance sampling, subset sampling and line sampling. A sampling method around MPP was provided in [22]; Reduced region importance sampling was developed in [33], [46]; Quasi MCS techniques were developed in [66], in which sampling was done in the important regions that include the region in the failure domain that contributed significantly to the probability of failure. Importance sampling was also employed to improve sampling efficiency and estimation accuracy in [58], [42]. Subset simulation was used in [27], in which an RBDO problem with surrogate model was solved by a double-loop approach; A three-step approach was proposed to solve RBDO in [14], in which reliability constraint was transformed into nonprobabilistic one by estimating the failure probability function and the confidence intervals using subset

simulation. A line sampling approach proposed in [101] employed lines instead of random points to probe the failure domain of interested.

As mentioned before the SORA method solves two optimization problems sequentially. The first optimization problem is as follows:

$$\begin{aligned} &\text{Minimize}_{\mathbf{d},\mu_{\mathbf{X}}} \quad f(\mathbf{d},\mu_{\mathbf{X}}) \\ &\text{Subject to} \quad G_i(\mathbf{d},\mu_{\mathbf{X}}-\mathbf{s}) \geq 0 \quad i=1,2,\ldots,n \end{aligned} \tag{4.1}$$

where **s** denotes the shifting vector derived from the reliability assessment step, and **s** is set to **0** in the first cycle. The random parameter vector is ignored in the above formulation for simplicity.

Based on the optimum **d** and $\mu_{\mathbf{X}}$, the reliability assessment is implemented as:

$$Prob[G_i(\mathbf{d},\mathbf{X}) \geq 0] = \int_0^{\infty} f_{G_i}(G_i)dG_i \geq R_i \tag{4.2}$$

where $f_{G_i}(G_i)$ is the probability density function (pdf) of $G_i(\mathbf{d},\mathbf{x})$. For low dimension and simple constraint function formulation, the pdf of $G_i(\mathbf{d},\mathbf{x})$ can be derived. However, it is typically very difficult to obtain $f_{G_i}(G_i)$ in highly nonlinear case. Then a multi-dimensional integration is derived as:

$$Prob[G_i(\mathbf{d},\mathbf{x}) \geq 0] = \int_{G_i(\mathbf{d},\mathbf{x})\geq 0} f_{\mathbf{X}}(\mathbf{x})d\mathbf{x} \geq R_i \tag{4.3}$$

where $f_{\mathbf{X}}(\mathbf{x})$ is the joint pdf of random vector **X**, and $G_i(\mathbf{d},\mathbf{x}) \geq 0$ is the integration region. Since the computational work for direct multi-dimensional integration in reliability assessment is unaffordable, a variety of approximate reliability assessment methods have been proposed in literature. SORA employs the MPP-based reliability analysis method, in which the probabilistic constraint evaluation is converted to an MPP optimization problem based on the concept of MPP and reliability index.

By the inverse reliability PMA, this optimization problem is as

$$\begin{aligned} &\text{Minimize}_{\mathbf{u}} \;\; G(\mathbf{u}) \\ &\text{Subject to} \;\; \| \mathbf{u} \| = \beta_{\text{target}} \end{aligned} \tag{4.4}$$

where the optimal solution, $\mathbf{u}_{\text{MPPIR}}$, is called the most probable point of inverse reliability (MPPIR) [25]. MPPIR is the point on the target reliability level which has the smallest performance function value in the U-space. Once the MPPIR is obtained, $G^R = G(\mathbf{u}_{\text{MPPIR}}) = G(\mathbf{x}_{\text{MPPIR}})$ is called the target probabilistic performance measure [84]. If $G^R \geq 0$, it indicates that the performance $G(\mathbf{x}) \geq 0$ for all the points within target reliability level. If $G^R < 0$, it indicates that the target reliability level in $i^{th}$ cycle is not satisfied, a shifting vector $\mathbf{s}^{i+1} = {\mu_{\mathbf{X}}}^i - \mathbf{x}^i_{\text{MPPIR}}$ is derived in the original X-space.

The design optimum from the first deterministic optimization has high probability of violating design constraints, as it does not consider uncertainties. If so, a shifting vector which starts from MPPIR and points to design variable $\mu_{\mathbf{X}}$ is derived to compensate the gap between actual reliability and target reliability. Then the algorithm enters a new cycle and the constraint in deterministic design optimization is revised by the shifting vector. Uncertainties are considered adaptively in each cycle until the decision variable vector $\mu_{\mathbf{X}}$ satisfies the target reliability level.

In this chapter, simulation methods are employed in the reliability assessment step because it can provide a more accurate probability estimation than the MPP-based method and also because it can handle general constraint functions, no matter they are linear or nonlinear, explicit or implicit functions. The probabilistic constraint evaluation by MCS can be expressed as

$$P_F = \int_{\mathbf{x}} I_F(\mathbf{x}) f_{\mathbf{X}}(\mathbf{x}) d\mathbf{x} = E(I_F(\mathbf{x})) = \lim_{N \longrightarrow \infty} \frac{1}{N} \sum_{k=1}^{N} I_F(\mathbf{x_k}) \tag{4.5}$$

where $N$ is the simulation sample size, and $\mathbf{x}_k$ is the sample distributed with the pdf $f_{\mathbf{X}}(\mathbf{x})$. $I_F(\mathbf{x})$ is an indicator function

$$I_F(\mathbf{x}) = \begin{cases} 1, & \text{if } \mathbf{x} \in F \\ 0, & \text{if } \mathbf{x} \notin F \end{cases} \qquad \text{and} \qquad F = \{\mathbf{x} | G_i(\mathbf{d}, \mathbf{x}) < 0\} \tag{4.6}$$

where $F$ represents the failure domain corresponding to the problem definition. When the sample size is $N$, the failure probability can be replaced by the estimator $\hat{P}_F$ as

$$\hat{P}_F = \hat{E}(I_F(\mathbf{x})) = \frac{1}{N} \sum_{k=1}^{N} I_F(\mathbf{x}_k) \tag{4.7}$$

The expectation and variation of the $\hat{P}_F$ are

$$E(\hat{P}_F) = P_F, \qquad Var(\hat{P}_F) = \frac{(1 - P_F)P_F}{N} \tag{4.8}$$

The confidence interval for the failure probability is $[P_F - z_{\alpha/2}\sqrt{\frac{(1-P_F)P_F}{N}}, P_F + z_{\alpha/2}\sqrt{\frac{(1-P_F)P_F}{N}}]$, which does not depend on the dimension of the input variable $\mathbf{x}$. When the failure probability $P_F$ is extremely small, however, the MCS approach is not longer feasible as the required sample size becomes extremely large. In this chapter, particle splitting, which is an improved sequential Monte Carlo simulation method [19], is employed for reliability assessment and it is integrated with the first optimization step of RBDO.

## 4.3 SORA with Particle Splitting-Based Reliability Analysis

To assess the extremely small but important probabilities of rare events, such as the structural failure probability, subset simulation has been developed in literature [4]. We will show how to integrate this technique with RBDO in this section. As the ultimate purpose of RBDO is to find the optimal setting of design variables, the rare-event simulation is only one step, but an important step, in the optimization

process. In the SORA algorithm, the reliability assessment is performed by an MPP optimization, which is to evaluate the worst case scenario of system reliability. Here, we replace it with the simulation-based reliability assessment method so that the reliability analysis would not be too conservative. On the other hand, similar to SORA which employs MPP points to find the shifting vector to improve the RBDO solution iteratively, we utilize the statistical property of sample points from simulation to find the target probability point (TPP) to define the shifting vector. As such, the rare-event simulation implemented in RBDO is different from its typical applications.

*Particle Splitting*

Particle splitting method extends the subset simulation by deploying multiple particles (multiple Markov chain Monte Carlo sampling pathes) to enhance sample diversity. Subset simulation was first proposed in [4] to compute small failure probabilities encountered in reliability analysis of engineering systems. It was considered for improving the efficiency of MCS in [101]; an innovative method called stochastic simulation optimization and sensitivity analysis was proposed in [81], [82];

The main idea of subset simulation is to formulate the small failure event probability as a product of larger conditional failure probabilities by introducing intermediate events. Suppose we need to evaluate a small failure probability $F = \{\mathbf{x} : G(\mathbf{x}) \leq G\}$ by simulation, subset simulation derives a sequence of events such that $F_1 \supset F_2 \cdots \supset F_m = F$. Then a series of limit values are generated as $G_1 > G_2 > \cdots > G_m$ corresponding to the event sequence. The original failure probability can

be expressed as a product of conditional probabilities as

$$\begin{aligned} P_F = P(F_m) &= P(F_m|F_{m-1})P(F_{m-1}|F_{m-2})\dots P(F_2|F_1)P(F_1) \\ &= P(F_1)\prod_{i=1}^{m-1} P(F_{i+1}|F_i) \end{aligned} \tag{4.9}$$

where $m$ denotes the number of subsets. The probability $P_F$ is determined by estimating $P(F_1)$ and the partial failure probabilities $P(F_{i+1}|F_i)$ in two steps: In the first step, the probability $P_1 = P(F_1) = Prob[G(\mathbf{x}) \leq G_1]$ is evaluated by a direct MCS, so

$$\hat{P}_1 = \frac{1}{N_1}\sum_{k=1}^{N_1} I_{F_1}(\mathbf{x}_k^{(1)}) \tag{4.10}$$

where $I_{F_1}(\mathbf{x})$ is an indicator function which is equal to 1 if $\mathbf{x} \in F_1$ and 0 if $\mathbf{x} \notin F_1$. In the second step, the conditional probabilities $P(F_{i+1}|F_i)$ are evaluated by the Markov chain Monte Carlo (MCMC) simulation in conjunction with Metropolis-Hastings algorithm. The conditional probability $P_{i+1} = P(F_{i+1}|F_i) = Prob[G(\mathbf{x}) \leq G_{i+1}|G(\mathbf{x}) \leq G_i]$ is estimated by

$$\hat{P}_{i+1} = \frac{1}{N_{i+1}}\sum_{k=1}^{N_{i+1}} I_{F_{i+1}}(\mathbf{x}_k^{(i+1)}) \tag{4.11}$$

where the conditional probability density function $f(\mathbf{x}|F_i)$ needs to be evaluated by MCMC.

Some specific concerns are:

(1) The starting sample point of subset $i+1$ is from the samples that are in subset $i$ but lie in the failure region $F_i$. In particle splitting, instead of using a single starting sample point, multiple starting points of subset $i+1$ are defined as a set of sample points locating in the failure region of subset $i$. Each element of the starting point sample set is referred as a particle and a sampling path is generated from each particle by MCMC. Multiple particles and paths can enhance simulation diversity and lead to more stable simulation results.

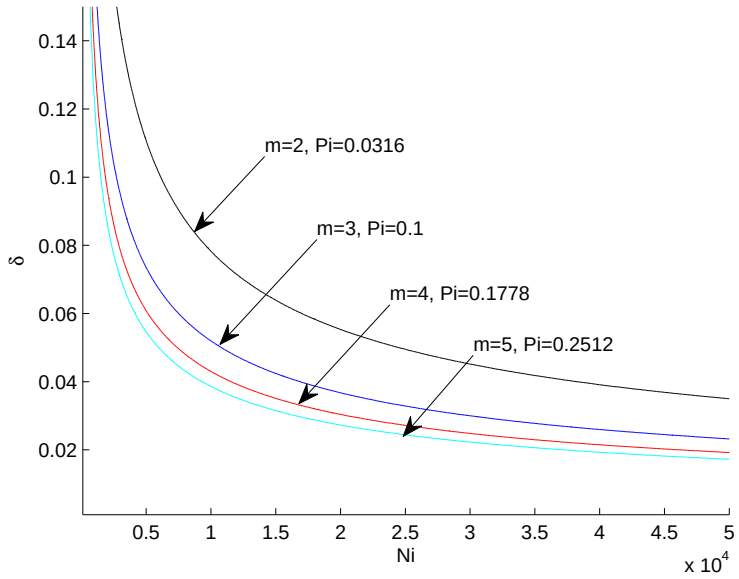


Figure 21.Sample size requirement for different coefficient of variation and number of subsets.

(2) The variation of estimator $\hat{P}_F$ is evaluated by the approximated coefficient of variation $\delta = \sqrt{\sum_{i=1}^{m} \delta_i^2}$, $i = 2, \ldots, m$, where $\delta_i = \sqrt{\frac{1-P_i}{P_i N_i}}$, $P_i$ and $N_i$ are the coefficient of variation, partial failure probability and the sample size of $i^{th}$ subset, respectively. For convenience we may set all $P_i$ to be equal, so $P_i = \sqrt[m]{P_t}$ under the target failure probability $P_t$, where $m$ is the number of subsets.

A plot of $\delta$ versus $N_i$ for different $m$'s or $P_i$'s is shown in Fig. 21. Suppose we would like to achieve $\delta = 0.1$, then the partial probability $P_i$ and sample size $N_i$ are shown in Table 12, where $N = N_i \times m$ is the total sample size. One can see that the sample size is minimal when four subsets are deployed.

The theoretical minimum sample size can be derived as such: As $\delta_i = \sqrt{\frac{1-P_i}{P_i N_i}}$ and $N_i = \frac{(1-P_i)m}{P_i \delta^2}$, we have the total sample size to be $N = N_i \times m = (\frac{1}{P_i} -$

Table 12.Sample Size Requirement for Different Number of Subsets When $\delta = 0.1$

| $m$ | $P_i$ | $N_i$ | $N$ |
|---|---|---|---|
| 2 | 0.0316 | 61246 | 12248 |
| 3 | 0.1 | 2700 | 8100 |
| 4 | 0.1778 | 1849 | 7396 |
| 5 | 0.2512 | 1491 | 7455 |

$1)\frac{m^2}{\delta^2}$. Since all $P_i$ are the same, i.e., $P_i = \sqrt[m]{P_t}$, we obtain the following formula,

$$N = m^2 P_t^{\frac{1}{m}} - m^2 \tag{4.12}$$

Taking the derivative $\frac{dN}{dm}$ and set it to be zero, we have

$$2m - 2mP_t^{\frac{1}{m}} + lnP_t = 0 \tag{4.13}$$

when $P_t = 0.001$, the solution of above equation is $m = 4.3346 \approx 4$, which matches the result obtained in Table 12.

Typically once partial failure probability $P_i, i = 1, \ldots, m$ are predefined, the corresponding limit values $G_i, i = 1, \ldots, m$ are determined adaptively during the simulation according to the target partial failure probability $P_i$. The method mentioned above provides only a reference for selecting $P_i$ since it has some assumptions such as equal partial failure probability and selecting coefficient of variation as accuracy measure. In addition, other considerations such as the burn-in duration and the acceptance rate of MCMC should be included to determine the number of subsets. A longer MCMC chain will generally reduce the burn-in effect and guarantee samples are generated from the target distribution. Therefore, the final selection of $P_i$ should be from a comprehensive evaluation of all criteria and computational burdens based on specific problems.

In this section we introduce the concept of TPP, which, like MPPIR, is used to constructing the shifting vector for improving the SORA solution to decision variables.

TPP is defined as the sample point that can separate all simulation samples into successful ones and failure ones, where the ratio of failure ones to total samples is equal to the target probability. For example, 1000 samples are simulated and listed in an ascending order $\mathbf{x}_1, \ldots, \mathbf{x}_{1000}$ by their performance values. Then we can find the $10^{th}$ sample to be TPP when the target probability is 0.01. Thus the first 10 samples are in failure region since their performance values are less or equal to the TPP measure. The ratio of failure samples is $\frac{10}{1000}$, which is equal to target probability level. To enhance the robustness, TPP is defined as the centroid of a set of points located between the upper bound and lower bound of the performance value $G_m$, where $G_m$ is the limit value of $m^{th}$ subset probability and is the target probabilistic performance measure. By applying the particle splitting method, we evaluate the probabilistic constraint in RBDO by finding a sequence of $G_i$ values. If $G_m \geq 0$, then the probabilistic constraint is satisfied.

TPP is different from MPP in the following aspects: First, MPP is an analytical function-based point. MPP could not be accurate if there is a large prediction error in approximated constraint function. TPP is a simulation-based point, which does not need analytical function. As long as the target probability is given, we can find the TPP from all simulation sample points. Second, MPP is the worst case point derived by optimization, it ignores the region that is out of target probability level but still feasible. TPP can be simulated in any region and reflects the target probability requirement, so it is not as conservative as MPP.

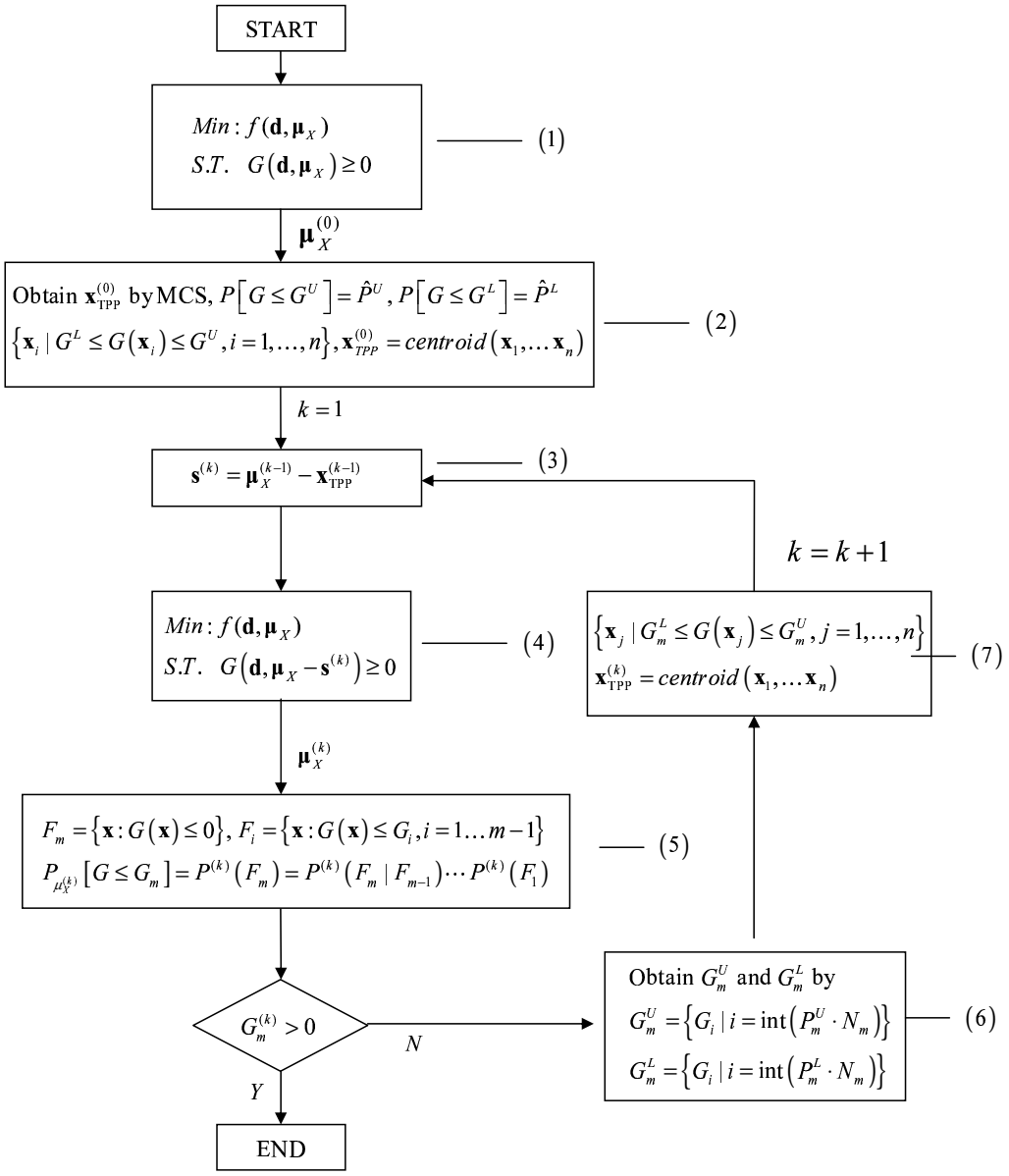


Figure 22.Particle splitting-based reliability assessment

The flowchart shown in Fig. 22 depicts the algorithm of SORA with particle splitting-based reliability assessment. It is explained below:

(1) A deterministic optimization problem with constraint $G_i(\mathbf{d}, \mu_X) \geq 0$ is solved and the solution $\mu_X^{(0)}$ is typically obtained on the deterministic boundary $G_i(\mathbf{d}, \mu_X) = 0$.

(2) As no uncertainties are considered in the deterministic optimization, the current reliability performance of $\mu_X^{(0)}$ can be evaluated by direct MSC because it is relative large comparing with the target failure probability. $N_1$ samples are simulated to obtain the estimated failure probability as $\hat{P}_F = \frac{1}{N_1}\sum_{k=1}^{N_1} I_F(\mathbf{x}_k)$. The upper bound and lower bound of target failure probability are $P_t^U = P_t + z_{\alpha/2}\sqrt{\frac{(1-P_t)P_t}{N_1}}$ and $P_t^L = P_t - z_{\alpha/2}\sqrt{\frac{(1-P_t)P_t}{N_1}}$, respectively.

In order to satisfy $Prob(G \leq G^U) = P_t^U$, we find the value $G^U = \{G_i | i = int(P_t^U \cdot N_1)\}$ in the sequence $(G_1, G_2, \ldots G_{N_1})$, where $G_1 < G_2 < \ldots < G_{N_1}$. Similar logic can be applied to obtain the value $G^L$. A set of samples $\{\mathbf{x}_i | G^L \leq G(\mathbf{x}_i) \leq G^U, i = 1, \ldots, n\}$ are collected between $G^L$ and $G^U$. Then the TPP is derived as the centroid of $(\mathbf{x}_1, \ldots, \mathbf{x}_n)$.

(3) Based on the TPP, a shifting vector $\mathbf{s}^{(1)} = \mu_X^{(0)} - \mathbf{x}_{\text{TPP}}^{(0)}$ is derived to modify the decision variable $\mu_X$, so that the TPP is moved at least onto the deterministic boundary to ensure the feasibility.

(4) Solve the updated deterministic optimization problem with constraint $G(\mathbf{d}, \mu_X - \mathbf{s}^{(k)}) \geq 0$ and derive the solution $\mu_X^{(k)}$.

(5) Given $\mu_X^{(k)}$, the particle splitting process with predefined equally $P_i$ can be implemented in Fig. 23, where $P^{(k)}(F_1)$ is evaluated by MCS and $P^{(k)}(F_2|F_1), \ldots,$ $P^{(k)}(F_m|F_{m-1})$ are evaluated by MCMC adaptively.

Based on the samples in the $m^{th}$ subset, we can find the limit value $G_m = \{G_i | i = int(P_m \cdot N_m)\}$. If $G_m > 0$, it can be concluded that $P_{\mu_X^{(k)}}[G \leq 0] < P_t$ because $P_{\mu_X^{(k)}}[G \leq G_m] = P_t$ and $G_m > 0$. Thus the optimal solution $\mu_X^{(k)}$ is feasible and the algorithm converges. If $G_m < 0$, it means the actual failure probability is greater than target failure probability $P_t$ and the current optimal solution is infeasible.

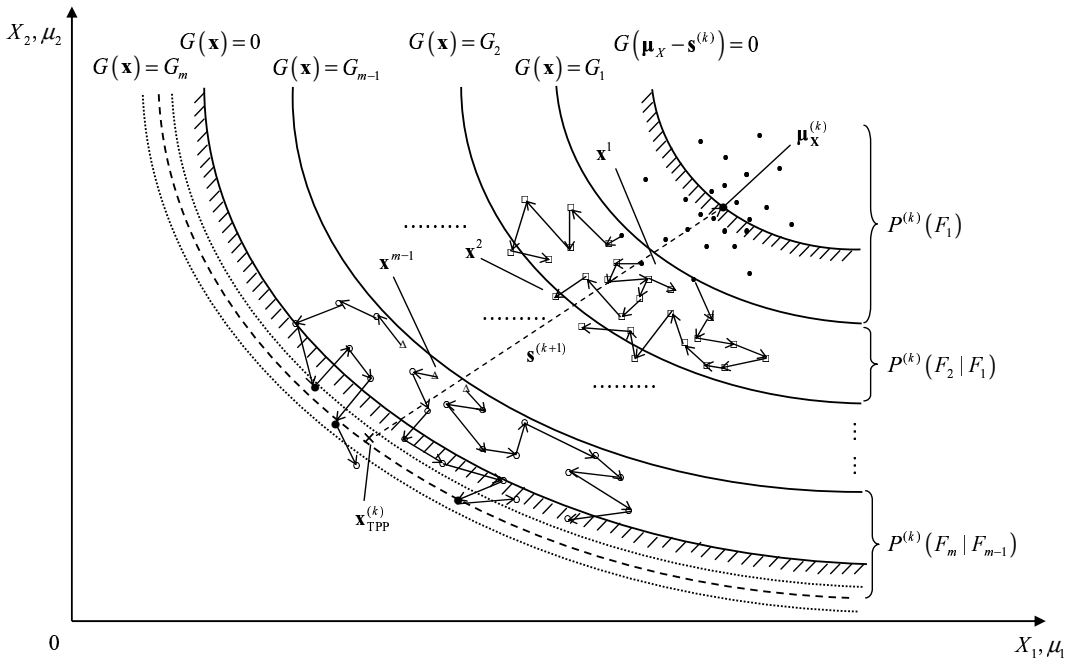


Figure 23.Particle splitting samples

(6) To derive TPP and moving vector, the upper bound and lower bound of $P_m$ are derived as $P_m^U = P_m + z_{\alpha/2}\sqrt{\frac{(1-P_m)P_m}{N_m}}$ and $P_m^L = P_m - z_{\alpha/2}\sqrt{\frac{(1-P_m)P_m}{N_m}}$, respectively. Then the limit values $G_m^U = \{G_i | i = int(P_m^U \cdot N_m)\}$ and $G_m^L = \{G_i | i = int(P_m^L \cdot N_m)\}$ are obtained in the ascending sequence $G_1 < G_2 < \ldots < G_{N_m}$. In Fig. 23, two dotted curve $G_m^U$ and $G_m^L$ are used to represent the upper and lower bound of $G(\mathbf{x}) = G_m$, respectively.

(7) A set of samples $\{\mathbf{x}_j | G_m^L \leq G(\mathbf{x}_j) \leq G_m^U, j = 1, \ldots, n\}$ are collected, which are represented by solid points in Fig. 23. Then a shifting vector $\mathbf{s}^{(k+1)} = \mu_{\mathbf{X}}{}^{(k)} - \mathbf{x}_{\mathrm{TPP}}^{(k)}$ is derived, where $\mathbf{x}_{\mathrm{TPP}}$ is the centroid of samples collected above. The probability of the sequential partial failure events and shifting vector are depicted in Fig. 24. The process is continued until $G_m^{(k)}$ is greater than zero, then the RBDO optimal solution based on particle splitting is obtained.

Comparing to other RBDO solutions, the proposed SORA with particle

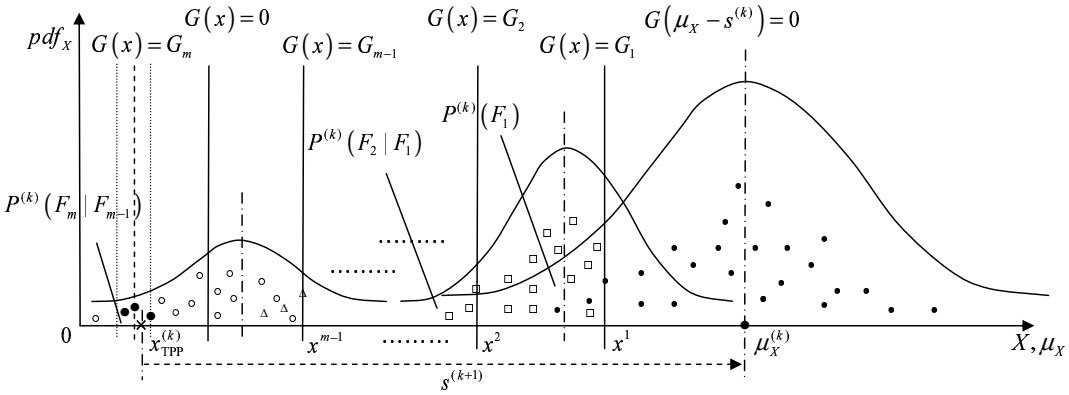


Figure 24.TPP location by particle splitting

splitting approach has the following advantages: First, the sequential optimization method is more computationally efficient than the double-loop methods such as [27], while it is more accurate than the single-loop methods such as [48], [76]. Second, the particle splitting-based reliability analysis is a simulation approach to the probabilistic constraint assessment, which is more accurate than the MPP-based method; at the same time, the particle splitting method improves the efficiency of random sampling in the design space. In addition, this approach can be easily extended to handle RBDO problems with multiple constraints without significantly increasing computation burden. Lastly, this approach is applicable to implicit constraint functions, e.g. a black-box computer model for evaluating product reliability, as long as the constraint function evaluation is affordable.

*Extension to RBDO with Multiple Probabilistic Constraints*

Simulation-based reliability assessment methods are, in general, dimensional free, but they require a large number of samples in the design space to estimate the probability. Engineering problems often encounter more than one probabilistic constraints. In this section, we discuss the extension of the particle splitting-based approach to the RBDO problem with multiple constraints. Without taking addi-

tional samples to assess more constraints, we share the samples among multiple constraints by combining multiple constraints into one constraint. Thus the computation of a complex RBDO problem with multiple constraints does not significantly increase comparing with the problem with a single constraint.

Suppose we have an RBDO problem with two probabilistic constraints $P = Prob[G_1(\mathbf{x}) < 0] < P_{t_1}$ and $P = Prob[G_2(\mathbf{x}) < 0] < P_{t_2}$, where $P_{t_1}$ and $P_{t_2}$ are target failure probabilities, respectively, to the two constraints. We can obtain the optimal solution $\mu_{\mathbf{X}}$ by iteratively solving following deterministic optimization problem,

$$\begin{aligned} &\text{Minimize } f(\mathbf{d}, \mu_{\mathbf{X}}) \\ &\text{Subject to } G_1(\mathbf{d}, \mu_{\mathbf{X}} - \mathbf{s}_1) \geq 0 \\ &\qquad\qquad G_2(\mathbf{d}, \mu_{\mathbf{X}} - \mathbf{s}_2) \geq 0 \end{aligned} \tag{4.14}$$

The particle splitting method is applied on evaluating the combination of two probabilistic constraints. Suppose $Prob[G_1(\mathbf{x}) < 0] = P(A)$ and $Prob[G_2(\mathbf{x}) < 0] = P(B)$, then the joint probability of $AB$ is given by $P(AB) = P(A)P(B|A)$, which is the same as $P_F = Prob[G_1 < 0, G_2 < 0] = Prob[G_1 < 0]Prob[G_2 < 0|G_1 < 0]$. We apply the particle splitting method on assessing the joint probability and the probability of the first constraint. If $P_F$ assessed to be less than $P_{t_1} \times P_{t_2}$ while guarantee the probability of the first constraint less than its own target $Prob[G_1 < 0] < P_{t_1}$, then the probability of the second constraint $Prob[G_2 < 0|G_1 < 0] < P_{t_2}$ will be automatically satisfied. In RBDO, $G_1$ and $G_2$ are two performance functions to describe two different aspects of the product or system. Also both $G_1 < 0$ and $G_2 < 0$ are rare events, the result of $G_2 < 0$ takes very little effects on $G_1 < 0$. Thus we can assume $G_1 < 0$ and $G_2 < 0$ to be independent, then $Prob[G_2 < 0] = Prob[G_2 < 0|G_1 < 0] < P_{t_2}$ is satisfied.

Suppose the target joint failure probability is $P_t = P_{t_1} \times P_{t_2}$ and $m$ subsets

are employed based on the scale of $P_t$. For the purpose of convenience, we set equal partial failure probability for each subset, i.e. $P_1 = P_2 = \cdots = P_m = \sqrt[m]{P_t} = \sqrt[m]{P_{t_1}}\sqrt[m]{P_{t_2}}$.

In the first subset, MCS is used to simulate $N_1$ samples. A critical value $G_1^1$ is obtained to satisfy $Prob[G_1(\mathbf{x}) < G_1^1] = \sqrt[m]{P_{t_1}}$, then $N_{11} = N_1\sqrt[m]{P_{t_1}}$ samples have the $G$ values to be less than $G_1^1$ in all $N_1$ samples. Similarly, a second critical value $G_2^1$ is obtained to satisfy $Prob[G_2 < G_2^1 | G_1 < G_1^1] = \sqrt[m]{P_{t_2}}$ in all $N_{11}$ samples. Thus the partial failure probability of the first subset is $P(F_1) = Prob[G_1 < G_1^1, G_2 < G_2^1] = Prob[G_1 < G_1^1]Prob[G_2 < G_2^1 | G_1 < G_1^1] = P_1$. By setting the partial failure probability and limit values in this way, we can guarantee the particle diversity since $P_1 \times N_1$ particles are selected to generate sample paths in the next subset.

From the second subset, the conditional probability $P(F_{i+1}|F_i)$ is evaluated by MCMC as shown in Fig. 25. When all $m$ subsets are evaluated, we can get the first constraint as $Prob[G_1 < G_1^m] = Prob[G_1 < G_1^1]Prob[G_1 < G_1^2]\cdots Prob[G_1 < G_1^m] = (\sqrt[m]{P_{t_1}})^m = P_{t_1}$. The joint probability $Prob[G_1 < G_1^m, G_2 < G_2^m] = (\sqrt[m]{P_{t_1}} \cdot \sqrt[m]{P_{t_2}})^m = P_{t_1} \cdot P_{t_2}$. Thus if $G_1^m \geq 0$ and $G_2^m \geq 0$, all constraints are satisfied.

A generic conditional probability formulation in $i^{th}$ subset is as follows:

$$\begin{aligned} P_i &= P(F_i|F_{i-1}) = Prob[G_1 < G_1^i, G_2 < G_2^i \cdots G_n < G_n^i | F_{i-1}] \\ &= Prob[G_1 < G_1^i | F_{i-1}] Prob[G_2 < G_2^i | G_1 < G_1^i, F_{i-1}] \\ &\cdots Prob[G_n < G_n^i | G_{n-1} < G_{n-1}^i \cdots G_1 < G_1^i, F_{i-1}] \\ &= \sqrt[m]{P_{t_1}}\sqrt[m]{P_{t_2}} \cdots \sqrt[m]{P_{t_n}} \end{aligned} \tag{4.15}$$

To derive the TPP of each constraint, we follow the similar procedure as in Step (6) and (7) in Fig. 22. A set of samples are located between the upper bound and lower bound of $G_1^m$ and $G_2^m$. As shown in Fig. 25, a set of samples for

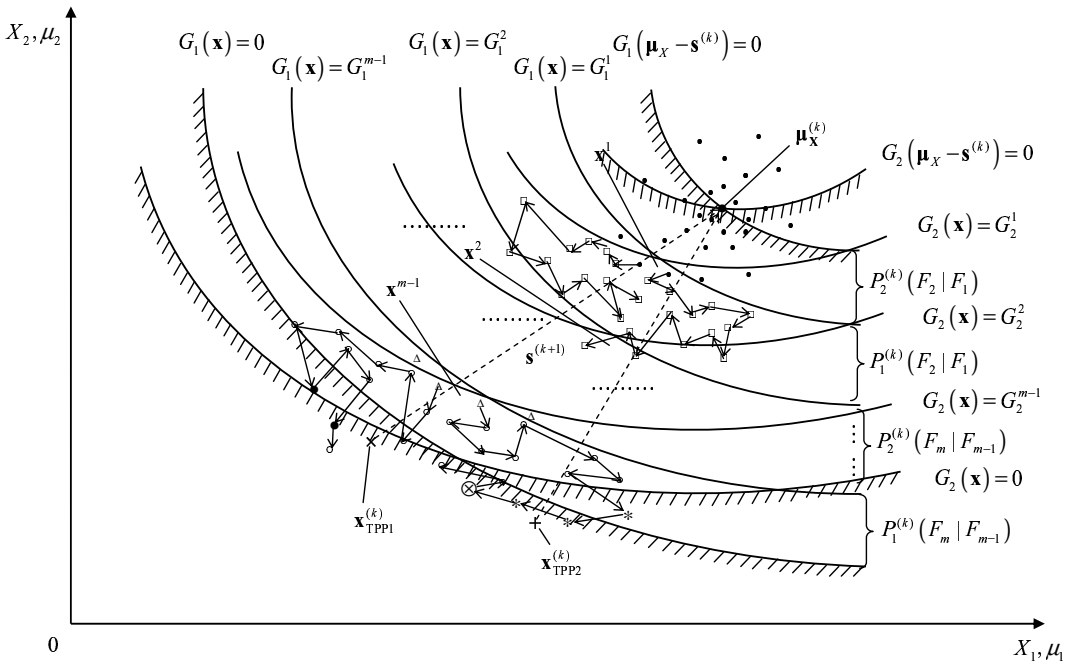


Figure 25.Particle splitting samples in multiple constraints

constraint $G_1$ are represented by the solid dots and cross circle point, and another set of samples for constraint $G_2$ are represented by the star and cross circle point. Thus TPPs are obtained by calculating the centroid of each set of samples. In particular, the cross circle falls in failure region and is used to calculate TPP for both constraints. If the targeted failure probabilities cannot be satisfied, shifting vectors $\mathbf{s}_1^{(k+1)} = \mu_{\mathbf{X}}{}^{(k)} - \mathbf{x}_{\mathrm{TPP}_1}^{(k)}$ or $\mathbf{s}_2^{(k+1)} = \mu_{\mathbf{X}}{}^{(k)} - \mathbf{x}_{\mathrm{TPP}_2}^{(k)}$ are derived, respectively. Thus the algorithm enters a new cycle and is continued until $Prob[G_1(\mathbf{x}) < 0, G_2(\mathbf{x}) < 0] < P_{t_1} \times P_{t_2}$ and $Prob[G_1(\mathbf{x}) < 0] < P_{t_1}$ are satisfied.

## 4.4 Examples

### *I-Beam Example*

The same I-beam RBDO problem in Section 2.5 is solved by the SORA with particle splitting in this section. First, the deterministic optimization loop is solved using genetic algorithm (GA), in which the initial population size is 1000 and GA

Table 13.Solution Steps by the Particle Splitting-Based Approach

| Cyc. | Method | $(\mu_1, \mu_2)$ | Obj | TPP | $P$ | Event No. | Samples |
|---|---|---|---|---|---|---|---|
| 1 | MCS | (43.26, 0.92) | 117.17 | (38.05, 0.96) | 0.497 | 1 | $10^3$ |
| 2 | PS | (47.42, 0.93) | 130.24 | (41.99, 0.97) | 0.0025 | 3 | $10^3$ |
| 3 | PS | (48.14, 0.93) | 132.40 | | 0.0009 | 3 | $10^3$ |

iteration number is set to be 3. Second, the reliability analysis loop is solved by particle splitting. Since the target failure probability is $1.3 \times 10^{-3}$, the failure event is subdivided into three sequential partial failure events, in which the failure probability is predefined to $P_i = 0.1$ for each subset. In order to keep the coefficient of variation $\delta$ to be about 0.1, $10^3$ samples are taken in each subset. The failure probability of the first subset is evaluated by MCS, and $10^3 \times 0.1 = 100$ particles used to generate the subsequent sampling path. In the following two subsets, MCMC in conjunction with the Metropolis-Hastings algorithm is employed. Three cycles are implemented in particle splitting-based decoupled-loop approach to obtain the RBDO optimal solution, which is shown in Table 13.

In each cycle, a shifting vector $\mathbf{s} = \mu - \mathbf{x}_{\text{TPP}}$ is derived if the failure probability is greater than the target failure probability. After three cycles, the optimal solution $(48.14, 0.93)$ with the objective value of 132.40 is obtained.

The accuracy and efficiency of the particle splitting-based approach are compared with the MCS-based method (ground truth) and the MPP-based method in Table 14. It is indicated that the optimal solution given by particle splitting is very close to the ground truth by MCS. Particle splitting only takes $3 \times 10^3$ samples to evaluate the target failure probability 0.0013 in one cycle under $\delta = 0.1$, while MCS needs to take about $10^5$ samples to evaluate the same target failure probability

Table 14.I-Beam Accuracy Comparison

| Method | $\mu_1$ | $\mu_2$ | Objective |
|---|---|---|---|
| MCS(ground truth) | 48.58 | 0.92 | 132.14 |
| Particle splitting | 48.14 | 0.93 | 132.40 |
| Decoupled-loop (SORA) | 49.73 | 0.92 | 135.16 |

under $\delta = 0.1$. Thus the efficiency of particle splitting is much higher with similar accuracy.

SORA is an MPP-based method. Table 14 shows that the optimal solution given by the particle splitting algorithm is closer to the ground truth comparing to the SORA solution. The efficiency of particle splitting-based approach and SORA can be compared by their sample sizes and computation times. In SORA, the reliability analysis step is converted to an optimization by PMA. It employs GA with 3 iterations, where 1000 initial samples are taken in each iteration. 9000 samples are taken in three SORA cycles, and the computation time is 2 minutes in Matlab 2010B. In the particle splitting-based method, each subset requires 1000 samples as shown in Table 13. There are 7000 samples being taken in three cycles and the computation time is 1.5 minutes in Matlab 2010B.

*An Example with Multiple Constraints*

In order to show the application of the particle splitting-based reliability analysis approach on multiple probabilistic constraints, a widely used numerical example in [76], [65], [39], [45], [40] is employed here. It has two random variables and three probabilistic constraints. The results are compared with the ground truth and other existing approaches, including SORA, double-loop methods (DLM) with PMA, traditional approximation method (TAM), single loop single variable (SLSV), mean

value method (MVM), and two-level approximation method (TLA). The problem formulation is:

$$
\begin{aligned}
&\text{Minimize: } f(\mu) = \mu_1 + \mu_2 \\
&\text{Subject to: } Prob[G_1(\mathbf{x}) = \frac{x_1^2 x_2}{20} - 1 \geq 0] \geq R_1 \\
&\qquad Prob[G_2(\mathbf{x}) = \frac{(x_1 + x_2 - 5)^2}{30} + \frac{(x_1 - x_2 - 12)^2}{120} - 1 \geq 0] \geq R_2 \\
&\qquad Prob[G_3(\mathbf{x}) = \frac{80}{x_1^2 + 8x_2 + 5} - 1 \geq 0] \geq R_3 \\
&\qquad 0 \leq \mu_1 \leq 10, 0 \leq \mu_2 \leq 10 \\
&\qquad X_1 \sim N(\mu_1, 0.3^2), X_2 \sim N(\mu_2, 0.3^2)
\end{aligned}
\tag{4.16}
$$

where three reliability level $R_1 = R_2 = R_3 = 0.9987$, thus the target failure probability is 0.0013.

Table 15 shows the solution when the particle splitting-based reliability assessment method is applied on this example. The first cycle is evaluated by $10^3$ MCS samples since the target failure probability is approximated to be 0.5. The second and third cycles are evaluated by particle splitting. The coefficient of variation $\delta$ is selected as the estimator accuracy criterion as in [49]. Since the target failure probability is 0.0013, we will have three subsets if we set the partial failure probability $P(F_1) = P_1 \approx 0.11$, $P(F_2|F_1) = P_2 \approx 0.11$, $P(F_3|F_2) = P_3 \approx 0.11$ and $P(F_1)P(F_2|F_1)P(F_3|F_2) \approx 0.0013$. Under the level of $\delta = 0.1$, $10^3$ samples are taken to estimate the target probability 0.11. According to the result from the first cycle, the constraint $Prob[G_3(\mathbf{x}) \geq 0] \approx 0$ since the decision variable $\mu$ is far from the constraint of $G_3$ as shown in Fig. 26. Thus the constraint of $G_3$ can be dropped and we only need to consider constraints of $G_1$ and $G_2$. We set $Prob[G_2 < 0|G_1 < 0] \approx \sqrt{0.11} = 0.33$ and $Prob[G_1 < 0] \approx 0.33$, so that $P(F_1) = Prob[G_2 < 0|G_1 < 0]Prob[G_1 < 0] \approx 0.11$. After three cycles, the optimal solution

Table 15.Results by the Particle Splitting-Based Approach

| Cycle | $(\mu_1, \mu_2)$ | Objective | Method | Events | Event Target probability | samples |
|---|---|---|---|---|---|---|
| 1 | (3.1068,2.1008) | 5.2076 | MCS | 1 | 0.5 | $10^3$ |
| 2 | (3.3185,3.2192) | 6.7064 | PS | 6 | 0.33 | $6 \times 10^3$ |
| 3 | (3.4374,3.2719) | 6.7093 | PS | 6 | 0.33 | $6 \times 10^3$ |

achieves $(3.4374, 3.2719)$ with the minimum objective 6.7093.

In Fig. 26, the optimal solution of the particle splitting-based reliability assessment approach is denoted as a cross sign from Cycle 1 to Cycle 3. Each optimal solution has a circle region where 99.87% samples are located. If the current optimal solution is feasible, the circle region should be included in the deterministic feasible region by $G_1 \geq 0$, $G_2 \geq 0$ and $G_3 \geq 0$. From Fig. 26 we can see the circle of Mu Cycle 3 is completely included in the deterministic feasible region, thus the optimal solution in Cycle 3 is feasible.

The true solution, $\mu = (3.4106, 3.1577)$, with the objective value of 6.5683 is obtained by the double-loop Monte Carlo simulation approach. From Table 16 we can see that particle splitting-based approach can give an accurate optimal solution which is very close to ground truth. There are $10^3$ samples taken to estimate the each partial event target probability 0.33, and totally $1.3 \times 10^4$ samples are taken in three cycles. In MCS, $10^5$ samples are required to estimate the target probability $1.3 \times 10^{-3}$ in Cycle 2 and Cycle 3 under the $\delta = 0.1$ level, and the total sample size could be over $2 \times 10^5$. Thus the efficiency of particle splitting-based approach is much higher than MCS.

In Table 16, the particle splitting-based approach is compared with other

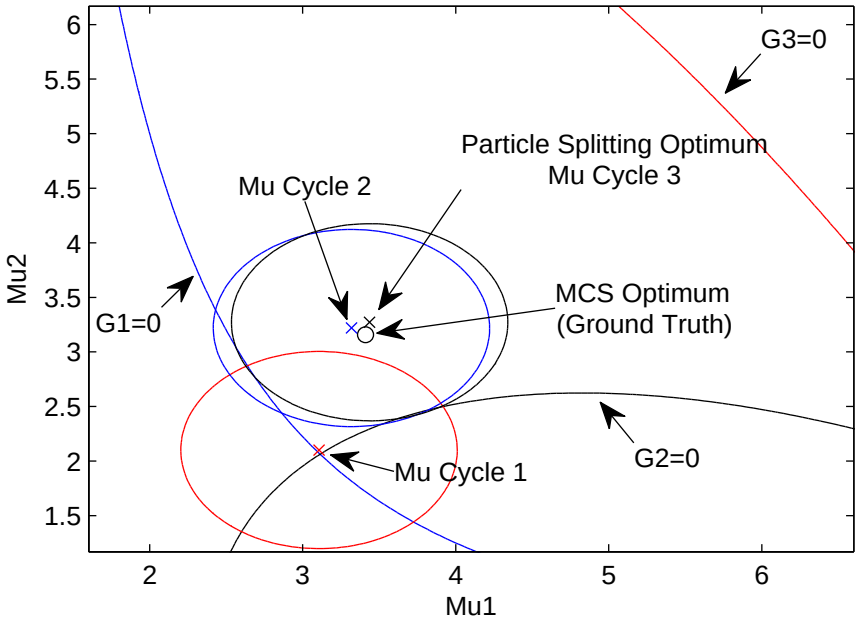


Figure 26.Particle splitting optimal solution

existing popular RBDO methods [65]. It is indicated that the optimal solutions by DLM, SLSV, TAM, TLA, MVM, SORA and SLM are more conservative than the optimal solution by particle splitting-based approach. One important reason is that these methods make approximations of constraint functions in reliability assessment. For examples, SORA has a first-order reliability method (FORM) approximation in reliability assessment; TLA uses a reduced second-order approximation in the first level and uses a linear approximation in the second level. In reality, the true constraint function can be highly nonlinear, so lower order approximation cannot capture the irregular function shape very well. These approximations usually lead to inaccurate optimal solutions, either conservative or infeasible. The solution given by particle splitting-based approach is the closest one to the ground truth. However, the particle splitting-based approach is a simulation method, so its computational efficiency is lower than other methods.

Table 16.Comparing Accuracy of the Solutions by Different Methods

| Method | Objective | Overall constraint evaluations | Iterations |
|---|---|---|---|
| PS | 6.709 | $1.3\times10^4$ | 3 |
| DLM | 6.737 | 636 | 5 |
| MVM | 7.148 | 72 | 5 |
| SLSV | 6.729 | 156 | 5 |
| TAM | 6.733 | 372 | 5 |
| TLA | 6.732 | 60 | 4 |
| SORA | 6.732 | 455 | 5 |

## 4.5 Conclusion and Future Work

In this chapter, a new simulation-based reliability analysis approach, the particle splitting method, is introduced to be integrated with the traditional sequential optimization method to solve RBDO problems. The simulation-based probability estimation is typically more accurate than the worst case analysis as in the MPP-based solutions, but it is more computationally intensive. In order to reduce computational burden and to enhance efficiency, we propose to use the particle splitting rare-event simulation method to replace MCS. Comparing to other rare-event simulation methods, particle splitting uses multiple particles to enhance the simulation diversity and consistency. In addition, this approach can be extended to address problems with multiple constraints without significantly increasing sample size. The strength of our proposed method lies on that we combine the merits of SORA and simulation-based reliability assessment such that it can provide a balanced solution, which is as accurate as the Monte Carlo simulation method, but with greatly reduced number of samples.

As mentioned in Section 4.3, the total sample size in particle splitting is equal to the product of number of subsets, number of particles and the length of

MCMC chain. Typically, the more subsets we have, the fewer samples are required in each subset evaluation since the partial probability is higher; the more particles in one subset we have, the larger simulation diversity it will be; the longer MCMC chain is, the closer it will get to the target distribution. The trade-offs among these three factors should be further investigated, especially for complex RBDO problems, e.g., RBDO with multiple objectives and/or multiple constraints. In addition, as mentioned in Section 4.2, subset simulation is one type of rare-event simulations. In future work, other rare-event simulation methods such as line sampling can be employed in reliability analysis in RBDO.

# CHAPTER 5

# RELIABILITY-BASED ROBUST DESIGN OPTIMIZATION UNDER IMPLICIT PERFORMANCE FUNCTIONS

## 5.1 Introduction

At the stage of product design and development, RBDO is used to address various uncertainties and improve product quality and reliability. From the point of view of mechanical engineering, the main task of RBDO is to keep the product design safe or reliable under the minimum production cost. However, traditional RBDO formulation and method have two drawbacks: First, most RBDO methods do not consider the impacts of noise variables in solving the problem. Although the random parameters or noise variables $\mathbf{p}$ are formulated in the performance function, they are often replaced by their mean values or ignored for the purpose of simplicity. Actually, two main issues can be considered based on the noise variables [69]: One is the design feasibility since the effect of variations due to noise variables will lead to feasible region shrinkage. The other one is the transmitted variation of performance function due to noise variables. Second, the objective cost function in RBDO only considers the production cost. However, the transmitted performance variation will cause the potential cost due to quality loss, which is the cost of quality-related efforts and deficiencies. In order to decrease the impacts of noise variables on both quality cost and design feasibility, robust design is introduced to address both feasibility robustness and objective robustness. Thus a reliability-based robust design optimization (RBRDO) problem is proposed in product design under implicit performance functions.

Robust design, first proposed by Taguchi, is an approach for improving the quality of a product by minimizing the effect of the causes of variation without eliminating the sources of variation [22]. Taguchi said robustness was the state where

the product or process performance was minimally sensitive to factors causing variability [68]. The key reason why impacts from uncontrollable noise variables could be minimized lies in the existence of interactions between controllable design variables and uncontrollable noise variables. Thus the objective of robust design is to select design variables to minimize the variability impact produced by the noise variables, and make the objective performance response close to the target value.

To encompass noise variables in robust design, one method is to assign probabilistic distributions to noise variables. Apley in [2] assigned normal distributions $N \sim (\mu_P, \sigma_P^2)$ to noise variables, then the performance response was also viewed as probabilistic; Tang in [83] assigned probabilistic distributions to noise variables and derived a robustness index measure. The other method is to employ non-probabilistic methods such as worst case analysis [69] and moment matching method [22]. Xu in [87] employed worst case analysis of maximum design parameter deviation $\Delta_P$, and proposed the robust design model based on maximum variation estimation. Under the consideration of noise variables, three typical robust design theories were proposed [68, 69]:

1. *Taguchi method* – In the early design stage, Taguchi provided a three-stage design: system design, parameter design and tolerance design [9], in which parameter design was the most important and used to derive optimal design parameters to satisfy the quality requirement. Comparing with ordinary optimization, Taguchi's method accounts for the performance variations due to noise factors. Suppose $G_i(\mathbf{x}, \mathbf{p}_i)$ is the performance function, where $\mathbf{x}$ and $\mathbf{p}_i$ are controllable variables and noise variables, respectively. A signal-to-noise ratio (SNR) is proposed to measure quality loss in Taguchi method as in Equation 1.1. In order to maximize SNR, design of experiments (DOE)

techniques are employed to assign the control factors to an experimental matrix. By evaluating different designs, the best condition can be selected from the full combinations of control factors. However, the orthogonal array and design variables in Taguchi method are defined in discrete space and difficult to be extended to wide design range. Also it is not efficient for a large size problem since the full combinations are costly. In addition, a general product design may have many design constraints which may not be solved by Taguchi method. To overcome the above disadvantages, robust optimization is proposed.

2. *Robust optimization* – Robust optimization (RD) approach explores the inherent nonlinear relationship among the design variables, noise variables and product performance. By introducing a well-developed optimization model, RD achieves the objective of optimizing the performance mean and minimizing the performance variation. It is a cost effective and efficient method to reduce the transmitted performance variation without eliminating the variation sources and suffer smaller quality loss. A generic form of RD model is given as follows:

$$\begin{aligned} &\text{Minimize } Var[G_i(\mathbf{d},\mathbf{x},\mathbf{p})] \\ &\text{Subject to } E[G_i(\mathbf{d},\mathbf{x},\mathbf{p})] \geq T_i \quad i = 1,2,\ldots,m \\ &\qquad \mathbf{d^L} \leq \mathbf{d} \leq \mathbf{d^U}, \mu_{\mathbf{X}}^{\mathbf{L}} \leq \mu_{\mathbf{X}} \leq \mu_{\mathbf{X}}^{\mathbf{U}}, \mu_{\mathbf{P}}^{\mathbf{L}} \leq \mu_{\mathbf{P}} \leq \mu_{\mathbf{P}}^{\mathbf{U}} \end{aligned} \tag{5.1}$$

where $G_i(\mathbf{d},\mathbf{x},\mathbf{p})$ is the $i^{th}$ product performance function, and $Var[G_i(\mathbf{d},\mathbf{x},\mathbf{p})]$ represents its variance and can be considered as quality loss measure. $T_i$ is the given target performance for the $i^{th}$ performance function. The robust design objective, quality loss function, can be measured by many methods, for examples, a performance percentile difference method was proposed in

[60], in which the performance variation was expressed by the spread of its PDF; a robust index derived from the acceptable performance variation was proposed in [47]; a coefficient of variation measure was provided in [1].

3. *Robust design with axiomatic approach* – The axiomatic design was first proposed by Suh in [79, 80]. Two fundamental axioms were provided in the framework for robust design: The independence axiom was used to maintain the independence of functional requirements; the information axiom was used to minimize the information content in a design. An integration design optimization framework of robust design, axiomatic design and reliability-based design was proposed in [77]. A review of robust design in axiomatic design was given in [68].

Our research contributions are: Firstly, the quality loss objective of robust design is integrated into RBDO to formulate an RBRDO problem. Secondly, different from traditional RBDO problems with explicit performance functions, we consider implicit performance functions in formulating and solving RBRDO problems. The metamodels are used and updated by a sequential EI criterion-based sampling approach. Finally, we extend the sequential sampling approach to address both random variables and random parameters (or noise variables) in order to improve RBRDO solutions.

The remaining part of the chapter is organized as follows: Section 5.2 presents an RBRDO formulation with implicit performance functions. Section 5.3 proposes a sequential sampling approach to improve both reliability and robustness in RBRDO problem. Section 5.4 illustrates the proposed method by I-beam example. Section 5.5 presents the conclusion and future work.

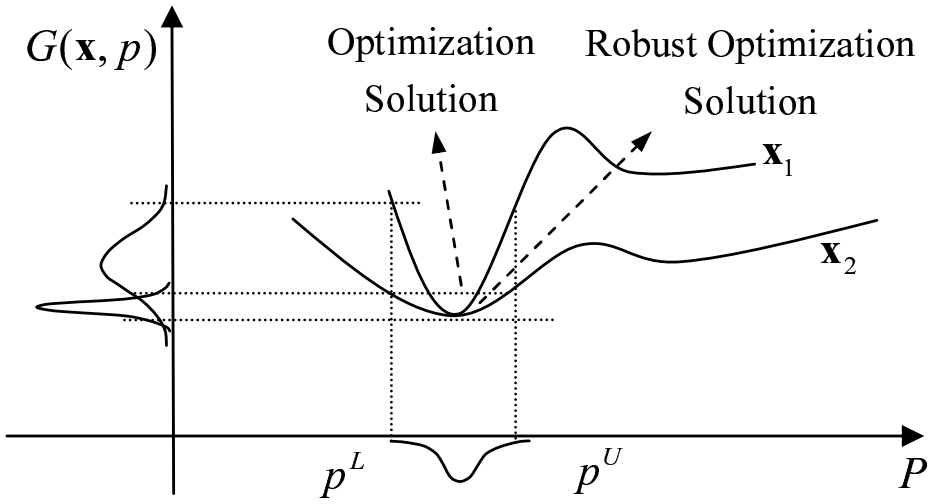


Figure 27.Noise variable impacts on performance function

## 5.2 Reliability-Based Robust Design Optimization

As mentioned in Section 5.1, RBDO concentrates to guarantee the design feasibility by probabilistic constraints under the existence of random variables. The design objective is to minimize the production cost, but it does not attempt to minimize the performance variation transmitted from the noise variables. A comparison between optimization solution and robust optimization solution is shown in Fig. 27, in which both decision variables $\mu_X^1$ and $\mu_X^2$ can achieve the same performance value. However, the performance value derived by $\mu_X^2$ is insensitive to the fluctuation from noise variable **p**. Thus the goal of robust design is to find a set of decision variables **d**, $\mu_{\mathbf{X}}$, in which mean performance value can satisfy target reliability requirement and the variability produced by the noise variables can be minimized. It is our belief to consider two major paradigms reliability and robustness together in a united RBRDO formulation.

*RBRDO Formulation*

In order to integrate robustness and reliability, a formulation is proposed as follows:

$$\begin{aligned} &\text{Minimize } E[f(\mathbf{d},\mathbf{x},\mathbf{p})] \\ &\text{Minimize } Var[G_i(\mathbf{d},\mathbf{x},\mathbf{p})] \\ &\text{Subject to } P[G_i(\mathbf{d},\mathbf{x},\mathbf{p}) \geq 0] \geq R_i \quad i = 1,2,\ldots,m \\ &\qquad \mathbf{d^L} \leq \mathbf{d} \leq \mathbf{d^U}, \mu_{\mathbf{X}}^{\mathbf{L}} \leq \mu_{\mathbf{X}} \leq \mu_{\mathbf{X}}^{\mathbf{U}}, \mu_{\mathbf{P}}^{\mathbf{L}} \leq \mu_{\mathbf{P}} \leq \mu_{\mathbf{P}}^{\mathbf{U}} \end{aligned} \tag{5.2}$$

where $E[f(\mathbf{d},\mathbf{x},\mathbf{p})]$ is the expectation production cost objective. $Var[G_i(\mathbf{d},\mathbf{x},\mathbf{p})]$ is transmitted performance variation produced by noise variables and is employed to represent quality loss objective. In this chapter, Delta method [69, 68] is used to estimate $Var[G_i(\mathbf{d},\mathbf{x},\mathbf{p})]$ as:

$$\begin{aligned} Var[G_i] &= \sum_{j=1}^{nx} \left(\frac{\partial G}{\partial x_j}\sigma_{X_j}\right)^2 + \sum_{j=1}^{np} \left(\frac{\partial G}{\partial p_j}\sigma_{P_j}\right)^2 \\ &= \sum_{j=1}^{nx} [G'(\mu_{X_j})]^2\sigma_{X_j}^2 + \sum_{j=1}^{np} [G'(\mu_{P_j})]^2\sigma_{P_j}^2 \end{aligned} \tag{5.3}$$

where $Var[G_i]$ is a function of $\mu_{\mathbf{X}}$ and is denoted as $V(\mu_{\mathbf{X}})$. $nx$ and $np$ are the number of random variables and noise variables, respectively. This expression does not assume underlying distribution for $x$ and $p$.

Under the formulation of multi-objectives, the optimal solution of RBRDO is known as a Pareto set or Pareto frontier, which denotes the trade-off between production cost and quality loss.

*Sequential Optimization and Reliability Analysis (SORA) in RBRDO*

In this chapter, SORA is extended to solve an RBRDO problem, a deterministic optimization loop is first solved as follows:

$$\begin{aligned} &\text{Minimize } f(\mathbf{d}, \mu_{\mathbf{X}}) \\ &\text{Minimize } V(\mu_{\mathbf{X}}) \\ &\text{Subject to } G_i(\mathbf{d}, \mu_{\mathbf{X}}, \mu_{\mathbf{P}}) \geq 0 \quad i = 1, 2, \ldots, m \end{aligned} \tag{5.4}$$

Based on the design variable $\mu_{\mathbf{X}}$ and given $\sigma_{\mathbf{X}}$, the X-space is transformed to U-space. Then another optimization loop in Formulation 3.5 is solved in U-space by PMA, the optimal solution is the inverse MPP ($\mathbf{u}_{\text{MPP}}$) locating on the targeted reliability surface. Then we can find the R-percentile $G^R = G(\mathbf{u}_{\text{MPP}})$. If $G^R = G(\mathbf{u}_{\text{MPP}}) \geq 0$, design variable $\mu_{\mathbf{X}}$ is feasible and it is the final optimal solution; otherwise, a shifting vector $\mathbf{s}^{(2)} = \mu_{\mathbf{X}}{}^{(1)} - \mathbf{x}_{MPP}^{(1)}$, derived in Formulation 3.7, is used to modify the current decision variable. The algorithm continues until $G^R(\mathbf{d}, \mathbf{x}_{MPP}) \geq 0$ in some iteration.

In this chapter, RBRDO is solved with implicit performance function and metamodel-based approach is used. Thus performance function $G$ is replaced by a Kriging metamodel $\hat{G}$, which is constructed based on samples by conducting computer experiments.

## 5.3 Sequential Sampling Strategy in RBRDO Under Implicit Performance Function

In order to obtain an RBRDO solution, a multi-objective optimization needs to be solved, in which probabilistic constraints evaluation may dominate the computational effort. The decoupled-loop methods such as SORA is well accepted because of the high efficiency and good accuracy. However, traditional SORA only deals

with problems with explicit performance (constraint) functions. Also the transmitted variation of performance function due to noise variables is not considered. In this section, a sequential sampling approach is proposed to address epistemic uncertainty due to implicit performance function and improve the solution of RBRDO.

*Hybrid Design and Combined Metamodel in RBRDO*

A hybrid design is proposed in this chapter to build a Kriging model to consider both random variables and noise variables. In particular, a Latin hypercube sampling (LHS) [56, 36] is employed for controllable variables since it is efficient for a complex computer model. A factorial design [59] is employed for noise variables or random parameters, since it can highlight the impact of noise variables.

Due to the existence of noise variables, the approximated performance model in this chapter is a combined metamodel of several Kriging models under different design levels of noise variables. For the purpose of simplicity, one noise variable $p$ with two levels $-1$ and $+1$ is considered in this chapter, then we have the combined metamodel as:

$$\hat{G}(\mathbf{x}, p) = \frac{1-p}{2}\hat{G}_{-}(\mathbf{x}) + \frac{1+p}{2}\hat{G}_{+}(\mathbf{x}) \tag{5.5}$$

where $\hat{G}_{-}(\mathbf{x})$ is the Kriging model built on the Latin hypercube samples under $p = -1$, and $\hat{G}_{+}(\mathbf{x})$ is the Kriging model built on the Latin hypercube samples under $p = +1$. Here $p = -1$ and $p = +1$ represent the values $\mu_P - \sigma_P$ and $\mu_P + \sigma_P$, respectively. $\mu_P$ is the value of the center point $p = 0$.

*Expected Improvement Criterion*

A Kriging model is constructed based on the samples from the hybrid design. Theoretically, the more samples are taken, the closer the Kriging model would get to the true model. In reality, the metamodel $\hat{G}$ has prediction errors since only limited

samples are available due to cost or computation effort. The prediction errors of $\hat{G}$ are different from area to area. Areas with more samples have smaller prediction errors and areas with fewer samples have larger prediction errors. Thus areas with fewer samples have the potential of containing true MPP instead of current minimum point. The EI criterion in Section 3.3 is extended in this section to tackle a multi-objective RBRDO problem with implicit performance functions.

*RBRDO Solution by Sequential EI-Based Sampling Strategy*

Based on the performance variation measure mentioned in Section 5.2, Formulation 5.3 is used to represent the quality loss. A weighted sum approach is employed to consider production cost and quality loss simultaneously. Then a pareto frontier is generated by different weight combinations. To consider the impact of noise variables, the combined metamodel is proposed and EI criterion is used to add new samples to update the combined metamodel. The detailed sequential EI-based sampling RBRDO strategy in Fig. 28 is as follows:

(1) Assign $m$ different weight combinations $w_0$ and $1-w_0$ to production cost objective and quality loss objective, respectively. Under each $w_0$ value, an optimization problem with weighted sum objective is solved.

(2) Similar as in SORA, an optimization problem is first solved with deterministic constraints as:

$$\begin{aligned} &\text{Minimize } w_0 f(\mathbf{d}, \mu_{\mathbf{X}}) + (1-w_0)V(\mu_{\mathbf{X}}) \\ &\text{Subject to } \hat{G}^k(\mathbf{d}, \mathbf{x}, p) \geq 0 \end{aligned} \tag{5.6}$$

where $\hat{G}^k = \frac{1-p}{2}\hat{G}^k_-(\mathbf{x}) + \frac{1+p}{2}\hat{G}^k_+(\mathbf{x})$ is the combined metamodel in $k^{th}$ iteration. Since $0 \leq \frac{1-p}{2}, \frac{1+p}{2} \leq 1$ and $\frac{1-p}{2} + \frac{1+p}{2} = 1$, $\hat{G}^k$ is a linear combination of $\hat{G}^k_-$ and $\hat{G}^k_+$. Then $\hat{G}^k \geq 0$ is guaranteed if $\hat{G}^k_- \geq 0$ and $\hat{G}^k_+ \geq 0$. Thus we can reformulate

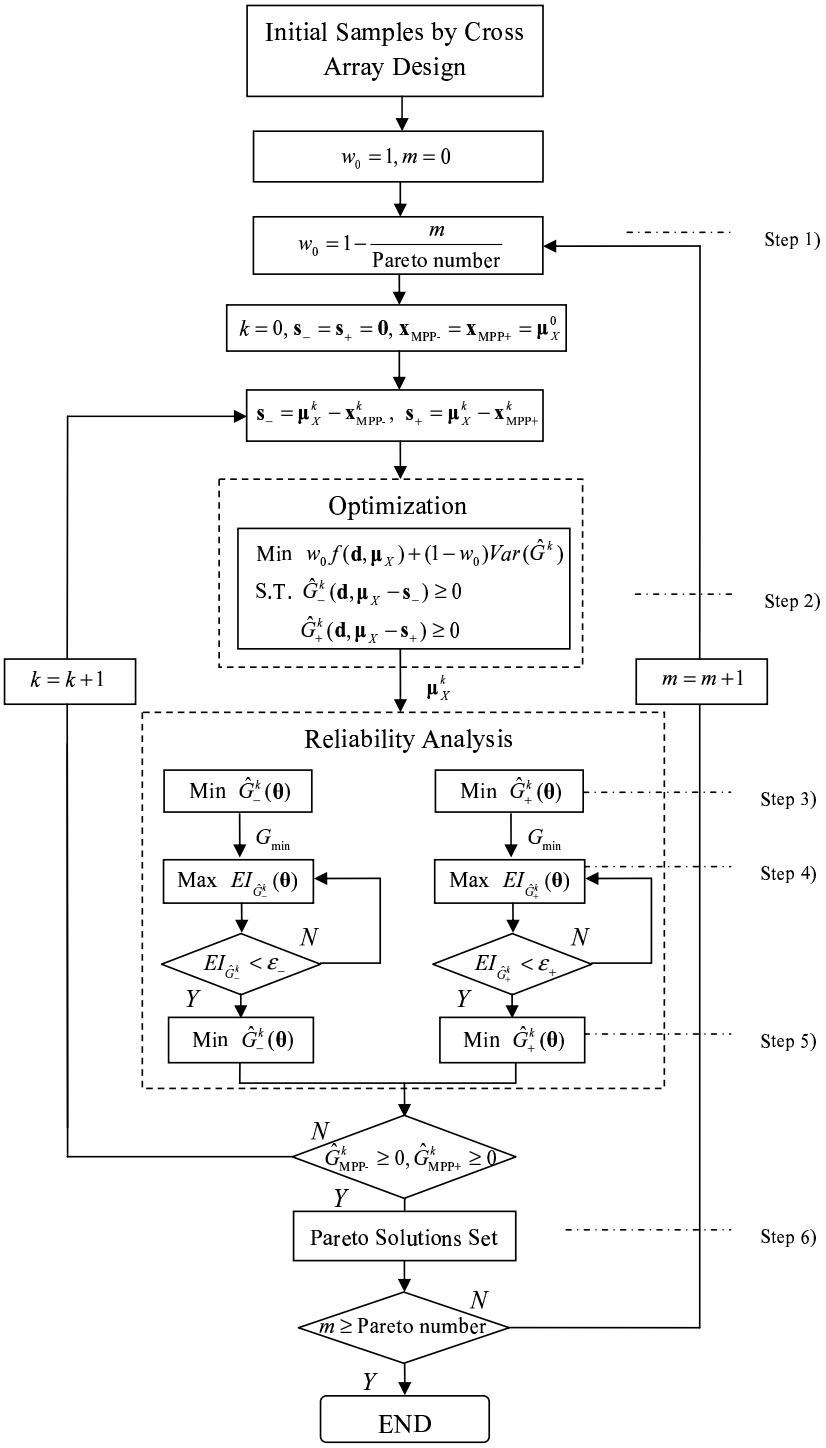


Figure 28.RBRDO algorithm

the optimization problem as follows:

$$\begin{aligned} &\text{Minimize } w_0 f(\mathbf{d}, \mu_{\mathbf{X}}) + (1-w_0)V(\mu_{\mathbf{X}}) \\ &\text{Subject to } \hat{G}_-^k(\mathbf{d}, \mu_{\mathbf{X}} - \mathbf{s}_-) \geq 0 \\ &\qquad\qquad \hat{G}_+^k(\mathbf{d}, \mu_{\mathbf{X}} - \mathbf{s}_+) \geq 0 \end{aligned} \tag{5.7}$$

According to Equation 5.3, the quality loss represented by transmitted performance variation is:

$$\begin{aligned} Var(\hat{G}) &= \left(\frac{\partial \hat{G}}{\partial x}\right)^2 |_{\mu_{\mathbf{X}}, \mu_P} {\sigma_{\mathbf{X}}}^2 + \left(\frac{\partial \hat{G}}{\partial p}\right)^2 |_{\mu_{\mathbf{X}}, \mu_P} \sigma_P^2 \\ &= \left[\frac{1-p}{2}\hat{G}'_- + \frac{1+p}{2}\hat{G}'_+\right]^2 |_{\mu_{\mathbf{X}}, \mu_P} {\sigma_{\mathbf{X}}}^2 + \left[\frac{1}{2}\hat{G}_+ - \frac{1}{2}\hat{G}_-\right]^2 |_{\mu_{\mathbf{X}}, \mu_P} \sigma_P^2 \\ &= \left[\frac{1}{2}\hat{G}'_-(\mu_{\mathbf{X}}) + \frac{1}{2}\hat{G}'_+(\mu_{\mathbf{X}})\right]^2 {\sigma_{\mathbf{X}}}^2 + \left[\frac{1}{2}\hat{G}_+(\mu_{\mathbf{X}}) - \frac{1}{2}\hat{G}_-(\mu_{\mathbf{X}})\right]^2 \sigma_P^2 \end{aligned} \tag{5.8}$$

Two constraints are considered, in which $\hat{G}_-$ and $\hat{G}_+$ are built on the Latin hypercube array samples when $p$ is on low level and high level in the factorial array, respectively. The optimal solution is a vector of decision variable $\mu_{\mathbf{X}}$.

(3) Given $\mu_{\mathbf{X}}$ and $\sigma_{\mathbf{X}}$, the original X-space can be transformed into the standardized U-space. To derive inverse MPP, PMA is employed in the following optimization problem as:

$$\begin{aligned} &\text{Minimize } \hat{G}_{-,+}(\mathbf{u}) \\ &\text{Subject to } \parallel \mathbf{u} \parallel = \beta_{\text{target}} \end{aligned} \tag{5.9}$$

where two parallel optimization problems are solved in Formulation 5.9 under models $\hat{G}_-$ and $\hat{G}_+$ in this step, respectively. Two MPP $\mathbf{x}_{\text{MPP}_-}$ and $\mathbf{x}_{\text{MPP}_+}$ are derived from the respective optimization problems under $\hat{G}_-$ and $\hat{G}_+$. However, $\hat{G}_-$ and $\hat{G}_+$ are only constructed based on the initial hybrid design and may not be accurate enough. Then EI criterion is employed to locate additional samples which make the largest expected improvement around current MPP $\mathbf{x}_{\text{MPP}_-}$ and $\mathbf{x}_{\text{MPP}_+}$, respectively.

Similar as in [100], in order to achieve the global minimum, a polar coordinate system is employed so that the above two optimization problems are transformed to two unconstrained optimization problems as:

$$\text{Minimize } \hat{G}_{-,+}(\theta) \tag{5.10}$$

The optimal solutions $\theta_{\text{MPP}_-}$ and $\theta_{\text{MPP}_+}$ are transformed back to be $\mathbf{x}_{\text{MPP}_-}$ and $\mathbf{x}_{\text{MPP}_+}$ in X-space and evaluated by computer experiment, then the current minimum $\hat{G}_{\text{Min}_-}$ and $\hat{G}_{\text{Min}_+}$ are obtained and added to the original sample pool to update the Kriging metamodels $\hat{G}_-$ and $\hat{G}_+$, respectively.

(4) In order to find additional sampling points and decrease the prediction error in the neighborhood of current MPP$_-$ and MPP$_+$, two maximization problems are solved to locate the samples which make largest expected improvement on $G_-$ and $G_+$ function estimation.

$$\text{Maximize}(G_{min_{-,+}} - \hat{G}_{-,+})\Phi\Big(\frac{G_{min_{-,+}} - \hat{G}_{-,+}}{s_{-,+}}\Big) + s_{-,+}\phi\Big(\frac{G_{min_{-,+}} - \hat{G}_{-,+}}{s_{-,+}}\Big) \tag{5.11}$$

After solving the two optimization problems in Formulation 5.11, the maximized EI sampling points are added into the original hybrid design sampling pool and used to update the respective metamodels $\hat{G}_-$ and $\hat{G}_+$. Step (4) is repeated until the maximum EIs of $\hat{G}_-$ and $\hat{G}_+$ are both less than a stopping criterion, which means that the prediction errors of $\hat{G}_-$ and $\hat{G}_+$ around the global minimum are small enough, so the current minimum of $\hat{G}_-$ and $\hat{G}_+$ are closer to the true global minimum.

(5) MPPs are derived based on the updated metamodels $\hat{G}_-$ and $\hat{G}_+$. If both $\hat{G}_{\text{MPP}_-} \geq 0$ and $\hat{G}_{\text{MPP}_+} \geq 0$, then $\mathbf{d}$ and $\mu_{\mathbf{X}}$ are the desired optimal solution under

current weight $w_0$. If any of $\hat{G}_{\text{MPP}_-}$ and $\hat{G}_{\text{MPP}_-}$ is less than zero, the respective shifting vector $\mathbf{s}_- = \mu_{\mathbf{X}} - \mathbf{x}_{\text{MPP}_-}$ or $\mathbf{s}_+ = \mu_{\mathbf{X}} - \mathbf{x}_{\text{MPP}_+}$ are derived to modify the deterministic constraint $\hat{G}_-$ and $\hat{G}_+$ in Step (2).

(6) As mentioned in Step (1), $m$ weight combinations $w_0$ and $1 - w_0$ are proposed, thus $m$ optimal solutions are derived with different production cost objective and quality loss objective values. In particular, the optimal solution in $i^{th}, i = 1, \ldots, m$ iteration is compared and added into pareto solution set if it is proved to be a non-dominated optimal solution. Finally, all non-dominated optimal solutions considering both reliability and robustness are in the pareto solution set.

## 5.4 I-Beam Example

The I-beam example in Section 3.4 is used in this section to implement the RBRDO formulation under implicit performance (constraint) epistemic uncertainty. In order to consider robust design, the vertical load $P$ is considered to be a noise variable which follows normal distribution with $\mu_P = 600kN$ and $\sigma_P = 10kN$. The lateral load $Q$ is assumed to be constant $50kN$ for the purpose of convenience.

Two objectives are considered in the I-beam example. The first objective is to minimize the beam material cost, which is derived as $f(\mu) = 2\mu_1\mu_2 + \mu_2(\mu_1 - 2\mu_2) = 3\mu_1\mu_2 - 2\mu_2^2$. The second objective is to minimize the quality loss of performance function. An implicit bending stress performance function is considered in this example, thus a hybrid design is used to obtain initial samples including a Latin hyper cube design of $X_1$ and $X_2$ and a factorial design with low level $P = 570$ and high level $P = 630$. Based on the initial sampling points, a combined metamodel $\hat{G}$

is constructed as follows:

$$\hat{G}(\mathbf{x},p)=\frac{630-p}{60}\hat{G}_{-}(\mathbf{x})+\frac{p-570}{60}\hat{G}_{+}(\mathbf{x}) \tag{5.12}$$

where $\hat{G}_{-}(\mathbf{x})$ is the Kriging model built on the Latin hypercube samples under $p=570$, and $\hat{G}_{+}(\mathbf{x})$ is the Kriging model built on the Latin hypercube samples under $p=630$. In the objective function, quality loss from transmitted performance variation is considered as the function of $\mu_1$, $\mu_2$ and $\mu_P$ and represented by Delta method as follows:

$$\begin{aligned}V(\mu_i)&=Var(\hat{G})=\Big(\frac{\partial\hat{G}}{\partial x_i}|_{\mu_\mathbf{i},\mu_P}\sigma_i\Big)^2+\Big(\frac{\partial\hat{G}}{\partial p}|_{\mu_\mathbf{i},\mu_P}\sigma_P\Big)^2\\&=\Big[\frac{630-p}{60}\hat{G}'_{-}+\frac{p-570}{60}\hat{G}'_{+}\Big]^2|_{\mu_\mathbf{i},\mu_P}{\sigma_\mathbf{i}}^2+\Big[\frac{1}{60}\hat{G}_{+}-\frac{1}{60}\hat{G}_{-}\Big]^2|_{\mu_\mathbf{i},\mu_P}\sigma_P^2\\&=\Big[\frac{1}{2}\hat{G}'_{-}(\mu_\mathbf{i})+\frac{1}{2}\hat{G}'_{+}(\mu_\mathbf{i})\Big]^2{\sigma_\mathbf{i}}^2+\Big[\frac{1}{60}\hat{G}_{+}(\mu_\mathbf{i})-\frac{1}{60}\hat{G}_{-}(\mu_\mathbf{i})\Big]^2\sigma_P^2\end{aligned} \tag{5.13}$$

where $i=1,2$ respective to random variables $x_1$ and $x_2$.

One probabilistic constraint is considered in the example as $P[G(x_1,x_2)\geq 0]\geq R$, where $G(x_1,x_2)$ is the implicit performance which denotes the threshold $\sigma=0.016kN/cm^2$ deducted by the actual bending stress. Then the formulation of RBRDO becomes:

$$\begin{aligned}&\text{Minimize: } f(\mu_1,\mu_2)=3\mu_1\mu_2-2\mu_2^2\\&\text{Minimize: } V(\mu_1,\mu_2)\\&\text{Subject to: } Prob[\hat{G}(x_1,x_2)\geq 0]\geq 99.87\%\\&\qquad 10\leq\mu_1\leq 80, 0.9\leq\mu_2\leq 5\end{aligned} \tag{5.14}$$

Following the procedure in Fig. 28, a set of weights $w_0$ and $1-w_0$ are assigned to combine the two objective into a weighted sum single objective, where the pareto number is set to be 100 in this example. A hybrid design is employed

Table 17.Initial Samples by Hybrid Design

| | LHS | | Factorial | | | LHS | | Factorial | |
|---|---|---|---|---|---|---|---|---|---|
| No. | $x_1$ | $x_2$ | $G_-$ | $G_+$ | No. | $x_1$ | $x_2$ | $G_-$ | $G_+$ |
| 1 | 32.11 | 2.63 | 0.0046 | 0.0034 | 11 | 80.00 | 3.06 | 0.0146 | 0.0145 |
| 2 | 24.74 | 0.90 | -0.0332 | -0.0384 | 12 | 28.42 | 1.76 | -0.0045 | -0.0066 |
| 3 | 65.26 | 2.19 | 0.0131 | 0.0128 | 13 | 39.47 | 4.35 | 0.0111 | 0.0106 |
| 4 | 10.00 | 3.71 | -0.1643 | -0.1825 | 14 | 21.05 | 4.57 | -0.0062 | -0.0084 |
| 5 | 61.58 | 3.27 | 0.0137 | 0.0135 | 15 | 76.32 | 1.33 | 0.0127 | 0.0123 |
| 6 | 50.53 | 5.00 | 0.0135 | 0.0132 | 16 | 68.95 | 4.78 | 0.0147 | 0.0146 |
| 7 | 54.21 | 4.14 | 0.0135 | 0.0132 | 17 | 13.68 | 1.55 | -0.1002 | -0.1121 |
| 8 | 72.63 | 3.92 | 0.0146 | 0.0145 | 18 | 43.16 | 1.98 | 0.0084 | 0.0077 |
| 9 | 35.79 | 3.49 | 0.0088 | 0.0080 | 19 | 46.84 | 2.84 | 0.0113 | 0.0109 |
| 10 | 57.89 | 1.12 | 0.0091 | 0.0145 | 20 | 17.37 | 2.41 | -0.0338 | -0.0388 |

and 40 samples are generated in Table 17 to build the metamodel $\hat{G}$. Then a deterministic optimization is solved by using GA with 100 initial population and 10 iterations, and a vector of decision variable $\mu_1$ and $\mu_2$ is derived. The reliability analysis is implemented for the implicit performance functions of $\hat{G}_-$ and $\hat{G}_+$ in, respectively. We set the stopping criterion of sequential EI-based sampling strategy to be maximum $EI < 0.05$. Once both MPP$_-$ and MPP$_+$ are satisfied, the optimal solution $(\mu_1, \mu_2)$ is considered as a Pareto optimal solution candidate and the algorithm enters the next iteration with a new set of weights. In order to achieve the trade-off between material cost and quality loss, the quality loss objective is multiplied by $10^5$ to keep two objectives in similar scale level in this example. The final Pareto solution set is shown in Table 18, in which the two objective values and the corresponding weight $w_0$ are indicated.

Comparing with the traditional RBDO with implicit performance function, the optimal solution in RBRDO is a Pareto frontier not a single optimal solution in Fig. 29. As indicated in Table 18, when weight $w_0$ is equal to 1.00, the robustness

Table 18.Pareto Solutions for I-Beam Design

| $w_0$ | $\mu_1$ | $\mu_2$ | Material cost | Increase% | Quality loss | Decrease% |
|---|---|---|---|---|---|---|
| 1.00 | 50.24 | 0.91 | 136.10 | – | 1.88 | – |
| 0.69 | 49.94 | 0.93 | 138.09 | 1.46% | 0.52 | 72.34% |
| 0.65 | 51.41 | 0.91 | 138.37 | 1.67% | 0.48 | 74.47% |
| 0.63 | 49.77 | 0.94 | 138.87 | 2.04% | 0.45 | 76.06% |
| 0.43 | 51.86 | 0.91 | 139.37 | 2.40% | 0.39 | 79.26% |
| 0.19 | 48.45 | 1.02 | 145.90 | 7.20% | 0.38 | 79.79% |
| 0.13 | 54.33 | 0.93 | 149.44 | 9.80% | 0.33 | 82.45% |
| 0.05 | 53.07 | 0.98 | 154.67 | 13.64% | 0.23 | 87.77% |
| 0.02 | 47.86 | 1.29 | 182.98 | 34.45% | 0.14 | 92.55% |
| 0.00 | 36.96 | 2.47 | 261.62 | 92.23% | 0.09 | 95.21% |

objective is ignored. Thus the traditional RBDO optimal solution is $(50.24, 0.91)$ with material cost 136.10 and quality loss 1.88. When we change the weight, other non-dominated solutions are derived, in which the material cost is increased and quality loss is decreased. Although the absolute value of material cost increase and quality loss decrease cannot be compared due to different numerical scales, the increase and decrease percentages compared with traditional RBDO solution are listed in Table 18. Based on the trade-off between material cost increase and quality loss decrease, the optimal solution $(51.86, 0.91)$ is the desired solution that considers both reliability and robustness simultaneously, in which a maximum 76.85% decrease is obtained totally with 2.40% material cost increase and 79.26% quality loss decrease.

## 5.5 Conclusion and Future Work

In this chapter, an RBRDO problem is proposed in product design with implicit performance function. The quality loss objective is integrated into traditional RBDO problem to add performance robustness consideration. In order to evaluate the impacts of noise variables, we employ the hybrid design and construct a combined

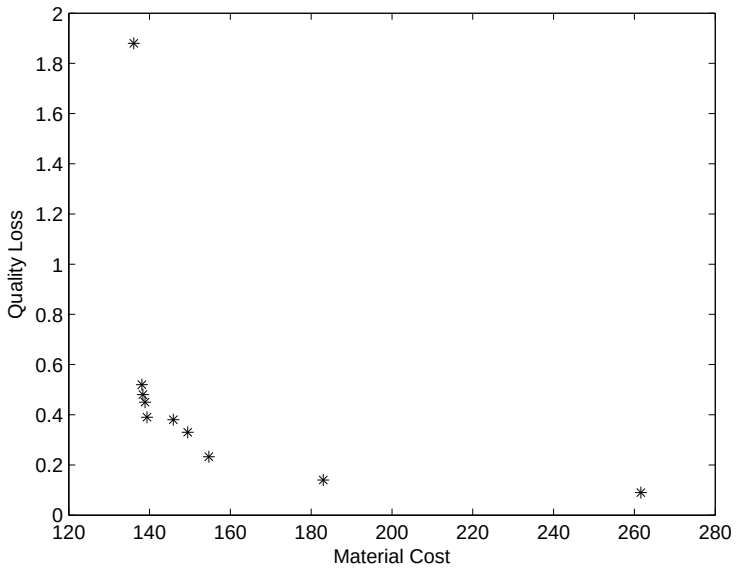


Figure 29.RBRDO Pareto frontier

Kriging metamodel. Then a sequential sampling approach is employed to update the metamodel and improve RBRDO solutions. Finally a Pareto solution frontier is derived to make a trade-off between production cost of RBDO and quality loss of robust design.

The RBRDO formulation in this chapter only handles one performance function, but there are typical multiple performance functions in realistic engineering design. In future work, multiple quality characteristics are required to measure different product performances, and the interactions between them should be further developed.

# CHAPTER 6

# CONCLUSION AND FUTURE RESEARCH

## 6.1 Conclusions

This dissertation proposes methods and formulations of product design optimization under epistemic uncertainty. Two major aspects of product design optimization, reliability and robustness, are addressed by RBDO and robust design, respectively. A comprehensive review of uncertainty including aleatory uncertainty and epistemic uncertainty is proposed in Chapter 2. The main contributions of the dissertation are the metamodel-based approximation methods and simulation-based methods in solving RBDO under epistemic uncertainty of implicit constraint functions. By extending the metamodel approximation methods, the robust design is integrated with RBDO to formulate an RBRDO problem under implicit performance functions.

In Chapter 3, a sequential sampling strategy is proposed to address the RBDO problem under implicit constraint function. Based on the Kriging metamodel, an ERI criterion is proposed to select additional samples and improve the solution of RBDO. The sampling strategy focuses on the neighborhood of current RBDO solution and maximally improves the MPP estimation. It is proved to be more reliable and accurate than other methods such as MPP-based sampling, lifted response function and non-sequential random sampling.

In Chapter 4, a new simulation-based reliability analysis approach, the particle splitting method, is introduced to be integrated with the traditional sequential optimization method to solve RBDO problems. The proposed strategy combines the merits of SORA and particle splitting reliability assessment method, which not only can provide more accurate solutions than worst case analysis as in MPP-

based method, but also is more efficient than traditional Monte Carlo simulation and enhances the simulation diversity by using multiple particles. In addition, the approach can be extended to address problems with multiple constraints without significantly increasing sample size.

In Chapter 5, a reliability-based robust design optimization is formulated to consider RBDO and robust design simultaneously. A trade-off balance between production cost objective of RBDO and quality loss objective of robust design is obtained in a multi-objective optimization problem under implicit performance function epistemic uncertainty. The sequential sampling strategy in Chapter 3 is extended to address noise variables and tackle a multi-objective optimization problem. A Pareto frontier is derived which includes all non-dominated solutions.

## 6.2 Future Work

This research has highlighted the algorithms and formulations to address product design optimization under epistemic uncertainty. Some extensions of work include:

- Implicit constraint (performance) function in Chapter 3 is just one type of epistemic uncertainty due to lack of knowledge. Strategies for other types such as unknown random variables distribution could be developed in future work;

- In particle splitting method, the trade-offs among number of subsets, number of particles and the length of MCMC chain could be further developed. Different combinations could lead to different simulation diversity, efficiency and accuracy;

- Subset simulation in Chapter 4 is one type of rare-event simulations. Other rare-event simulation methods such as line sampling can be employed in re-

liability analysis in future work;

- The RBRDO formulation in Chapter 5 could be extended to the case of multiple performance functions. Metrics could be developed to represent the total quality loss among different product performance functions.

REFERENCES

[1] Antonio, C., and L. Hoffbauer. 2009. An approach for reliability-based robust design optimization of angle-ply composites. *Composite Structures* 90(1):53–59.

[2] Apley, D., J. Liu, and W. Chen. 2006. Understanding the effects of model uncertainty in robust design with computer experiments. *Jounal of Mechenical Design* 128(4):945–958.

[3] Arenbeck, H., S. Missoum, A. Basudha, and P. Nikravesh. 2010. Reliability-based optimal design and tolerancing for multibody systems using explicit design space decomposition. *Jounal of Mechenical Design* 132(2):0210101–02101011.

[4] Au, S., and J. Beck. 2001. Estimation of small failure probabilities in high dimensions by subset simulation. *Probabilistic Engineering Mechanics* 16(4):263–277.

[5] Basudhar, A., and S. Missoum. 2008. Adaptive explicit decision functions for probabilistic design and optimization using support vector machines. *Computer and Structures* 86(19–20):1904–1917.

[6] Basudhar, A., and S. Missoum. 2009. A sampling-based approach for probabilistic design with random fields. *Computer Methods in Applied Mechanics and Engineering* 198(47–48):3647–3655.

[7] Basudhar, A., and S. Missoum. 2010. An improved adaptive sampling scheme for the construction of explicit boundaries. *Structural and Multidisciplinary Optimization* 42(4):517–529.

[8] Basudhar, A., S. Missoum, and A. Sanchez. 2008. limit state function identification using support vector machines for discontinous responses and disjoint failure domains. *Probabilistic Engineering Mechanics* 23(1):1–11.

[9] Beyer, H., and B. Sendhoff. 2007. Robust optimization – A comprehensive survey. *Computer methods in applied mechanics and engineering* 196(33-34):3190–3218.

[10] Bichon, B., M. Eldred, L. Swiler, S. Mahadevan, and J. McFarland. 2007. Multimodal reliability assessment for complex engineering applications using efficient global optimization. In *48th AIAA/ASME/ASCE/AHS/ASC Sturctures, Structural Dynamics and Materials Conference*.

[11] Bichon, B., M. Eldred, L. Swiler, S. Mahadevan, and J. McFarland. 2008. Efficient global reliability analysis for nonlinear implicit performance functions. *AIAA Journal* 46(10):2459–2468.

[12] Bichon, B., S. Mahadevan, and M. Eldred. 2009. Reliability-based design optimization using efficient global reliability analysis. In *48th AIAA/ASME/ASCE/AHS/ASC Sturctures, Structural Dynamics and Materials Conference*.

[13] Chen, X., and T. Hasselman. 1997. Reliability-based structural design optimization for practical applications. In *38th AIAA/ASME/ASCE/AHS/ASC Sturctures, Structural Dynamics and Materials Conference and Exhibit and AIAA/ASME/AHS Adaptive Structural Forum*.

[14] Ching, J., and Y. Hsieh. 2007. Approximate reliability-based optimization using a three-step approach based on subset simulation. *Jounal of Engineering Mechenics* 133(4):481–493.

[15] Chiralaksanakul, A., and S. Mahadevan. 2004. Reliability-based design optimization methods. In *30th Design Automation Conference*, Volume 1.

[16] Choi, J., D. An, and J. Won. 2010. Bayesian approach for structural reliability analysis and optimization using the Kriging dimension reduction method. *Journal of Mechanical Design* 132(5):0510031–05100311.

[17] Choi, K., and B. Youn. 2001. Hybrid analysis method for reliability-based design optimization. Volume 121.

[18] Choi, S., R. Grandhi, and R. Canfield. 2007. *Reliability-based Structural Design*. Springer.

[19] Dirk, P., T. Thomas, and I. Zdravko. 2011. *Handbook of Monte Carlo Methods*. Wiley.

[20] Du, L., K. Choi, B. Youn, and D. Gorsich. 2006. Possibility-based design optimization method for design problems with both statistical and fuzzy input data. *Journal of Mechanical Design* 128(4):928–935.

[21] Du, X. 2007. Interval reliability analysis. In *International Design Engineering Technical Conferences and Computers and Information in Engineering Conference*.

[22] Du, X., and W. Chen. 2000. Towards a better understanding of modeling feasibility robustness in engineering design. *Journal of Mechanical Design* 122(4):385–394.

[23] Du, X., and W. Chen. 2002. Sequential optimization and reliability assessment for probabilistic design. In *International Design Engineering Technical Conferences*.

[24] Du, X., and W. Chen. 2004. Sequential optimization and reliability assessment method for efficient probabilistic design. *Journal of Mechanical Design* 126(March):225–233.

[25] Du, X., A. Sudjianto, and W. Chen. 2004. An integrated framework for optimization under uncertainty using inverse reliability strategy. *Transactions of the ASME* 126(4):562–570.

[26] Du, X., A. Sudjianto, and B. Huang. 2005. Reliability-based design with the mixture of random and interval variables. *Transactions of the ASME* 127(6):1068–1075.

[27] Dubourg, V., B. Sudret, and J. Bourinet. 2011. Reliability-based design optimization using kriging surrogates and subset simulation. *Structural and Multidisciplinary Optimization* 44(5):673–690.

[28] Enevoldsen, I., and J. Sorensen. 1994. Reliability-based optimization in structural engineering. *Struct. Saf.* 15(3):169–196.

[29] Frangopol, D., and F. Moses. 1994. Reliability-based structural optimization. *Advances in design optimization*:492–570.

[30] Guanwan, S., and P. Papalambros. 2006. A Bayesian approach to reliability-based optimization with incomplete information. *Journal of Mechanical Design* 128(4):909–918.

[31] Guo, X., K. Yamazaki, and G. Cheng. 2001. A new three-point approximation approach for design optimization problems. *International Jounal for Numerical Methods in Engineering* 50(4):869–884.

[32] Hanss, M., and S. Turrin. 2010. A fuzzy-based approach tocomprehensive modeling and analysis ofsystems with epistemic uncertainties. *Structural Safety* 32(6):433–441.

[33] Hasofer, A., and N. Lind. 1974. Exact and invariant second-moment code format. *Journal of the Engineering Mechanics Division* 100(1):111–121.

[34] Hu, C., and B. Youn. 2011a. Adaptive-sparse polynomial chaos expansion for reliability analysis and design of complex engineering systems. *Structural and Multidisciplinary Optimization* 43(3):419–442.

[35] Hu, C., and B. Youn. 2011b. An asymmetric dimension-adaptive tensor-product method for reliability analysis. *Structural Safety* 33(3):218–231.

[36] Iman, R., J. Helton, and J. Campbell. 1981. An approach to sensitivity analysis of computer models, Part 1. Introduction, input variable selection and preliminary variable assessment. *Journal of Quality Technology* 13(3):174–183.

[37] Jin, R., X. Du, and W. Chen. 2003. The use of metamodeling techniques for optimization under uncertainty. *Struct Multidisc Optim* 25(2):99–116.

[38] Jones, D., M. Schonlau, and W. Welch. 1998. Efficient global optimization of expensive black-box functions. *Journal of Global Optimization* 13(4):455–492.

[39] Ju, B., and B. Lee. 2008. Reliability-based design optimization using a moment method and a Kriging metamodel. *Engineering Optimization* 40(5):421–438.

[40] Kim, C., and K. Choi. 2008. Reliability-based design optimization using response surface method with prediction interval estimation. *Journal of Mechanical Design* 130(12):121401–121412.

[41] Kiureghian, A., and O. Ditlevsen. 2009. Aleatory or epistemic does it matter. *Structural Safety* 31(2):105–112.

[42] Kuczera, R., Z. Mourelatos, E. Nikolaidis, and J. Li. 2009. A simulation-based RBDO method using probabilistic te-analysis and a trust region approach. In *International Design Engineering Technical Conferences and Computers and Information in Engineering Conference*.

[43] Lee, I., K. Choi, and D. Gorsich. 2010. Sensitivity snalysis of FORM-based and DRM-based performance measure approach (PMA) for reliability-based design optimization (RBDO). In *International Journal for Numerical Methods in Engineering*, Volume 82, 26–46.

[44] Lee, S., and W. Chen. 2007. A comparative study of uncertainty propagation methods for black-box type functions. In *International Design Engineering Technical Conferences and Computers and Information in Engineering Conference*, Volume 6 PART B, 1275–1284.

[45] Lee, T., and J. Jung. 2008. A sampling technique enhancing accuracy and efficiency of metamodel-based RBDO: constraint boundary sampling. *Computers and Structures* 86(13–14):1463–1476.

[46] Li, F., and T. Wu. 2007. An importance sampling based approach for reliability analysis. In *The 3rd Annual IEEE Conference on Automation Science and Engineering*.

[47] Li, M., S. Azarm, and V. Aute. 2005. A multi-objective genetic algorithm for robust design optimization. In *Genetic and Evolutionary Computation Conference*, 771–778.

[48] Liang, J., Z. Mourelatos, and E. Nikolaidis. 2007. A single-loop approach for system reliability-based design optimization. *Journal of Mechanical Design* 129(12):1215–1224.

[49] Liebscher, M., S. Pannier, J. Sickert, and W. Graf. 2006. *Efficiency improvement of stochastic simulation by means of subset sampling*. TU Dresden, Dresden, Germany: LS-DYNA Anwenderforum, UIM. Technical report.

[50] Lin, P., C. Hae, and Y. Jaluria. 2009. A modified reliability index approach for reliability-based design optimization. In *International Design Engineering Technical Conferences and Computers and Information in Engineering Conference*.

[51] Liu, D., W. Yue, P. Zhu, and X. Du. 2006. New approach for reliability-based design optimization minimum error point. *Chinese Journal of Mechanical Engineering* 19(4).

[52] Liu, H., W. Chen, J. Sheng, and H. Gea. 2003. Application of the sequential optimization and reliability assessment method to structural design problems. In *Design Engineering Technical Conferences and Computers and Information in Engineering Conference*.

[53] Liu, P., and A. Kiureghian. 1991. Optimization algorithms for structural reliability. *Structural Safety* 9(3):161–177.

[54] Lophaven, S., H. Nielsen, and J. Sondergaard. 2002. *A matlab Kriging toolbox*. Kongens Lyngby: Technical University of Denmark. Technical report.

[55] Madsen, H., S. Krenk, and N. Lind. 2006. A single-loop approach for system reliability-based design optimization. *Journal of Mechanical Design* 129(12):1215–1224.

[56] McKay, M., R. Beckman, and W. Conover. 1979. A comparison of three methods for selecting values of input variables in the analysis of output from a computer code. *Technometrics* 21(2):239–245.

[57] Minguez, R., and E. Castillo. 2009. Reliability-based optimization in engineering using decomposition techniques and FORMS. *Structural Safety* 31(3):214–223.

[58] Mok, C., N. Sitar, and A. Kiureghian. 2002. Improving accuracy of first-order reliability estimate by importance sampling simulations. In *ModelCARE*.

[59] Montgomery, D. 2009. *Design and Analysis of Experiments*. John Wiley.

[60] Mourelatos, Z., and J. Liang. 2005. A methodologh for trading-off performance and robustness under uncertainty. In *International Design Engineering Technical Conferences and Computers and Information in Engineering Conference*.

[61] Mourelatos, Z., and J. Zhou. 2004. Reliability estimation and design with insufficient data based on possibility theory. In *10th AIAA/ISSMO Multidisciplinary Analysis and Optimization Conference*, Volume 5, 3147–3162.

[62] Myers, R., and D. Montgomery. 1995. *Response Surface Methodology: Process and Product Optimization Using Designed Experiments*. New York: Wiley & Sons.

[63] Nikolaidis, E., S. Chen, H. Cudney, R. Haftka, and R. Rosca. 2004. Comparison of probability and possibility for design against catastrophic failure under uncertainty. *Transactions of the ASME* 126(3):386–394.

[64] Noh, Y., K. Choi, I. Lee, D. Gorsich, and D. Lamb. 2011. Reliability-based design optimization with confidence level for non-Gaussian distributions using bootstrap method. *Journal of Mechanical Design* 133(9):091001–091012.

[65] Oza, K., and H. Gea. 2004. Two-level approximaiton method for reliability based design optimization. In *International Design Engineering Technical Conferences and Computers and Information in Engineering Conference*.

[66] Padmanabhan, D., H. Agarwal, J. Renaud, and S. Batill. 2006. A study using Monte Carlo simulation for failure probability calculation in reliability-based optimization. *Optimization and Engineering* 7(3):297–316.

[67] Panda, S., and C. Manohar. 2008. Applications of meta-models in ginite element based reliability analysis of engineering structures. *Computer Modeling in Engineering and Sciences* 28(3):161–184.

[68] Parker, G., T. Lee, K. Lee, and K. Hwang. 2006. Robust design: an overview. *AIAA Journal* 44(1):181–191.

[69] Parkinson, A., C. Sorensen, and N. Pourhassan. 1993. A general approach for robust optimal design. *Transactions of the ASME* 115(1):74–80.

[70] Picheny, V., N. Kim, and R. Haftka. 2007. Conservative estimations of reliability with limited sampling. In *International Design Engineering Technical Conferences and Computers and Information in Engineering Conference*.

[71] Rahman, S., and H. Xu. 2004. A univariate dimension-reduction method for multi-dimensional integration in stochastic mechanics. *Probabilistic Engineering Mechanics* 19(4):393–408.

[72] Reh, S., J. Beley, S. Mukherjee, and E. Khor. 2006. Probabilistic finite element analysis using ANSYS. *Structural Safety* 28(1-2):17–43.

[73] Sacks, J., W. Welch, T. Mitchell, and H. Wynn. 1989. Design and analysis of computer experiments. *Statistical Science* 4(4):409–423.

[74] Samson, S., S. Thoomu, G. Fadel, and J. Reneke. 2009. Reliable design optimization under aleatory and epistemic uncertainties. In *International Design Engineering Technical Conferences and Computers and Information in Engineering Conference*.

[75] Sanchis, J., M. Martinez, and X. Blasco. 2008. Integrated multiobjective optimization and a priori preferences using genetic algorithms. *Information Sciences* 178(4):931–951.

[76] Shan, S., and G. Wang. 2008. Reliable design space and complete single-loop reliability-based design optimization. *Reliability Engineering & System Safety* 93(8):1218–1230.

[77] Shen, L., J. Yang, and Y. Zhao. 2011. An integration design optimization framework of robust design, axiomatic design and reliability-based design. *Quality and Reliability Engineering International* 27(7):959–968.

[78] Sopory, A., S. Mahadevan, Z. Mourelatos, and J. Tu. 2004. Decoupled and single loop methods for reliability-based optimization and robust design. In *Design Engineering Technical Conferences and Computers and Information in Engineering Conference*.

[79] Suh, N. 1990. *The Principles of Design*. New York: Oxiford University.

[80] Suh, N. 2001. *Axiomatic Design: Advances and Application*. New York: Oxiford University.

[81] Taflanidis, A., and J. Beck. 2008. Stochastic subset optimization for reliability problems. *Probabilistic Engineering Mechanics* 23(2–3):324–338.

[82] Taflanidis, A., and J. Beck. 2009. Stochastic subset optimization for reliability optimization and sensitivity analysis in system design. *Computers and Structures* 87(5–6):318–331.

[83] Tang, Y., J. Chen, and J. Wei. 2012. A sequential algorithm for reliability-based robust design optimization under epistemic uncertainty. *Journal of Mechanical Design* 134(1):014502–1–014502–10.

[84] Tu, J., and K. Choi. 1999. A new study on reliability-based design optimization. In *IDETC/CIE*, Volume 121.

[85] Wei, D., Z. Cui, and J. Chen. 2008. Uncertainty quantification using polynomial chaos expansion with points of monomial cubature rules. *Computer & Structures* 86(23-24):2102–2108.

[86] Xiong, F., S. Greene, W. Chen, Y. Xiong, and S. Yang. 2010. A new sparse grid based method for uncertainty propagation. *Structural and Multidisciplinary Optimization* 41(3):335–349.

[87] Xu, H., H. Huang, Z. Wang, B. Zheng, and D. Meng. 2011. Research on multi-objective robust design. In *International Conference on Quality, Reliability, Risk, Maintenance, and Safety Engineering*, 885–890.

[88] Yang, R., and L. Gu. 2003. Experience with approximate reliability-based optimization methods. *Springer-Verlag*.

[89] Youn, B., and K. Choi. 2004a. A new response surface methodology for reliability-based design optimization. *Computer and Structures* 82(2–3):241–256.

[90] Youn, B., and K. Choi. 2004b. An investigation of nonlinearity of reliability-based design optimization approaches. *Journal of Mechanical Design* 126(3).

[91] Youn, B., K. Choi, R. Yang, and L. Gu. 2004. Reliability-based design optimization for crashworthiness of vehicle side impact. *Struct Multidisc Optim* 26(3–4):272–283.

[92] Youn, B., and P. Wang. 2006. Bayesian reliability based design optimization under both aleatory and epistemic uncertainty. In *11th AIAA/ISSMO Multidisciplinary Analysis and Optimization Conference*.

[93] Youn, B., and P. Wang. 2008. Bayesian reliability-based design optimization using eigenvector dimension reduction (EDR) method. *Structural and Multidisciplinary Optimization* 36(2):107–123.

[94] Youn, B., and Z. Xi. 2009. Reliability-based robust design optimization using the eigenvector dimension reduction (EDR) method. *Structural and Multidisciplinary Optimization* 37(5):475–492.

[95] Youn, B., Z. Xi, and P. Wang. 2008. Eigenvector dimension reduction (EDR) method for sensitivity-free probability analysis. *Struct Multidisc Optim* 37:13–28.

[96] Youn, B., Z. Xi, L. Wells, and P. Wang. 2006. Enhanced dimension reduction (EDR) method for sensitivity-free uncertainty quantification. In *Multidisciplinary Analysis and Optimization Conference*.

[97] Yu, X., K. Choi, and K. Chang. 1997. A mixed design approach for probabilistic structural durability. *Structural and Multidisciplinary Optimization* 14(2–3):81–90.

[98] Zhang, X., and H. Huang. 2010. Sequential optimization and reliability assessment for multidisciplinary design optimization under aleatory and epistemic uncertainties. *Structural and Multidisciplinary Optimization* 40(1-6):165–175.

[99] Zhao, L., K. Choi, and I. Lee. 2009. Response surface method using sequential sampling for reliability-based design optimization. In *IDETC/CIE*, Volume 1.

[100] Zhuang, X., and R. Pan. 2012. A sequential sampling strategy to improve reliability-based optimization under implicit constraints. *Journal of Mechanical Design* 134(2):021002–1–021002–10.

[101] Zio, E., and N. Pedroni. 2009. *Subset simulation and line sampling for advanced Monte Carlo reliability analysis*. Milano, Italy: Energy Department, Politeconico di Milano. Technical report.